Development and Applications of Particle Induced Gamma-ray Emission Methods for Low Z Elements

By

SUMIT CHHILLAR

CHEM01200904013

BHABHA ATOMIC RESEARCH CENTRE, MUMBAI

A thesis submitted to the
Board of Studies in Chemical Sciences
In partial fulfillment of requirements for the Degree of

DOCTOR OF PHILOSOPHY

Of

HOMI BHABHA NATIONAL INSTITUTE

January 2016

STATEMENT BY AUTHOR

This dissertation has been submitted in partial fulfillment of requirements for an advanced degree at **Homi Bhabha National Institute** (HBNI) and is deposited in the Library to be made available to borrowers under rules of the HBNI. Brief quotations from this dissertation are allowable without special permission, provided that accurate acknowledgement of source is made. Requests for permission for extended quotation from or reproduction of this manuscript in whole or in part may be granted by the Competent Authority of HBNI when in his or her judgment the proposed use of the material is in the interests of scholarship. In all other instances, however, permission must be obtained from the author.

(Sumit Chhillar)

DECLARATION

I hereby declare that the investigation presented in the thesis has been carried out by me. The work is original and has not been submitted earlier as a whole or in part for a degree / diploma at this or any other Institution / University.

(Sumit Chhillar)

List of Publications Arising from the Thesis

Journal

1. Application of particle induced gamma-ray emission for non-destructive determination of fluorine in barium borosilicate glass samples, **Sumit Chhillar**, R. Acharya, S. Sodaye, K. Sudarshan, S. Santra, R.K. Mishra, C.P. Kaushik, R.K. Choudhury, P.K. Pujari, *J. Radioanal. Nucl. Chem.*, **2012**, 294, 115–119.
2. A simple and sensitive particle induced gamma-ray emission method for non-destructive quantification of lithium in lithium doped $Nd_2Ti_2O_7$ ceramic sample, **Sumit Chhillar**, R. Acharya, R.V. Pai, S. Sodaye, S.K. Mukerjee, P.K. Pujari, *J. Radioanal. Nucl. Chem.*, **2012**, 293, 212-216.
3. Non-destructive compositional analysis of sol–gel synthesized lithium titanate (Li_2TiO_3) by particle induced gamma-ray emission and instrumental neutron activation analysis, **Sumit Chhillar**, R. Acharya, T.V. Vittal Rao, Y.R. Bamankar, S.K. Mukerjee, P.K. Pujari, S.K Aggarwal, *J. Radioanal. Nucl. Chem.*, **2013**, 298, 1597-1603.
4. Compositional characterization of lithium titanate ceramic samples by determining Li, Ti and O concentrations simultaneously using PIGE at 8 MeV proton beam, **Sumit Chhillar**, R. Acharya, R. Tripathi, S. Sodaye, K. Sudarshan, P. C. Rout, S. K. Mukerjee, P. K. Pujari, *J. Radioanal. Nucl. Chem.*, **2015**, DOI 10.1007/s10967-015-4037-1
5. Simultaneous determination of Si, Al and Na concentrations by particle induced gamma-ray emission and applications to reference materials and ceramic archaeological artifacts K.B. Dasaria, **Sumit Chhillar**, R. Acharya, D.K. Ray, A. Behera, N. Lakshmana Das, P.K. Pujari, *Nucl. Instrum. Meth. B*, **2014,** 339, 37-41.
6. Development of particle induced gamma-ray emission methods for nondestructive determination of isotopic composition of boron and its total concentration in natural and

enriched samples, **Sumit Chhillar**, Raghunath Acharya, Suparna Sodaye, Pradeep K. Pujari, *Anal. Chem.*, **2014**, 86(22), 11167-11173.

7. Compositional Characterization of borosilicate glass samples for low Z elements using *in situ* current normalized particle induced gamma-ray emission methods, **Sumit Chhillar**, R. Acharya, R.K. Mishra, C.P. Kaushik, P.K. Pujari *(Submitted)*

Conference

1. Non-destructive Determination of Fluorine in Borosilicate Glass Samples by a PIGE Method; **S. Chhillar**, R. Acharya, S. Sodaye, K. Sudarshan, S. Santra, R.K. Mishra, C.P. Kaushik, R.K. Choudhury, P.K. Pujari, Fourth International Symposium on Nuclear Analytical Chemistry (NAC-IV), BARC, Mumbai, **November 15-19, 2010**, p.196.
2. Setting up of PIGE facility at FOTIA, BARC and its application to Borosilicate Glass Samples for determination of fluorine by an internal standard method; **S. Chhillar**, R. Acharya, S. Sodaye, K. Sudarshan, S. Santra, R.K. Mishra, C.P. Kaushik, S.K. Gupta, A. Agarwal, P. Singh, R.K. Choudhury, P.K. Pujari, Proceedings of DAE Symposium on Nuclear Physics (SNP-55), BITS, Pilani, Rajasthan, **December 20-24, 2010**, p.780-781.
3. An internal standard particle induced gamma ray emission methodology for non-destructive determination of Lithium in ceramic samples, **S. Chhillar**, R. Acharya, S. Sodaye, R. Pai, S. K. Mukerjee, P. K. Pujari, Proceedings of Tenth DAE-BRNS biennial symposium on Nuclear and Radiochemistry (NUCAR-2011), GITAM University, Visakhapatnam, **February, 22-26, 2011**, p.523-524.
4. Proton Induced Gamma-ray Emission Reaction for Quantification of Lithium in Lithium Titanate Samples, **S. Chhillar**, R. Acharya, K.B. Dasari, R. Tripathi, P.K. Pujari, T.V. Vittal Rao, Y. R. Bamankar, S. K. Mukerjee, S.K Aggarwal, Proceedings of DAE

Symposium on Nuclear Physic (SNP-56), Andhra University, Visakhapatnam, **December 26-30, 2011**, p.630-631.

5. Non-destructive quantification of boron and ^{10}B to ^{11}B ratios in neutron absorber materials by PIGE using proton beam from FOTIA, BARC, **S. Chhillar**, R. Acharya and P.K. Pujari, Proceedings of DAE Symposium on Nuclear Physic (SNP-57), Delhi University, Delhi, **December 3-7, 2012**, p. 920-921.
6. Applications of PIGE and PIXE for analysis of ceramic and archaeological artifacts, K.B. Dasari, R. Acharya, **Sumit Chhillar**, D.K. Ray, A. Behera, N.L. Das, P.K. Pujari, Proceedings of Eleventh DAE-BRNS biennial symposium on Nuclear and Radiochemistry (NUCAR-2013), R.D. University, Jabalpur, **February 19-23, 2013**, p.473-474.
7. Application of particle induced gamma-ray emission methodology for simultaneous quantification of low Z elements in borosilicate glass, **Sumit Chhillar**, R. Acharya, R. K. Mishra, C. P. Kaushik and P. K. Pujari, Proceedings of Eleventh DAE-BRNS biennial symposium on Nuclear and Radiochemistry (NUCAR-2013), R.D. University, Jabalpur, **February 19-23, 2013**, p.479-480.
8. Application of *in situ* current normalized PIGE method for determination of total boron and its isotopic composition, **Sumit Chhillar**, R. Acharya, S. Sodaye, P.K. Pujari, Fifth Symposium on Nuclear Analytical Chemistry (NAC-V), BARC, Mumbai, **January 20-24, 2014**, p.224-225.
9. Simultaneous quantification of Li, Ti and O in lithium titanate by particle induced gamma-ray emission using 8 MeV proton beam, **S. Chhillar**, R. Acharya, R. Tripathi, S. Sodaye, K. Sudarshan, P.C. Rout, S.K. Mukerjee, P.K. Pujari, Proceedings of Fifth Symposium on Nuclear Analytical Chemistry (NAC-V), BARC, Mumbai, **January 20-24, 2014**, p.210-211.

10. R&D work on particle induced gamma-ray emission using proton beam at FOTIA, BARC: Present status and future Prospects, R. Acharya, **S. Chhillar**, P.K. Pujari, A. Agarwal, S.K. Gupta and P. Singh, Fifth Symposium on Nuclear Analytical Chemistry (NAC-V), BARC, Mumbai, **January 20-24, 2014**, p.212-213.
11. Determination of isotopic composition of boron in various neutron absorbers by a Particle Induced Gamma-ray Emission method, R. Acharya, **Sumit Chhillar**, J.K. Sonber, D.S. Arati, T.S.R. Ch Murthy, P. K. Pujari, Proceedings of Twelfth DAE-BRNS biennial symposium on Nuclear and Radiochemistry (NUCAR-2015), BARC, Mumbai, **January 20-24, 2015**, p.417-418.

(Sumit Chhillar)

Dedicated to

My

Grand Parents and Parents

ACKNOWLEDGEMENTS

*I would like to thank my supervisor **Prof. Pradeep K. Pujari,** Head, Nuclear Chemistry Section (NCS), Radiochemistry Division (RCD), BARC, for providing a platform and allowing me to join his research group. It has been a privilege to work in his research group and I have received firm support and encouragement throughout my tenure. I appreciate his willingness to let me work on projects that challenged me intellectually and provided the sustenance that I needed to grow as a nuclear analytical chemist. I am grateful to him for his support and guidance.*

*I am grateful to **Dr. R. Acharya**, NCS, RCD, BARC who was the main pillar of my strength while carrying out the research work. I have been immensely benefited from his in-depth knowledge on the subject, valuable suggestions and effective mentoring which led to successful completion of my PhD thesis work. I sincerely thank him for being there whenever I needed.*

*I thank **Prof. D. Srivastava**, Material Science Division, BARC, for his guidance and valuable suggestions and also for being my co-guide as well as a member of my doctoral committee.*

*I am grateful to **Prof. A. Goswami**, Head, RCD, BARC for giving me the opportunity to carry out my research work and providing me all the infrastructure and access to required facilities during the course of this research. I also thank **Prof. Goswami** for being the chairman of my doctoral committee. His constructive suggestions, comments and moral help are gratefully acknowledged. I also thank **Prof. V.K. Manchanda,** Ex-Head, RCD, BARC for his support and encouragement.*

*Special thanks are due, to **Prof. B.S. Tomar**, Associate Director RC&I Group & Head RACD, BARC and Dean, Academic Chemical Sciences, **Homi Bhabha National Institute (HBNI)** for his valuable suggestions as a member of my doctoral committee and an advisor during my training school days. I sincerely thank **Prof. R. Mukhopadhyay** Ex-Head, SSPD, BARC for being a doctoral committee member and also for his valuable suggestions which helped in improving the quality of this research work.*

*It has been a great privilege to have valuable discussions with **Dr. (Mrs.) S. Sodaye, Dr. Rahul Tripathi, Dr. K. Sudarshan, Dr. D. Dutta, Dr. S.K. Sharma**, **Dr. (Ms.) P. Maheshwari** and **Dr. S.K. Mukherjee** of NCS, RCD. I also thank **Dr. S.K. Mukerjee**, Head, PDD, **Dr. S. Santra** and **Dr. P.C. Rout**, NPD, **Dr. R.V. Pai**, and **Mr. T.V. Vittal Rao**, FCD, **Dr. C.P. Kaushik**, **Dr. R.K. Mishra**, WMD and **Dr. T.S.R.Ch. Murthy**, MPD BARC for their help during this work.*

*I sincerely thank **Dr. K.L. Ramkumar**, Director, RC&I Group, BARC for the support and encouragement. I acknowledge **Dr. Swapan K. Ghosh,** former Dean Academic, Chemical Sciences, **HBNI**, for his whole hearted help and constant support from the very first day in BARC. I am thankful to **HBNI, Department of Atomic Energy** for providing financial*

support during the course of this research work. I thank all administrative staff of HBNI, RCD and RC&I Group for their help.

I am indeed thankful to ***Dr. P. Singh****, Head, IADD,* ***Mr. S.K. Gupta****,* ***Mr. A. Agarwal****, and operational staff members of FOTIA, IADD, BARC, for their help during experiments.Thanks are also due to staff members of accelerator facilities at IOP and TIFR.*

I feel extremely fortunate to have ***Dr. K.B. Dasari****,* ***Dr. Amol D. Shinde, Dr. Pushkar N. Patil, Mr. Prashant Gaikwad*** *and* ***Dr. Rakesh N. Shinde*** *as my lab mates. Their kind cooperation, friendly company, suggestions and invaluable help during my research work has provided a stimulating and friendly environment to learn and grow.*

I would like to place my special thanks ***Dr. A.V.R. Reddy****, Head, ACD, BARC and* ***Dr. Tulsi Mukherjee,*** *Ex-Director Chemistry Group, BARC who have always lent their helping hand and constant encouragement. My special thanks and gratitude are due to* ***Dr. S. Jeykumar****, RACD and (late)* ***Dr. P.N. Pathak****, RCD, BARC for encouraging me during my PhD work. I would like to thank my close friends at BARC* ***Dr. R.K. Singal****,* ***Dr. K.K. Swain, Mr. K.Venkatesh, Mr. Praveen K. Verma, Mr. Adish Tyagi, Mr. Deepak Rawat, Mr. Ashwani Kumar*** *and* ***Ms. Diksha*** *for their help and encouragement.*

I am thankful to ***Shri Krishan Chand Katoch*** *and* ***Shri Rajendar Singh Bedi*** *for standing by my side not as my school teachers but as real Guru for enlightening my path and making me self aware. I gratefully acknowledge my (late)* ***grandparents****,* ***father****,* ***mother****,* ***sister (MANDY)*** *and* ***brothers (MARK, NIKKA and MIKKA)*** *for their love, care, moral support and encouragement as well as for being a ray of hope and standing by my side as my biggest strength. Last but not the least I thank* ***ADI*** *for making my life so special and for being with me always. Finally, I would like to thank one and all who have contributed directly or indirectly for the successful realization of this thesis.*

SUMIT CHHILLAR

CONTENTS

Synopsis

Homi Bhabha National Institute

Ph. D. PROGRAMME

1.	**Name of Student**	**Sumit Chhillar**
2.	**Name of the Constituent Institution**	Bhabha Atomic Research Centre
3.	**Enrolment Number**	CHEM01200904013
4.	**Title of the Thesis**	Development and Applications of Particle Induced Gamma-ray Emission Methods for Low Z Elements
5.	**Board of Studies**	Chemical Sciences

Chemical characterization of materials is the most important step under chemical quality control (CQC) exercise. CQC helps in ensuring the quality of the fabricated material with respect to the required chemical specifications. CQC involves quantitative and qualitative analysis of major, minor and trace elements present in the finished product. Conventional wet chemical as well as spectroscopic methods are routinely used for chemical analyses. Though these techniques are sensitive and give high quality results at low concentration levels but they are destructive methods requiring tedious sample preparation procedure and are not free from reagent blank corrections. For solid samples with complex matrices like ceramics and glass samples, non-destructive as well as radio-analytical methods like ED-XRF, neutron activation analysis (NAA), Prompt gamma ray NAA (PGNAA) and ion beam analysis (IBA) like particle induced X-ray emission (PIXE) and particle induced gamma-ray emission (PIGE) are preferred. These techniques are capable of simultaneous multi-element determination from major to trace element concentration determination without any spectral interference. Most of the techniques give results of medium to high Z elements. There are a few methods which are capable of determining low Z elements in complex matrices non-destructively. Between PGNAA and PIGE, PIGE is capable of determining Li to S using proton beam ($\geq$2 MeV). In view of these aspects, present thesis work is focused for developing PIGE methods for quantification of low Z elements starting from Li using low and medium energy proton beam an applying them to various solid samples relevant to nuclear technology for determination of low Z elements (F, Li, Si, Al, Na and B) as well as boron isotopic composition in boron based neutron absorbers. An *in situ* current normalized method has been developed and used in addition to the current measurement by RBS method using Au foil or from the target with graphite as matrix,. In this method an element, like F or Li is mixed with the samples and their gamma-rays are used to correct for variation in the total number of incident particle from sample to sample. PIGE

methods were applied for analysis of barium borosilicate glass, lithium based ceramics (like Li doped neodymium dititanate and lithium titanate), boron based compounds (like boron carbide, boric acid, carborane, borazine) and several reference materials. The thesis is divided into six chapters whose details are briefly given below:

Chapter 1: This chapter gives introduction and motivation for the present studies. One of the important aspects of chemical characterization of a material is determination of its composition. Wet chemical methods, used for this purpose, consists of broad range of techniques like AAS, AES, ICP-OES, photometry, various mass spectrometric techniques, and conventional analytical techniques. However, for many types of samples, like glass, ceramics etc. these methods would time consuming. On the other hand, most of the nuclear/ radio analytical techniques such as PIGE, PIXE, NRA, NAA, PGNAA and XRF are non-destructive in nature and involve minimal sample preparation. Nuclear analytical methods utilize the properties of nucleus which makes them isotope specific, selective and sensitive towards a particular analyte. In the present work, PIGE method has been utilized for concentration determination and RBS method was used current measurement of proton beam.

In this chapter, basic principles of PIGE and RBS have been described. PIGE involves on-line measurement of characteristic γ-rays emitted from different nuclear reactions like (p, p'γ), (p,γ), (p, nγ) and (p,αγ). Sippel and Glover in 1960 showed that PIGE with protons could be used for the determination of Mg and F in geological samples [**1**]. Pierce et al. showed that deuterons could be used to determine carbon and Pierce et al. used 4 MeV protons to determine the amount of Si in several kinds of steel [**2,3**]. PIGE has been standardized and applied for the simultaneous determination of low Z elements [**4**] PIGE method has been applied to analyze biological samples, archaeological samples, and environmental samples [**5-7**].

In the present work, *in situ* PIGE methodology has been developed and applied to various materials for quantification of low Z elements (like Li, B, F, Na, Al and Si) in barium borosilicate glass (BaBSG), lithium in lithium based ceramics like lithium doped neodymium dititanae (NTO) and lithium titanate and Li, Ti and O in lithium titanate. Isotope specific nature of PIGE was exploited to determine isotopic composition of boron ($^{10}B/^{11}B$ atom ratio) along with total boron content in boron based enriched and natural samples. In order to validate the PIGE method, reference materials from IAEA and NIST were analyzed. The scope of thesis is given in this Chapter.

Chapter 2: Experimental details are given in this chapter. Different samples of borosilicate glass, lithium doped neodymium dititanate, lithium titanate reference materials and enriched and natural boron based compounds and samples have been analyzed. The samples analyzed were solid and were in powdered form. No special chemical treatment was given to any sample before experiment. The powdered samples were mixed homogenously with cellulose or graphite, as matrix or binder. These mixtures were pelletized using hydraulic press. The beam current variations were normalized either by RBS method or directly from the sample (here graphite was used as matrix). *In situ* approach was also developed for normalizing the beam current variations. In this approach an element of high sensitivity towards PIGE like Li, F or Al, not present in the sample was mixed in the sample and matrix (cellulose or graphite). The sample and standards were irradiated at folded tandem ion accelerator (FOTIA), BARC, IOP, Bhubaneswar and at pelletron facility of TIFR-BARC at TIFR, Mumbai. The targets were irradiated using 4MeV/8MeV proton beam, the prompt gamma-rays were measured using high resolution gamma-ray spectrometry using HPGe detector coupled with 8k PC based multi-channel analyzer (MCA). The elemental concentrations were determined using relative method. The sensitivity (count rate per unit concentration) of *in situ* current

normalizer, which would vary depending on the variation in beam current, was used to normalize the count rate of isotope of interest from the target.

Chapter 3: Barium borosilicate glass (BaBSG) is being extensively studied as a vitrification of high level radioactive liquid waste (HLW) generated from spent nuclear fuel. Various BaBSG are being prepared with varying amount F (0.1-4 wt%) and subjected vitrification at high temperature. Therefore it is important to know the extent of F retention/loss in the BaBSG samples. PIGE method was used to determine the F content in different glass samples. The detection limit obtained for F was 19 mg kg^{-1}. In different samples the F concentrations obtained were in the range of 0.4-3.8 wt%. The uncertainties in the results were in the range of ±1-4%.

Different physico-chemical properties (like pouring temperature, melting point and refractive index) of glass depend on concentration of different low Z elements (like Li, B, Na, Al and Si). In order to have better understanding of properties of said glass as well as to optimize its composition for specific purposes, it is important to quantify the composition of glass. PIGE method was utilized for simultaneous determination of Si, Al, Na, B and F. For method validation, reference materials (RMs) from IAEA and standard reference materials (SRMs) from NIST have been analyzed to determine concentrations of Na, Al and Si.

Chapter 4: This chapter describes the analysis of lithium based ceramics, namely, lithium doped neodymium dititanate and lithium titanate. Neodymium dititanate is a high temperature ferroelectric material. Its ferroelectric properties can be tailored by doping it with lithium. In order to correlate the ferroelectric properties of this ceramic with Li ion concentration, it was important to determine the concentration of lithium in as prepared and heat treated samples. An *in situ* PIGE method, using F as *in situ* current normalizer, was applied and Li

concentration was determined in three as prepared and heat treated samples of lithium doped neodymium dititanate. The Li concentrations obtained were in the range of 0.30-0.85wt%. The Li loss was in the range of 5-37%. The uncertainties in the results were in the range of 1.5-3.3%. The detection limit of Li was 7 mg kg^{-1}.

Lithium titanate is a proposed tritium breeder material in D-T based fusion reactor. An i*n situ* PIGE method using 4 MeV proton beam from FOTIA, BARC with F as *in situ* current normalizer has been used for non-destructive quantification of Li in Li_2TiO_3 pebbles synthesized by sol-gel method. Ti quantification was carried out by INAA using pneumatic carrier facility (PCF) of DHRUVA reactor at BARC. Li/Ti mole ratio and Li concentrations were used to confirm the composition of sol-gel synthesized finish product. The Li concentrations obtained were in the range of 11.20-12.68 wt% of lithium. The uncertainties in the results were less than 2% where as the uncertainties in the results of Ti were in the range of 2-3%. It was necessary to determine Li, Ti and O concentrations in this material for complete compositional analysis, and for this PIGE method using 8MeV proton beam from BARC-TIFR pelletron facility was standardized and applied. The Li, Ti and O concentrations were in the range of 12.0-12.6wt% of Li, 43.7-43.9wt% of Ti and 43.5-44.3 wt% of O, respectively.

Chapter 5: Boron finds applications in many fields including nuclear industry. Due to its high neutron absorption cross-section (3837 barn for ^{10}B), it is used in reactors as control shutoff material, burnable poison and neutron shielding material. PIGE method, using F and Al foil as *in situ* current normalizers, was used for non-destructive determination of isotopic composition of boron ($^{10}B/^{11}B$ atom ratio) and total boron content. Various natural and enriched boron samples and compounds including boron carbide, boric acid, carborane, borazine and borosilicate glass were analyzed. The $^{10}B/^{11}B$ atom ratios obtained in these

samples were found in the range of 0.247-2.032 that corresponds to 19.8-67.0 atom% with respect to ^{10}B. Total boron concentrations were also obtained which were in the range of 5.32-78.29 wt% of boron. The uncertainties in the results were less than ±2%. The ratio of $^{10}B/^{11}B$ in various targets and hence the enrichment factor with respect to ^{10}B in the range of 20–67%.

Chapter 6: This chapter gives conclusions of the present study as well as future perspectives of PIGE method. In summary, PIGE methodologies have been optimized for non-destructive determination of low Z elements like B, Li, F, Na, Al and Si in BaBSG, Si, Al and Na concentrations in RMs, Li in lithium doped neodymium dititanate and lithium titanate samples and simultaneous quantification of Li, Ti and O in lithium titanate samples using 8MeV proton beam. Simultaneous determination of isotopic composition (^{10}B and ^{11}B) and total boron concentrations in various boron based natural and enriched samples including B_4C could be carried out by PIGE. Detection limits of F, Li and B obtained are 19, 7 and 8 mg kg^{-1} respectively, using 4MeV proton beam, whereas detection limits for Li, Ti and O were 0.62 mg kg^{-1} 0.23 mg kg^{-1} 5.0 mg kg^{-1} respectively using 8MeV proton beam. PIGE methods optimized are unique for these samples compared wet-chemical and other radioanalytical methods particularly for Li, F, B and Si. The work carried out resulted in three international journal publications, more than 10 conference presentations and three manuscripts have been submitted to journal for favor of publications.

Utilization of medium energy (8 MeV) proton beam is advantageous for simultaneous determination of less sensitive low Z elements like C, N, O, P, S, K, Cl and Ca in addition to Li, B, Be, F, Na, Al and Si. In addition to boron isotopic composition, isotopic composition of Li ($^{6}Li/^{7}Li$) is a challenging work. Future scope includes quantification of Li in Pb-Li-alloy, C, N and O in steel and stainless steel, Be in BeO and applications of PIGE for low Z elements in U-Th based ceramics.

References

1. R.F. Sippel, E.D. Glover, **1960**, *Nucl. Instrum. Meth.*, 9, p.37–48.
2. T.B. Pierce, P.F. Peck, W.M. Henry, **1965**, *Analyst*, 90, p.339–345.
3. T.B. Pierce, P.F. Peck, D.R.A. Cuff, **1967**, *Anal. Chim. Acta*, 39, p.433–436.
4. R.B. Boulton, G.T. Ewan, **1977**, *Anal. Chem.*, 49, p.1297–1304.
5. Gene S. Hall, Eliahu Navon, **1986**, *Nucl. Instrum. Meth. B*, 15, p.629-631.
6. A. Climent-Font, A. Munoz-Martina, M.D. Ynsaa, A. Zucchiatti, **2008**, *Nucl. Instrum. Meth. B*, 266, p.640–648.
7. G. Robaye, J.M. Delbrouck-Habaru, I. Roelandts, G. Weber, L. Girard-Reydet, J. Morelli and J.P. Quisefit, **1985**, *Nucl. Instrum. Meth. B*, 6, p.558-561.

List of Figures

List of Tables

Chapter 1

Introduction

1.1 Material characterization

Characterization of materials refers to the broad and general process by which the material structure and its properties are probed and measured. Applications of materials are dependent on its structure and properties which are directly related to their composition. Thus, characterization of a material is important to assess whether the material fabricated or procured conforms to the required specifications or not. It is also an important aspect in the field of material science, which helps in ascertaining the scientific understanding of engineered materials. The techniques utilized for material characterization (like compositional and microscopic characterization studies) are dependent on the nature of the material being investigated [**1,2**]. **Fig. 1.1** gives in brief the most common techniques used for material characterization. Various techniques are being used for characterization of materials and a few of which are shown under composition sub-heading of **Fig.1.1**. Material characterization generally involves morphological and surface studies along with measurement of physical properties (like melting point, boiling point, refractive index) and chemical compositional analysis. To deal with modern age advanced materials, new techniques and methodologies are constantly emerging. With the advancement of technology, materials scientists are able to probe the actual structure of materials in two-dimensional/three-dimensional with proper positions of atoms in a solid.

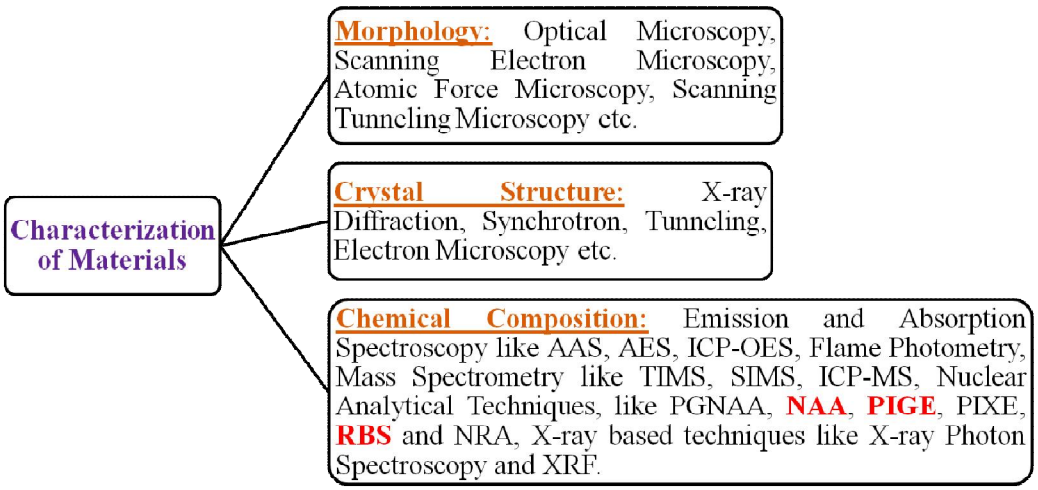

Fig.1.1: Different techniques used for characterization of materials.

Among various material characterization techniques, chemical characterization is the most important aspect for certifying material acceptability/suitability for the specific purpose. To get quantitative information of elements at major to ultra trace concentrations, though various techniques are available, there is always scope for improving the sensitivities and detection limits of elements of interest.

1.2 Chemical characterization of materials

Chemical characterization is the first and most important step under chemical quality control (CQC) exercise. Different definitions exist for 'chemical characterization of materials', but most appropriately stated one is the application of a process or series of processes for quantification of a substance, the component of a solution or mixture, or to resolve the structures of a crystal or material. It means that the scope of chemical characterization is very wide and broad and covers a wide range of chemical and instrumental techniques. With the advancement of technology and increase demand for improved material with better quality, the analytical chemist has a greater role to play. Manufacturing industries are dependent upon qualitative and quantitative analysis of chemicals to ensure that the required material or finished product meets the interest of consumer satisfactorily. Chemical quality control (CQC) helps in ensuring the quality of the fabricated material with respect to the required chemical specifications. CQC involves compositional analysis as well as trace impurity determination present in the raw materials as well as in the finished products. The raw materials are examined to ensure absence of unwanted substance that may hinder the manufacturing process or appear as impurity in the final product. Quantitative analysis of raw materials helps in establishing the proportion of essential constituents. The final product is subjected to quality control (QC) exercise to ensure the presence of its essential components in specified range of composition and impurities do not exceeds the upper limit of

specification. CQC exercise also helps in managing the risk factors associated with the fabricated material.

For CQC, different analytical methods are being used for quantitative analysis of raw as well as finished products. The analysis is done through application of reference analytical techniques to get information on major to ultra trace elemental concentrations in materials. Sometimes two or more techniques may be hyphenated to obtain required information of a material of interest.

1.3 Analytical techniques for chemical characterization

Different analytical techniques which can be used for CQC of materials are described here briefly. Analytical techniques are broadly classified as: (i) classical wet chemical, (ii) electro-analytical, (iii) chromatographic, (iv) atomic and mass spectroscopic and (iv) radio or nuclear analytical techniques **[3]**.

Classical wet-chemical techniques include gravimetry and titrimetry, electro-analytical techniques include potentiometry, voltammetry, amperommetry, as well as coulometry and chromatographic techniques that include ion-exchange and liquid chromatography. Methods based on absorption of radiations include atomic absorption spectroscopy (AAS), inductively coupled plasma AAS (ICP-AAS), graphite furnace AAS (GF-AAS), and, methods involving emission of radiations includes flame emission spectroscopy (FES), atomic emission spectroscopy (AES), inductively coupled plasma atomic/optical emission spectroscopy (ICP-AES or ICP-OES) as well as directly coupled plasma OES (DCP-OES). Colorimetry or visible spectroscopy which involves visible radiations is used for determination of cations (like ammonia, arsenic, boron, chromium, titanium and tungsten), anions (chloride, phosphate, sulphate) and organic compounds like primary amines and anionic detergents. The technique which utilizes the measurement of mass to charge ratio as final signal for both

qualitative as well as quantitative comes under mass spectrometric (MS) techniques. Various mass spectrometric techniques are thermal ionization mass spectrometry (TIMS), secondary ion mass spectrometry (SIMS), inductively coupled mass spectrometry (ICP-MS) and gas chromatographic mass spectrometry (GC-MS). It can be used for the analysis of gases, petroleum products, semiconductors for impurities and determination of isotopic composition and particularly useful in establishing the structure of organic compounds.

Radio and nuclear analytical techniques (NATs) utilize gamma-rays, X-rays and energetic particles emitted during nuclear or atomic processes for analytical information. These techniques are element/isotope specific and can be used for non-destructive analysis of materials. Radio-analytical techniques are carried out by alpha, X-ray and gamma-ray spectrometry as well as detection of energetic particles. Among the X-ray based techniques, Wave length dispersive XRF (WDXRF), energy dispersive XRF (EDXRF) and particle induced X-ray emission (PIXE) are used for non-destructive determination of concentrations of elements.

1.3.1 Nuclear analytical techniques (NATs)

Nuclear analytical techniques (NATs) namely activation analysis as well as ion beam analysis (IBA) is carried out by neutron, charge particle or photon as projectiles. The techniques are neutron activation analysis (NAA), prompt gamma-ray NAA (PGNAA), charge particle activation analysis (CPAA), photon activation analysis (PAA) and IBA techniques like particle induced gamma-ray emission (PIGE), Rutherford backscattering spectroscopy (RBS) and nuclear reaction analysis (NRA). Sensitivities that could be achieved by some NATs are comparable or better to conventional techniques like AAS, ICP-OES and ICP-MS. NATs are multi-elemental in nature ranging from H to U and are used for simultaneous determination of elements non-destructively. Depending on sample matrix and

elements of interest, instrumental (direct analysis) or chemical (involved sample dissolution) nuclear analytical methods are used. NATs based on measuring the delayed gamma-rays emitted from neutron activated products include instrumental neutron activation analysis (INAA), pre-concentration NAA (PNAA) and radiochemical NAA (RNAA). RNAA and PNAA are destructive methods, unlike INAA, but they yield precise and accurate results at low concentration levels. In prompt gamma-ray NAA (PGNAA) method, which is an online measurement technique, sample is irradiated with a flux of neutrons and prompt gamma-rays are measured using high resolution gamma-ray spectrometry with the help of HPGe detector system. PGNAA is useful for low Z elements (like H and B) as well as elements whose isotopes have high (n,γ) cross-sections. PGNAA is truly a non-destructive method and thus analysis of complex matrix samples like, alloys and ceramics as well as geological and archaeological samples can be analyzed.

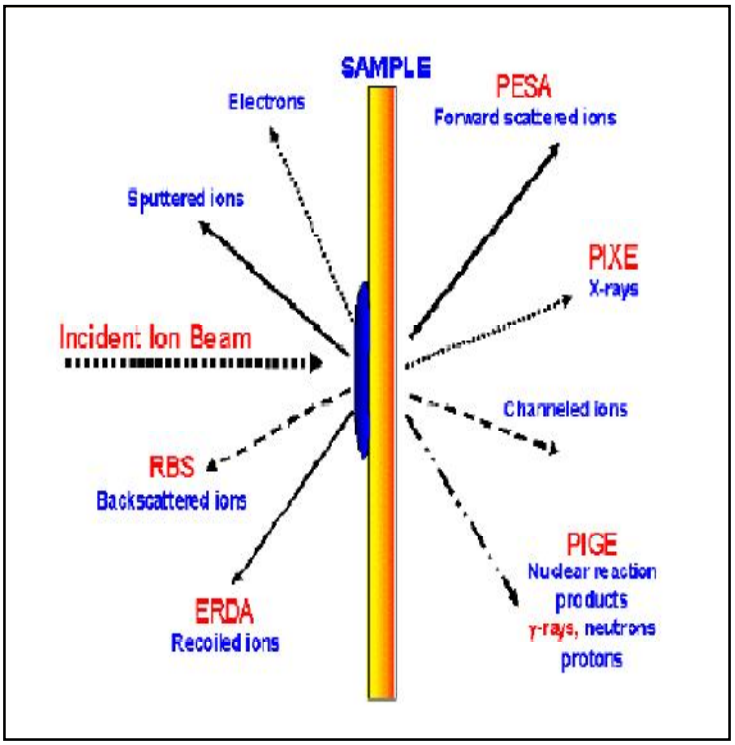

Fig. 1.2: Schematic principle of ion beam analysis techniques *(Source: http://www2.ulg.ac.be/ipne/ipne/iba/IBA.html)*

Fig. 1.2 gives the principles of different IBA techniques using energetic charge particles like proton, deuteron, alpha and other higher Z charge particle. It includes a wide range of techniques that mainly includes PIGE, NRA, RBS, channeling, elastic (non-Rutherford) backscattering spectrometry (EBS) and elastic recoil detection analysis (ERDA). Though PIXE is included in IBA, this is not a nuclear analytical technique as this involves X-ray measurements. The choice of IBA techniques depend on the sample/material which is under investigation. IBA techniques are based on phenomena of nuclear reactions caused due to interaction of energetic charged particles with the elements or isotopes of interest in the sample/material. The interaction leads to many processes like scattering of beam particles, nuclear reactions, emission of gamma-rays and X-rays and channeled ions from the target.

Depending on the interaction and the process of interest the IBA techniques have been classified as follows:

- **Particle induced gamma-ray emission (PIGE):** It involves detection and measurement of prompt gamma-rays when energetic charged particles (p, d and α) are bombarded on the target. This technique is sensitive for low Z elements from Li to S using low energy proton beam. It is also useful for medium Z elements above S and also for C, N and O using medium energy proton beam (7-10 MeV).
- **Nuclear reaction analysis (NRA):** The energetic charged particle beam on hitting the target initiates particular nuclear reaction/phenomena with specific isotope of an element present in the sample as analyte. The emitted radiation/particle with a specific energy is characteristic signature of a particular nuclear process. The measurement of the intensity of the emitted radiation/particle enables depth profiling and determines the concentration of the particular isotope of interest in the target. Using NRA, depth profiling of low Z elements in high Z matrix is feasible using energetic beams of ^{3}He, ^{7}Li, ^{15}N and ^{19}F.

- **Rutherford backscattering (RBS):** It involves measurement of backscattered charge particles (projectiles) from the target using surface barrier detectors. Generally, it is used for quantification as well as elemental depth profiling of heavy elements in a matrix of light elements. RBS is a conventional method for beam current measurement using thin foils of high Z metals like Au, Ag and W for PIGE and PIXE experiments.
- **Elastic (non-Rutherford) resonance scattering (ERS):** The compound nucleus in excited state is formed when the energetic incident projectile penetrates the Coulomb barrier of the target. The reaction probability or cross-section of nuclear reaction is considerably high if the incident projectile energy matches with the excited levels of compound nucleus. The excited compound nucleus may decay by either re-emission of the incident particle or emission of gamma-rays. If it decays by re-emission of incident particle then the phenomena is known as elastic resonance scattering. This technique is used for analyzing low Z elements (like ^{4}He-^{16}O).
- **Elastic recoil detection (ERD):** This IBA method is based on the detection and measurement of recoiled particles from the target after collision with the energetic heavy incident ions. This technique is highly sensitive for light elements (like H, Li, O and F) in a matrix of heavy elements.
- **Particle induced X-ray emission (PIXE):** It involves the detection and measurement of radiations (X-rays) induced by the bombardment of beam of energetic charged particles (like proton) on the target. The emitted X-rays are characteristic feature of a particular atom. PIXE is useful for medium (from Si) and high Z elements up to U.

1.4 Ion beam analysis using particle accelerators

Particle accelerators have been designed mainly as experimental tool for nuclear physics research. The development of accelerators has started through early Cockroft-Walton

accelerators to linear accelerators, cyclotrons and synchrotrons. These accelerators can generate the particles of energies from a few hundred eV to tera eV (TeV) needed in search for the sub-nucleonic particles. In 1960s use of focused MeV ion beams for material characterization and analysis arose when Van de Graff accelerators were found inadequate to generate high energy charge particles for nuclear physics experiments **[4]**. With the advancement of science in various fields' especially material science and microelectronics, there is a need for characterization and modifications of the materials. Therefore, it was necessary to develop new methodologies for characterization and investigation of materials in non-invasive manner for their compositional characterization, elemental depth profiling in the near surface region or layer of solids as well as understanding the lattice defects.

IBA is an important family of modern NATs for obtaining both qualitative as well as quantitative information on surface and near surface region using various ions in the range from few eV to MeV. IBA techniques help in studying the layer by layer structure of the material ranging from top of the surface to few microns depending on the beam energy. Collectively these techniques are very sensitive to almost all the elements of the periodic table and some of the techniques have the ability to determine even very small amounts of isotopes of an element present in the sample. Their non-destructive nature and ability to detect elements/isotopes in the sub-monolayer range makes them the method of choice for studying thin films or layers (nm thickness) on various materials and compositional characterization of ceramic and glasses, where wet chemical as well as spectroscopic methods fail to give the desired results. For IBA studies, it is necessary to have nuclear/atomic reactions using low to medium energy charged particles, knowledge of nuclear data about the range of projectile in various materials, stopping power offered by material to projectile and cross-section or yield.

In the present thesis the development and application work on determination of low Z

elements in materials relevant to nuclear technology was carried out by *in situ* current normalized PIGE methods using proton beams from tandem accelerators. The following section provides the principle, capability, methods and literature survey including applications of PIGE. Additionally, principle and capability of INAA is also given.

1.5 Introduction to Particle Induced Gamma-ray Emission (PIGE)

PIGE is an isotope specific nuclear analytical technique for the determination of low Z elements (usually $3 \leq Z \leq 16$) in different type of solid materials. Since characteristic prompt gamma-rays are measured, it experiences less matrix effect as compared to PIXE. These reactions used in PIGE are induced by energetic charged particle beams (e.g. protons, deuteron and alpha) from accelerators. For determination of elemental concentrations from gamma-ray spectra, it is important to have the knowledge of parameters like gamma-ray yields or cross-sections, stopping power of material and beam current.

In 1960 Sippel and Glover, **[5]** showed for the first time that gamma-rays emitted by using energetic protons (of MeV energy) could be used for determining the concentrations of Mg and F in geological samples. Pierce et al **[6]** used energetic deuteron beam for determination of carbon in steel samples. In 1967, Pierce et al. **[7]** quantified Si in different kind of steels by using 4 MeV proton beam. Advent of Ge based detectors in 1970 onwards, revolutionized the field of gamma-ray spectrometry. The Ge based detectors (Ge(Li) and HPGe) have much better energy resolution than NaI(Tl) and makes PIGE to quantify multi-elements simultaneously in a sample. Since then studies have been carried out with both light (like p and d) and heavy (like ^{3}H, α and ^{3}He) energetic particle beams **[8-11]**.

Though PIGE is unique in its applications for low Z elements, it is not fully exploited like other IBA techniques namely RBS and PIXE. PIGE has advantages over PIXE, as it can be used for determining low Z elements which are difficult to analyze by PIXE and other

analytical techniques. The gamma-ray lines of two neighboring elements or isotopes of same element are totally different, which is added advantage not to have gamma ray interference / peak-overlapping.

1.6 Principle of PIGE

Particle induced gamma-ray emission (PIGE) is an isotope specific nuclear analytical technique capable of determining low to medium Z elements mainly in solid samples using low to medium energy charge particles. After the nuclear reaction, the nuclei of the sample remain in the excited states and can decay either by emitting the charged particles (like p and α), neutrons or gamma-rays. The proton induced reactions involve measurement of prompt gamma rays from inelastic-scattering (p,p'γ) or from nuclear reactions like (p,αγ), (p,nγ) and (p, γ). Beam of deuteron and alpha particles can also be used in PIGE for specific elements including C, N and O **[6]**. The reactions used commonly in these cases are (d,pγ), (d,nγ) and (α,nγ). At relatively low beam energies (few MeV), nuclear reactions like (p,p'γ) and (p,αγ) show resonant reaction, whereas at higher beam energy, the probability of (p,γ) reaction decreases. The gamma-rays thus emitted are characteristic signature of the isotopes of elements. Thus PIGE can be advantageously utilized for isotopic composition of elements namely B (^{10}B/^{11}B) and Li (^{6}Li/^{7}Li). **Fig.1.3**. shows the schematic diagram of PIGE and PIXE using energetic proton beam. By measuring the intensity of a gamma-ray peak of interest from the target, one can identify and quantify the isotope of element(s) of interest present in the sample. For a nuclear reaction to occur between a beam particle and a sample nucleus, the beam particle energy must exceed the Coulomb barrier (E_c). The barrier energy (in MeV) can be estimated using following equation:

$$E_c = 1.44 \frac{Z_1 Z_2}{R} \, MeV \qquad (1.1)$$

where

where Z_1 and Z_2 are the number of protons of projectile and the target nuclei, respectively. R

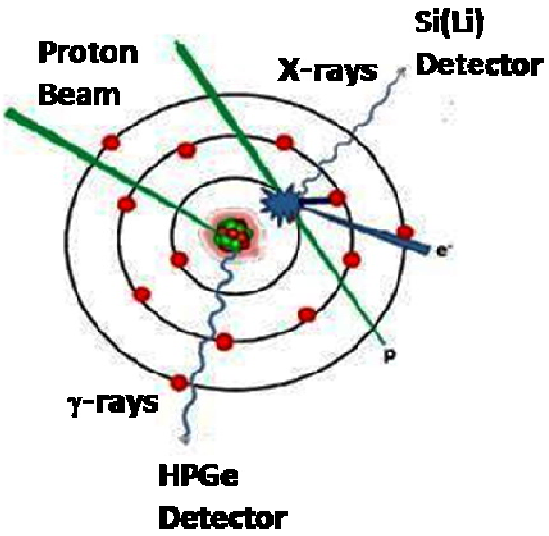

Fig. 1.3: Schematic diagram showing PIGE and PIXE induced by proton beam.

(in fm) represent the sum of respective radii of projectile and target nuclei; with A_1 and A_2 are the respective mass numbers. Above approximation is based on the idea that strong nuclear forces are short range (~1 fm) forces. If the energy of incident projectile beam is < E_c, the beam particles will be deflected by the target nucleus. In this case gamma-rays will be produced by process known as Coulomb excitation of the target nucleus. If the beam energy is greater than E_c other reactions will also occur which encompasses inelastic scattering, capture reactions and particle transfer. If the projectile used is proton, then above reactions can be represented as: (p,p'γ), (p,γ), (p,αγ) and (p,nγ) respectively. The most commonly used nuclear process for studying PIGE is via compound nucleus formation reaction, shown schematically as in equation given below:

$$a + A \longrightarrow C^* \longrightarrow B + b \qquad (1.2)$$

here ‘a’ representing the energetic particle beam, ‘A’ the target nucleus, ‘C*’, the compound nucleus (CN) in excited state. The excited CN may decays either by emitting the projectile, ‘a’ as ejectile or some other ejectile ‘b’ and gives the product nucleus either ‘A’ or ‘B’ which may be in excited state ‘B*’ or may be in ground state. The CN nucleus may decay by emitting gamma-rays or particles along with daughter nuclei ‘B*’which can decay to ground state by emitting gamma-rays or particles. One can use either of the gamma-rays for determining concentration of ‘A’ in the sample. **Fig. 1.4** explains the schematics of the above discussion **[12]**. The CN model is based on the assumption that the decay probability of CN into any specific set of final products is independent of path of formation of CN **[13]**. The decay mode of the CN depends on its energy. If the excitation energy (E_x) of CN is greater than the particle’s binding energy, the CN will decay via the particle emission channel mode. The excitation energy of CN (C*) can be calculated using equations:

$$E_x = Q + \frac{E_p * m_A}{m_a + m_A} \qquad (1.3)$$

$$\text{where } Q = [m_A + m_a - m_C)]c^2 \qquad (1.4)$$

where Q is the reaction Q value (in MeV). For an exothermic nuclear reactions Q is positive i.e. mass is converted into energy and vice-versa for an endothermic nuclear reaction. The kinetic energy, E_{KE}, of the center-of-mass can be calculated by the following equation:

$$E_{KE} = \frac{E_p * m_A}{m_A + m_a} \qquad (1.5)$$

This energy appears as kinetic energy of the recoiling CN completely. If gamma-rays are emitted during the recoiling of CN i.e. if the life time of the nuclear states involved in the decay process of the CN is shorter than slowing down time of the recoiling CN in the sample then the emitted in flight gamma-rays will show a shift and Doppler broadening in energy. The measured gamma-ray energy is then given by the following equation:

The gamma-ray yield is another important factor in PIGE as it is directly related to the reaction cross-section and emission probabilities and hence the sensitivity of the method

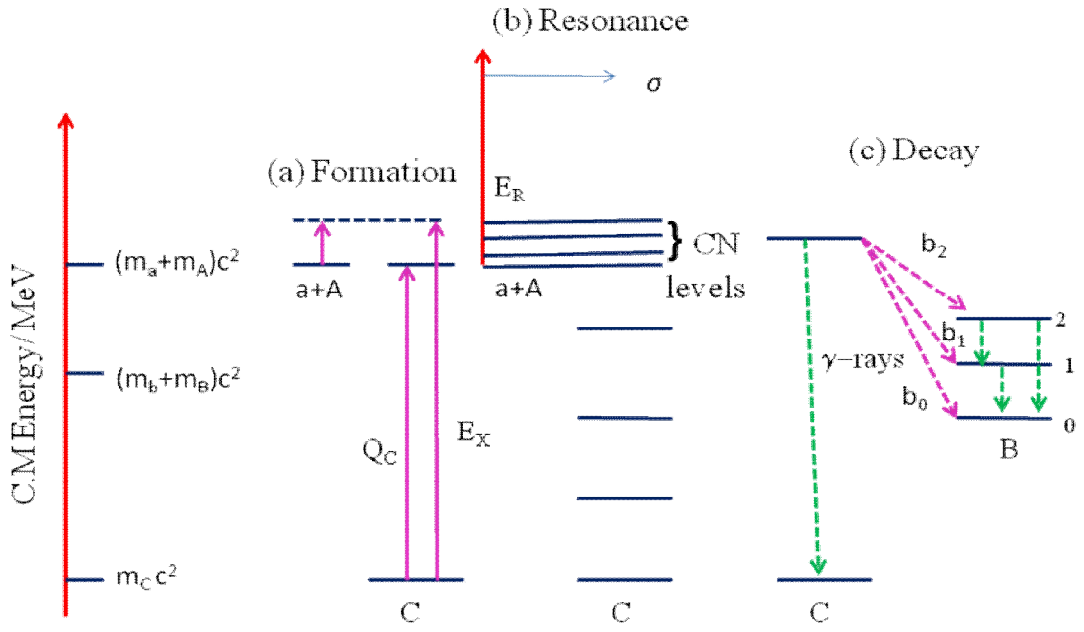

Fig. 1.4: (a) Formation of CN 'C*' in an excited state (CN level).

(b) Decay of CN either by γ-rays or by particle emission ('a' or 'b').

(c) Decay of CN by particle emission form the reaction product 'A*' or 'B*' in excited states or in the ground state **[12]**.

towards a particular isotope of an element. The reaction probability is expressed by the reaction cross-sections, which represents an imaginary surface of the nucleus through which the projectile has to interact and penetrate for inducing a particular nuclear reaction.

For practical applications, knowledge of reaction cross-section values is very important as it helps in determining the sensitivity of the process. Many other resonant or non-resonant nuclear reactions may yields gamma-rays like inelastic-scattering (p,p'γ) which can be used

for elemental analysis using protons as projectiles. Beam of deuteron and alpha particles can also be used in PIGE for specific elements including C, N and O **[6,14]**. The reactions used commonly in these cases are (d,pγ), (d,nγ) and (α,nγ). At relatively low beam energies, in the few MeV region, the (p,p'γ) and the (p,αγ) reactions also show resonant structures. In the cases where the cross-section does not show resonant behavior, but varies only slowly with beam energy, the cross-section can be taken to be constant or averaged over the relevant energy region. For non-resonant reactions the following expression (**Eq. 1.7**) can be used to obtain the gamma-ray yield $Y(E_0)$ when particle 'x' of incident energy 'E_0', hitting the target, containing an analyte of interests "A" of atomic mass M (in g mol^{-1}), concentration C_A and cross-section $\sigma_{(x,\gamma)}(E)$:

$$Y(E_0) = N_p \frac{C_A}{M} N_{Av} \varepsilon(E_\gamma) \frac{\Omega}{4\pi} \int_{E_0}^{E_f} \frac{\sigma_{x,y}(E)}{S(E)} dE \qquad (1.7)$$

here, N_p is the number of charge particles 'x' falling on the target and can be determined from the measured beam current and time for which the target is irradiated. N_{Av} is the Avogadro number, $\varepsilon(E_\gamma)$ is the detector efficiency for the gamma-ray of interest from the target and Ω is the solid angle of the detector (in steredians). The cross-section $\sigma_{(x,\gamma)}(E)$(cm^2) and the stopping power $S(E)$ (MeV g^{-1}cm^2) are integrated over the energy range from E_0 to E_f for thin target and $E_f = 0$ for thick target. The above equation can be used to evaluate the thick target gamma-ray yields (counts per unit of charge falling on the target and per unit of solid angle, count/(μC-Sr)) and can be obtained from **Eq. 1.7** by dividing out the N_p (expressed as charge) and Ω. The thick target gamma-ray yields, way to express the sensitivity of different elements towards PIGE, are presented in **Table 1** for different elements at different proton energies. Experimentally, the thick target pellet yield (Y_{Pel}) can be determined using following equation:

$$Y_{Pel} = \frac{Net\ Counts}{Charge\ (in\ C) \times 4\pi \times \varepsilon(E_\gamma)} \qquad (1.8)$$

$$\text{where,} \quad \varepsilon(E_\gamma) = \frac{\Omega_e(E_\gamma)}{4\pi}$$

To get isotopic yield (Y) of the element from the pellet yield (Y_{Pel}), the following expression (**Eq. 1.9**) is used:

$$\frac{Y}{Y_{Pel}} = \frac{100}{C_A \times \theta} \times \frac{S(E)_{Pel}}{S(E)_{Element}} \qquad (1.9)$$

The cross-sections and the stopping power [$S(E)$] of projectile 'x' slowed down in the sample have been reported in various publications for many projectiles, energies and stopping materials **[15,16]**. Care should be taken for self absorption of gamma-rays in thick targets, particularly when gamma-ray energies are low **[12]**.

The absolute reaction cross-sections for different isotopes of different elements and stopping powers for various matrices are not known. In order to overcome this, the measurements of internal or external standards are often compared with the measurement of the real sample. In the case of internal standard where elements are added, their concentrations and cross-sections must be known precisely. In the case of an external standard, a synthetic sample is prepared with exactly the similar composition as the sample of interest. It is convenient to add a standard element of high sensitivity and known concentration 'C_s'. When comparing the gamma-ray yields of element 'A' and standard 'S', parameters like solid angle, number of beam particles and stopping powers remain same. The unknown concentration C_A can easily be calculated by comparing measured gamma-ray yields of standard and sample (**Eq. 1.10**):

$$C_A = C_s \times \frac{Y_A \times I_A \times S_S}{Y_s \times I_S \times S_A} \qquad (1.10)$$

To make the method simple, thick targets in graphite or cellulose as major matrix (about 90% or more) are used for experiments where the stopping power ratio of sample to standard becomes unity (approx.). So above equation will further be simplified as:

$$C_A = C_s \times \frac{Y_A \times I_A}{Y_s \times I_S} \qquad (1.11)$$

In relative method by taking current normalized count rate (CPS_N), the concentration is calculated for identical experimental conditions of sample and standard by the following equation:

$$C_A = C_s \times \frac{CPS_{A,N}}{CPS_{S,N}} \qquad (1.12)$$

For thick targets the current measurements can be carried out either using conventional RBS method, charge measurement directly from the conducting target or by *in situ* current normalization methods using an externally added element in the target pellet (proposed method in this thesis), the details of which are discussed in **Chapter 2**.

1.7 Depth profiling using PIGE

PIGE can be used for depth profiling like NRA. A variety of charged particle induced resonance reactions **[17,18]** can be used for studying the depth profile of a particular analyte in a sample by tagging the gamma-ray emitted as a result of resonance reaction. The principle is based on the fact that as the beam particles move into the sample matrix, they slow down and when their energy matches with the resonance energy value of the reaction occurs. This is the principle behind NRA studies too. The depth Δx (cm) of the sample being analyzed, is a function of beam energy ΔE (keV). These two quantities are related via the stopping power S (keV cm^{-1}) by **Eq. 1.13**:

$$\Delta x = \frac{\Delta E}{S} \qquad (1.13)$$

1.8 Nuclear reactions and characteristic gamma-rays of low Z elements in PIGE

In PIGE, energetic beam (generally 2-9 MeV) of light particles (like protons, deuterons, tritons, ^{3}He and ^{4}He) is bombarded on the samples. The number of gamma-ray counts in a peak of a particular element corresponds to the concentration of the element in the sample. When an element has more than one isotope, gamma-rays can be produced in any of the isotopes and this will show up in the accompanying spectra as more lines belonging to one element but different isotopes. **Table 1** shows the list of some of the nuclear reactions induced by energetic proton beam in PIGE method **[19,20,37,43]**.

Table 1: Literature values of thick target gamma-ray yields of some of the PIGE reactions using different proton energies (2.4, 4, 7 and 9 MeV).

Element	Nuclear Reaction	E_γ	γ-ray yield (counts/μC-sr) at different proton energies			
			2.4 MeV	4 MeV	7 MeV	9 MeV
Li	^{7}Li(p,p′γ)^{7}Li	478	2.6×10^{7}	1.1×10^{8}	3.6×10^{8}	2.2×10^{9}
	^{7}Li(p,nγ)^{7}Be	429	-	3.3×10^{7}	4.3×10^{7}	2.2×10^{8}
	^{6}Li(p,γ)^{7}Be	429	-	1.1×10^{7}	-	-
Be	^{7}Be(p,αγ)^{6}Li	3526	2.5×10^{4}	2.5×10^{6}	2.0×10^{8}	1.9×10^{8}
	^{9}Be(p,γ)^{10}B	718	5.3×10^{3}	-	-	-
B	^{10}B(p,αγ)^{7}Be	429	3.5×10^{6}	1.1×10^{7}	-	-
	^{10}B(p,p′γ)^{10}B	718	1.2×10^{5}	3.0×10^{6}	1.2×10^{8}	1.5×10^{8}
	^{11}B(p,p′γ)^{11}B	2125	-	1.1×10^{6}	2.8×10^{8}	4.3×10^{8}
C	^{12}C(p,p′γ)^{12}C	4439	-	-	$7.5\text{x}10^{8}$	$2.9\text{x}10^{9}$
	^{13}C(p,p′γ)^{13}C	3089	-	4.1×10^{4}	-	-
N	^{14}N(p,p′γ)^{14}N	1635	-	-	1.3×10^{7}	3.2×10^{7}
	^{14}N(p,p′γ)^{14}N	2313	-	5.4×10^{4}	1.8×10^{7}	4.2×10^{7}
	^{14}N(p,p′γ)^{14}N	5106	-	-	2.2×10^{6}	2.5×10^{7}
O	^{16}O(p,γ)^{17}F	495	9.5×10^{2}	2.2×10^{3}	-	-
	^{17}O(p,p′γ)^{17}O	871	3.5×10^{1}	7.1×10^{3}	-	-
	^{18}O(p,p’γ)^{18}O	1982	-	2.7×10^{4}	-	-
	^{16}O(p,p′γ)^{16}O	6129	-	-	1.2×10^{7}	1.8×10^{9}
	^{16}O(p,p′γ)^{16}O	6919	-	-	-	8.3×10^{7}

	$^{16}O(p,p'\gamma)^{16}O$	7114	-	-	-	-
F	$^{19}F(p,p'\gamma)^{19}F$	110	3.5×10^{5}	$1.1x10^{7}$	-	-
	$^{19}F(p,p'\gamma)^{19}F$	197	2.9×10^{6}	4.3×10^{7}	-	-
	$^{19}F(p,p'\gamma)^{19}F$	1236	1.5×10^{5}	6.8×10^{6}	3.4×10^{8}	3.0×10^{8}
	$^{19}F(p,p'\gamma)^{19}F$	1346	-	9.7×10^{6}	1.4×10^{8}	7.7×10^{8}
	$^{19}F(p,p'\gamma)^{19}F$	1357	1.0×10^{5}	1.7×10^{7}	1.4×10^{8}	1.4×10^{8}
	$^{19}F(p,\alpha\gamma)^{16}O$	6129	6.0×10^{5}	5.0×10^{7}	1.9×10^{7}	9.4×10^{7}
Na	$^{23}Na(p,p'\gamma)^{23}Na$	440	3.4×10^{6}	3.9×10^{7}	7.3×10^{8}	6.7×10^{8}
	$^{23}Na(p,p'\gamma)^{24}Mg$	1636	1.5×10^{6}	-	4.8×10^{8}	4.8×10^{8}
	$^{23}Na(p,p'\gamma)^{23}Na$	1951	-	2.6×10^{7}	-	-
	$^{23}Na(p,p'\gamma)^{23}Na$	2391	-	5.1×10^{5}	-	-
Mg	$^{24}Mg(p,p'\gamma)^{24}Mg$	417	-	4.5×10^{5}	-	-
	$^{25}Mg(p,p'\gamma)^{25}Mg$	585	6.7×10^{4}	1.2×10^{6}	-	-
	$^{25}Mg(p,p'\gamma)^{25}Mg$	975	2.2×10^{4}	4.7×10^{5}	-	-
	$^{24}Mg(p,p'\gamma)^{24}Mg$	1369	1.5×10^{5}	6.5×10^{6}	-	-
	$^{24}Mg(p,p'\gamma)^{24}Mg$	2754	-	-	$7.3\ x10^{8}$	$9.3x10^{8}$
	$^{24}Mg(p,p'\gamma)^{24}Mg$	4239	-	-	$5.2\ x10^{7}$	$9.2\ x10^{7}$
Al	$^{27}Al(p,p'\gamma)^{27}Al$	844	1.5×10^{5}	7.5×10^{6}	2.1×10^{8}	3.8×10^{8}
	$^{27}Al(p,p'\gamma)^{27}Al$	1014	3.3×10^{5}	1.6×10^{7}	5.0×10^{8}	8.9×10^{8}
	$^{27}Al(p,p'\gamma)^{27}Al$	2210	-	2.1×10^{6}	4.2×10^{8}	8.0×10^{8}
	$^{27}Al(p,p'\gamma)^{27}Al$	2734	-	5.2×10^{4}	-	-
	$^{27}Al(p,p'\gamma)^{27}Al$	2981	-	-	7.3×10^{7}	1.0×10^{8}
	$^{27}Al(p,p'\gamma)^{27}Al$	3004	-	-	2.0×10^{8}	5.4×10^{8}
Si	$^{29}Si\ (p,p'\gamma)^{29}Si$	755	-	2.5×10^{5}	-	-
	$^{30}Si(p,\gamma)^{31}P$	1266	1.9×10^{5}	3.6×10^{5}	-	-
	$^{29}Si\ (p,\gamma)^{30}Si$	1273	1.8×10^{3}	8.7×10^{5}	-	-
	$^{29}Si\ (p,p'\gamma)^{29}Si$	1779	2.3×10^{2}	1.0×10^{7}	2.1×10^{8}	4.7×10^{8}
	$^{28}Si\ (p,p'\gamma)^{28}Si$	2028	-	8.8×10^{4}	4.9×10^{6}	1.1×10^{7}
	$^{29}Si\ (p,p'\gamma)^{29}Si$	2230	1.3×10^{2}	7.9×10^{4}	-	-
	$^{29}Si\ (p,\gamma)^{30}P$	2235	1.3×10^{2}	-	4.3×10^{6}	1.2×10^{7}
	$^{30}Si\ (p,p'\gamma)^{30}Si$	2839	-	-	4.9×10^{6}	2.2×10^{7}
	$^{28}Si\ (p,p'\gamma)^{28}Si$	3200	-	-	2.9×10^{6}	2.9×10^{7}
P	$^{31}P(p,p'\gamma)^{31}P$	1266	3.8×10^{4}	8.9×10^{6}	9.7×10^{7}	1.7×10^{8}
	$^{31}P(p,\alpha\gamma)^{28}Si$	1779	2.0×10^{3}	1.1×10^{6}	5.2×10^{7}	8.1×10^{7}
	$^{31}P(p,\gamma)^{32}S$	2230	3.5×10^{3}	1.0×10^{5}	7.0×10^{7}	1.3×10^{8}
	$^{31}P(p,p'\gamma)^{31}P$	2235	3.5×10^{3}	-	7.0×10^{7}	1.3×10^{8}
S	$^{32}S(p,p'\gamma)^{32}S$	841	1.4×10^{2}	2.9×10^{4}	-	-
	$^{34}S(p,\gamma)^{35}Cl$	1219	6.5×10^{1}	2.8×10^{5}	-	-
	$^{34}S(p,p'\gamma)^{34}S$	2127	-	4.8×10^{4}	-	-
	$^{32}S(p,p'\gamma)^{32}S$	2230	-	8.9×10^{5}	6.2×10^{7}	1.5×10^{8}
	$^{32}S(p,p'\gamma)^{32}S$	4282	-	-	6.0×10^{6}	3.7×10^{7}
Cl	$^{35}Cl(p,p'\gamma)^{35}Cl$	1219	3.5×10^{3}	1.5×10^{6}	5.7×10^{7}	8.6×10^{8}
	$^{35}Cl(p,n\gamma)^{35}Cl$	1410	-	2.1×10^{5}	-	-
	$^{35}Cl(p,p'\gamma)^{35}Cl$	1763	-	6.8×10^{5}	9.5×10^{7}	1.6×10^{8}
	$^{35}Cl(p,\alpha\gamma)^{31}P$	2230	1.2×10^{3}	1.8×10^{5}	5.1×10^{7}	1.1×10^{8}

	$^{35}Cl(p,p'\gamma)^{35}Cl$	3163	-	-	2.3×10^{7}	1.1×10^{7}
	$^{39}K(p,\gamma)^{40}Ca$	2168	2.6×10^{3}	1.6×10^{5}	-	-
	$^{39}K(p,p'\gamma)^{39}K$	2814	-	-	4.0×10^{7}	1.0×10^{8}
K	$^{39}K(p,p'\gamma)^{39}K$	3019	-	-	1.8×10^{7}	2.9×10^{7}
	$^{39}K(p,p'\gamma)^{39}K$	3598	-	-	7.0×10^{6}	1.5×10^{7}
	$^{41}K(p,p'\gamma)^{41}K$	1294	-	1.4×10^{5}	-	-
	$^{40}Ca(p,p'\gamma)^{40}Ca$	755	-	-	5.7×10^{5}	2.6×10^{7}
Ca	$^{40}Ca(p,p'\gamma)^{40}Ca$	3736	-	-	7.4×10^{7}	2.6×10^{8}
	$^{40}Ca(p,p'\gamma)^{40}Ca$	3904	-	-	8.6×10^{7}	2.8×10^{8}
	$^{48}Ti(p,p'\gamma)^{48}Ti$	985	-	-	6.2×10^{7}	1.3×10^{8}
Ti	$^{48}Ti(p,p'\gamma)^{48}Ti$	1312	-	-	4.3×10^{6}	1.7×10^{7}
	$^{48}Ti(p,p'\gamma)^{48}Ti$	1437	-	-	7.0×10^{6}	1.7×10^{7}

1.9 Sensitivity and detection limit in PIGE

Sensitivity of an element refers to count rate per unit concentration for particular experimental condition with information on energy of beam, current, solid angle and detector efficiency. It can be seen from thick target gamma ray yield, which is a direct indication of isotopic/elemental sensitivity. Detection limit on the other hand refers to the minimum amount/concentration that can be detected by a particular method. It depends on background counts of sample spectrum and sensitivity. The standard way to determine detection limit is:

$$L_D = 3 \times \frac{\sqrt{C_B}}{S \times t_m} \qquad (1.14)$$

where C_B is the background counts, t_m is the measurement time and S is the sensitivity in terms count rate (cps) per unit concentration (ppm or mg kg^{-1}). **Eq. 1.14** is valid for the same beam current of sample and standard. Systematic studies about the sensitivities of different elements have been performed by Deconninck and Demortier **[21]** with protons, Clark et al **[22]** with protons, tritons and alpha particles, Borderie et al **[23,24]** with tritons and alpha particles and Giles and Peisach **[9]** with alpha particles. Out of 70 studied elements, 40 can be determined with high sensitivity (<100 mg kg^{-1}) using PIGE. Trace element detection limit (mg kg^{-1} range) can be obtained for the light elements Li, Be, B, N, O, F, Na and P **[25]**.

Borderie **[24,25]** has indicated possibilities for bulk analysis in prompt gamma-ray spectrometry (PIGE) using different charged projectiles. A general enumeration of PIGE is given about its analytical possibilities with expected sensitivities for different elements using different projectiles. Protons and alpha particles in the energy range 1-5 MeV appear to be the best choice for light element determinations. Like deuterons, tritons are well suited for determining carbon and oxygen. They can also be used for a rapid determination of some metallic elements (like Fe and Ti) in the percentage range.

Background, which is the important parameter for the detection limit, plays an important role for obtaining accuracy of analysis. Accurate determination of concentrations in samples depends on the limit of detection and on the presence of major and minor elements in the sample. The absolute amount can be calculated from the concentration of an element if the areal mass density (g/cm^2) of the sample is known. The minimal amount of light elements is in the range $10^{-11} – 10^{-10}$ g. The lower limit in the absolute amount is obtained with the ion microprobe technique. Here, a beam diameter below 1 μm can be used **[36]**, making detection of an absolute amount of $10^{-16} – 10^{-15}$ g possible, although measurement time can be very high if concentration distributions have to be determined.

Thick target gamma ray yields are direct indication of isotopic/elemental sensitivity and it is more sensitive to that using thin target. There is a strong energy dependence of the excitation curve, and the sample mass and composition and these should be known accurately **[26]**. Several authors have published data with thick-target yields **[9,19,20,27,28]**. Kenny et al **[27]** measured the absolute thick-target yield for several elements at incident proton energies of 2.0 and 2.5 MeV. They have measured the yields for several gamma-ray lines for elements ranging from F to Au. Other set of data have been presented by Anttila et al **[19]** and Kiss et al **[20]** in the proton energy range 1.0 - 4.2 MeV for isotopes with $3 \leq Z \leq 21$. Thick-target gamma-ray yields for heavy elements ($Z > 30$) were determined by Raisanen and Hanninen

[29] using 1.7 and 2.4 MeV protons. Thick-target gamma-ray yields for light elements with 2.4 MeV He^+ are given by Lappalainen **[28]** and prompt gamma-rays generated by 5 MeV alpha-particles were investigated by Giles and Peisach **[9]** who determined the sensitivity of elements ranging from lithium to hafnium in their work on PIGE.

The limit of detection of an element is calculated using **Eq. 1.14**, in which background counts under the peak of sample spectrum and elemental sensitivity are the input parameters. The background in the gamma ray spectrum is dependent upon sample/target composition, experimental condition like beam energy, current and detection system. The background is mainly caused by Compton scattering of gamma-rays in HPGe detector. If the isotopes of matrix elements have high energy characteristic gamma rays, they produce higher Compton background which leads to poor detection limit for the elements whose gamma rays fall in the low energy region. Additionally, higher energy gamma rays (> 1.022 MeV) will give rise to low energy single and double escape peaks in the spectrum. Gamma-rays can also be produced by reactions taking place on the target ladder made up of aluminium or stainless steel as well as the materials of vacuum chamber by scattered charge particle. Background from these materials can be reduced by using thick target and proper alignment of beam, target and detector combination. Deuteron based reactions lead to production of neutrons which interacts with target and structural materials of beam chamber and give rise to background gamma rays. Another problem could be natural radioactivity in the surroundings of the experimental set-up, thus adequate shielding for the detector needs to be provided. To prevent any influence of the surroundings background and X-rays from the shielding, graded shielding with lead as the outer shield is provided for the HPGe detector. However, PIGE spectra are less complicated and easier to analyse compared to other on-line spectrometry experiments like PGNAA and PIXE.

1.9 Advantages and limitations of PIGE

Advantages	Limitations
• Non-destructive and non-invasive nature of this technique makes it suitable method of choice, where sample dissolution is a problem, for simultaneous quantification of low to medium Z elements.	• Proton beam of lower energy (1-4 MeV) from low energy accelerators is capable of determination of low Z elements from Li to Al at major to trace concentrations but requires higher energy proton beam to determine medium Z elements.
• It is an on-line technique and thus rapid analysis of many samples is possible.	• For C, N and O and medium Z element determination higher proton beam energy (≥ 7 MeV) is required which is not possible to obtain from low energy particle accelerators. Though they can be determined using deuteron beam but emission of neutrons is a problem.
• Lower matrix effect is experienced compared to PIXE as measurement of gamma-rays is performed.	• Sensitivity and limit of detection of an element in PIGE is dependent on energy and beam current. Lower beam energy and beam current will lead to poor detection limit.
• In PIGE, minimal sample preparation is required and also no chemical treatment is required before analysis, leading to low/negligible contamination problem.	• Direct sample analysis is not possible like NAA, as it require exact values of cross-section and stopping powers as input parameters.
• Isotope specific nature of PIGE can be used for determination of isotopic composition of different elements (like $^{6}Li/^{7}Li$ and $^{10}B/^{11}B$) along with total concentration simultaneously.	• As it is a matrix dependent method, care should be taken to match the sample/target matrix with the reference /standard to have accurate analysis in relative method of PIGE.
• It can be used in combination with PIXE as an analytical tool for complete compositional characterization of different samples like geological, archeological, biological, ceramic and glass samples including nuclear materials.	

1.10 Neutron activation analysis

Neutron activation analysis (NAA) is an isotope specific quantitative nuclear analytical technique used for simultaneous concentration determination of multi-elements in diverse matrices. It finds applications in the fields of biology, geology, archaeology, environmental science, material science, forensic science and nuclear technology due to many advantages like multi-element determination capability, low or negligible matrix effect, high sensitivity and selectivity, and non-destructive nature. NAA is based on irradiation of a sample in a flux of neutrons, preferably in a nuclear reactor, and subsequent measurement of the induced radioactivity to evaluate the concentration of an element present in the sample. The nuclear reaction involves absorption of neutron which forms a compound nucleus in excited state. The excited nucleus, de-excites by the emission of prompt gamma rays and delayed gamma rays from activation products. The decay characteristics permit the unambiguous identification of the radio nuclides in the irradiated sample. PGNAA and NAA are two different approached which utilize prompt gamma-ray or delayed gamma-ray, respectively, for measurements. In practice many labs use conventional NAA. It is possible to determine more than 50 elements ranging from F to U in various samples using NAA.

Advantages of NAA

1. It is independent of the chemical state of the element in a sample.
2. The technique has high sensitivity, specificity and selectivity. The technique experiences negligible matrix effect.
3. Applicability to different matrices ranging from geological, biological, environmental, archaeological samples including nuclear materials. Analytical blank is absent in INAA and RNAA.
4. The INAA technique is non destructive in nature.
5. NAA has a capability of simultaneous multi-element determination.

1.11 Applications of PIGE technique: A literature survey

PIGE applications range from geological and archaeological samples, ceramic samples, steel samples, dust and aerosol samples to biomedical samples. In 1960, Sippel and Glover **[5]** for the first time showed that gamma-rays emitted by using energetic protons of the order of MeV could be used for determining low Z elements like Li, Be, C, N, O, F, Na, Mg Al and P in geological samples. They discussed about the general outline of PIGE method and experimental details comprehensively. Pierce et al **[6]** used energetic beam of deuterons for carbon determination in steel samples. In 1967, Moller and Starfelt applied the same technique for studying fluorine contamination of zircaloy cladding for reactor fuel **[30]**. Pierce et al **[7]** quantified Si in different kind of steels by using 4 MeV proton beam. Pierce et al. also studied the nuclear reactions for different low Z elements starting from Li to Cl using 0.5 MeV proton beam **[31]**. Use of Ge based detectors in 1970 onwards, revolutionized the field of gamma-ray spectrometry. The Ge based detectors (Ge(Li) and HPGe) with better energy resolution than NaI(Tl) helped PIGE to quantify multi-elements simultaneously in a sample. Since then, studies have been carried out with both light (like p and d) and heavy (like t, α and ^{3}He) projectiles. G. Deconninck at LARN, Belgium and other researchers (Boulton and Ewan) studied (p, p'γ), (p, γ) and (p,nγ) nuclear reactions for different elements like Li, B, F, Na, Al, P, Cr, Mn, Se, Rh, Pt and Au using proton beam of energy up to 3 MeV and reported the respective detection limits **[8,9,11,32]**.

The PIGE technique was utilized for determination of O, C, N, Si and S in coal samples using 9.5 MeV proton beam. Macias et al reported the accuracy of method ~5% of the concentration of each element and a precision of ~ 4% for elements constituting 1% of coal by weight **[33]**. J. Raisanen and R. Hanninen analyzed hafnium plate by bombarding with 10 mC of 2.4 MeV protons. They determined the following elements/isotopes: O (495 keV from

^{16}O and 871 keV from ^{17}O) (150 mg kg^{-1}), ^{23}Na (440 keV, 0.3 mg kg^{-1}), ^{27}Al (844, 1014 keV, 30 mg kg^{-1}) and ^{31}P (1266 keV, 5 mg kg^{-1}) including heavier elements /isotopes ^{92}Zr (657, 1083 and 1208 keV, 2.8%), Fe (1378 and 1920 keV, 100 mg kg^{-1}) and Cu (992 keV, < 50 mg kg^{-1}) **[29]**. Van Ijzendoorn et al **[34]** used the PIGE technique to quantify thin layers of SiF_x that were a result of reactive ion etching of Si wafers with CF_4 plasma. The quantification is important to understand the etching process. The $^{19}F(p,p'\gamma)^{19}F$ reaction was used to determine F on the Si wafer using proton beam of 2.78 MeV. The energy was so chosen to suppress a Si reaction and thus to limit the Compton background. G.E. Coote, in 1992 reviewed specifically the nuclear reactions for PIGE analysis of F and other low Z elements in different materials including biological (like teeth, bone and fish scales), archaeological and atmospheric samples. In the same review, brief description about the experimental part of PIGE method is discussed including excitation function and interferences **[35]**.

Volfinger et al determined Li, Be, B and F in the individual grains of micas using alpha particle beam of energy 1-3 MeV. The reported 20 mg kg^{-1} limit of detection is reached for Be, 25 mg kg^{-1} for Li, 900 mg kg^{-1} for B and 450 mg kg^{-1} for F in the granite samples **[36]**. Smectite Swy-1 clay samples were analyzed by Savidou et al using 4 MeV proton beam and they reported the concentrations of Li, B, F, Na, Mg, Al, Si and P in their work **[37]**. Nsouli et al analyzed F concentration in a drug as a part of chemical quality control exercise using proton beam for the first time **[38]**. A number of glass samples of archaeological importance have been studied using PIGE-PIXE combination. The elements reported by PIGE using proton beam were Na, Mg, Al and Si **[39]**. Boulton and Ewan determined boron in a bean leaf using PIGE, which is an essential nutrient to plants in trace quantities and poisonous in large quantities. The boron concentration reported in this sample was 600 mg kg^{-1} **[32]**. Yosnda et.al determined the F concentrations in teeth **[40]** samples using proton beam. Macias Edward et al analyzed aerosol samples for environmental studies using PIGE for the

determination of low Z elements **[41]**. Different samples of geological importance and environmental reference materials have been analyzed by Valkovic et al using PIGE methods **[42]**.

By increasing the beam energy, the excitation function also improves for a thick target which leads to increase in cumulative cross-section of a particular nuclear process and hence improved sensitivity of method with better detection limit can be achieved. In view of this it is important to have an idea of gamma-ray yield of most intense gamma-ray emitted during a nuclear process from the isotope of interest. Therefore the gamma-ray yields were measured using proton beams of energy from 2 to 10 MeV **[43]**. Saarela et.al showed that PIGE can be used for determination of Na, Mg, Al, P and Mn in plant samples using 3 MeV proton beam in external PIGE set-up. They also showed that the elemental concentrations to detection limit ratios were enhanced greatly by dry ashing of biological samples **[44]**.

In accelerator based experiments beam current or fluence normalizations is an important aspect of the experiment. If beam current or fluence variation is experienced during irradiation, than that can be normalized by measuring the current directly from the sample if the same is conducting **[5]**, by measuring the beam current using Faraday cup kept just behind the thin target **[45]** or by using RBS method. In RBS approach, backscattered ions from thin foils of high Z metals like Au, Ag and W are measured using a Si based surface barrier detector kept at a fixed backward angle with respect to the ion beam **[46]**. The beam current/fluence normalized count rates were utilized in relative PIGE methods for determining the concentrations of analytes in various samples. Relative PIGE method is more popular and simple to use over absolute PIGE method for concentration determination. Thus PIGE is a promising analytical tool for chemical characterization of materials (particularly for low Z elements) and when it combines with PIXE, complete compositional characterization of materials is feasible **[47]**.

1.13 Scope of the present thesis

The objective of the present thesis is to develop particle induced gamma-ray emission (PIGE) methods using proton beams for simultaneous determination of low Z elements and applications to materials relevant for nuclear technology. In this respect, both conventional as well as current normalized PIGE methods have been optimized using 4 or 8 MeV proton beams from tandem accelerators namely FOTIA (BARC, Mumbai), IOP (Bhubaneswar) and TIFR (Mumbai). The methods have been applied for non-destructive analysis of samples of borosilicate glass, lithium based ceramics and boron based compounds including carbides, which are otherwise difficult to be analyzed by wet chemical classical as well as spectroscopic methods. The concentrations of low Z elements like Li, B, O, F, Na, Si, Al and Ti have been determined in different samples using PIGE methods. The development of PIGE methodologies and applications are described briefly in the following:

In the present work, thick targets using cellulose or graphite matrix were used for the experiments in order to achieve higher analytical sensitivity and to obtain matrix matching composition of sample and standard. In accelerator based experiments, beam current measurement / normalization is carried out either by measuring current from the conducting target or by RBS method using thin foil of Au or Ag. A new approach i.e., *in situ* current normalization methodology is developed in this work wherein, an element, not present in the sample and having high sensitivity in PIGE, is mixed homogenously in the sample and standard in constant amount. One of the elements like F, Li and Al was used for *in situ* current normalization depending on the type of sample. This approach does not demand sample to be conducting and also does not require a separate arrangement (like RBS approach) for current measurement. The advantage is that the count rate of *in situ* current normalizer is measured simultaneously with that of sample and the count rates of externally

added element in the target give variation of beam current, if any. In addition to the *in situ* current normalized method, conventional PIGE method using RBS approach and beam current measurement from target (prepared in graphite matrix) were also carried out. The *in situ* current normalized PIGE methods have been applied for determination of: (i) F and other low Z elements like Li, B, Si, Al and Na in borosilicate glass samples, (ii) trace to major amount of Li in lithium based ceramic samples namely Li doped neodymium dititanate and sol-gel synthesized lithium titanate and (iii) total boron concentration in boron based compounds and neutron absorbers. The isotope specific nature of PIGE was utilized advantageously to determine isotopic composition of boron ($^{10}B/^{11}B$ atom ratio) in addition to total boron concentration in natural and enriched boron based compounds including B_4C. For complete compositional characterization of lithium titanate i.e., for simultaneous determination of Li, Ti and O, PIGE method utilizing 8 MeV proton beam was applied for the first time. The PIGE methods were validated by analyzing stoichiometric chemical compounds and/or reference materials from NIST and IAEA. Since in many cases, it was difficult to obtain suitable reference materials, the methods were validated by analyzing synthetic samples in cellulose or graphite matrix as the case may be.

Barium borosilicate glass (BaBSG) is a promising matrix for nuclear waste vitrification. BSG samples with varying composition of Si, B, Al and Na with F were prepared to examine the retention/loss of F during vitrification at high temperature. As a part of chemical quality control (CQC) exercise, it is important to accurately determine concentration of F as well as the major glass matrix forming low Z elements like Si, B, Al and Na in different BSG samples preferentially without any chemical dissolution. The *in situ* current normalized PIGE method using 4 MeV proton beam was applied for compositional analysis of two types of glass samples: (i) containing F, Si, B and Na (ten samples) and (ii) Si, B, Al, Na and Li (three samples). First four elements in the first set were determined by

relative PIGE method using Li as the current normalizer. Since, the second set of samples contain Li, F and Al together; the charge/current normalized PIGE method with conducting targets (prepared in graphite matrix) was used. The concentrations ranges of different elements determined were 0.1-3.76 wt% (F), 0.7-1.0 wt% (Li), 4.5-10.0 wt% (B), 8.0-13.0 wt% of Na, 16.0-18.0 wt% (Si) and 1.8-3.0 wt% (Al). The total propagated uncertainties in the results were less than 3.0%.

The *in situ* current normalized PIGE method (using F as current normalizer) was extended for determination of lithium in two types of ceramic samples namely (i) Li doped neodymium dititanate (NTO) and (ii) lithium titanate (Li_2TiO_3), which are difficult to be analyzed using wet chemical methods. Li doped NTO is a high temperature ferroelectric material and it is necessary to estimate Li in the heat-treated (at 800^oC) as well as precursor samples for studying the ferroelectric properties. The concentrations of Li were in the range of 0.3-0.6 wt% in heat treated Li doped NTO indicating a loss of 5-35% of Li with respect to precursor samples.

This method was further extended for determination of Li in sol-gel synthesized Li_2TiO_3 sample, which is a tritium breeder blanket material in proposed D-T based fusion reactor under ITER programme. This work was undertaken for optimizing synthetic procedure and ascertaining Li content in the sample with respect to its stoichiometric composition. Three types of samples (with starting materials LiCl, $LiNO_3$ and 1:1 (LiCl+$LiNO_3$) were analyzed by *in situ* current normalized PIGE. Li concentrations in the range of 11.0-12.7 wt% were obtained in this work. Since Ti could not be determined by PIGE using 4 MeV proton beam due to its lower thick target gamma-ray yield, INAA method using Pneumatic Carrier Facility (PCF) of Dhruva reactor was used for quantification of Ti (42.7-44.7 wt%) utilizing its short-lived activation product, ^{51}Ti (5.7 min, 320 keV). The total uncertainties in the results of Li and Ti concentrations were less than 3%, respectively. Since

complete compositional characterization was necessary for lithium titanate, PIGE method using 8 MeV proton beam is developed for simultaneous determination of Li, Ti and O. Experiments were carried out using samples in graphite matrix and RBS method using thin Au foil for the current measurement. The concentrations of Li, Ti and O in four samples were in the range of 11.8-12.7, 43.3-43.8 and 43.7-44.3 wt% with respect to their stoichiometric concentrations of 12.67, 43.51 and 43.85 wt%, respectively. The uncertainty values for Li, Ti and O concentrations were within ±3%, ±3% and ±8%, respectively.

Boron is an important element in nuclear technology and due to its high neutron absorption cross section; its compounds are used as control/shut-off material in nuclear reactors. Thus, determination of total B and its isotopic composition (IC, $^{10}B/^{11}B$ atom ratio) values is necessary for CQC purpose. PIGE is capable of estimating IC of boron due to the characteristic gamma-rays at 429 and 718 (^{10}B) and 2125 (^{11}B) keV by proton induced reactions. Using this advantageous property of PIGE, IC of boron and its total concentration were determined simultaneously in various boron based natural and enriched compounds samples including B_4C. *In situ* current normalized PIGE methods (using F or Al thin foil as *in situ* current normalizer) were used for total B concentration determination. For IC determination, the method was rather simpler as the peak area ratios of ^{10}B and ^{11}B of samples and standard (natural boric acid) were utilized without any current normalization. The method was applied to various boron based stoichiometric compounds and samples like boron carbide (natural and enriched), elemental boron, carborane and borosilicate glass. The total B concentrations determined were in the range of 5-78 wt%. Isotopic composition values of boron were in the range of 0.247-2.0 that corresponds to ^{10}B in the range of 19.8–67.0 atom%. The uncertainties in the total concentration of boron as well as in IC of B were in the range of 0.5-3%.

In summary, both conventional and *in situ* current normalized PIGE methods using 4 and 8 MeV proton beams were standardized for quantification of low Z elements. Relative PIGE methods were applied for non-destructive determination of (i) F, Si, Al, Na and Li in Ba borosilicate glass samples, (ii) Li in Li doped neodymium dititanate and lithium titanate (iii) Li, Ti and O simultaneously in lithium titanate and (iv) total boron and its IC ($^{10}B/^{11}B$ atom ratio) in boron based materials including B_4C. *In situ* current normalization is a novel approach in which an element not present in the sample is mixed with the target or a thin foil is wrapped on the target. For QA/QC, stoichiometric compounds, synthetic samples and/or reference materials were analyzed and concentrations of low Z elements were determined and compared with calculated / certified values. The quality of results was further evaluated by calculating total uncertainties in measurements and experimental detection limits.

Chapter 2

Experimental

Experimental details of PIGE methods are discussed in this Chapter. Solid samples of borosilicate glass, lithium doped neodymium dititanate, lithium titanate, enriched and natural boron based samples and reference materials from IAEA and NIST have been analyzed for determination of low Z elements namely F, Si, Al, Na, B, Li, O and Ti. To obtain similar matrix of standard and sample, the solid samples were powdered and mixed homogenously with cellulose or graphite. The homogenously mixed samples were pelletized using hydraulic press. The targets were irradiated using 4 or 8 MeV proton beam, as the case may be, from tandem accelerators namely FOlded Tandem Ion Accelerator (FOTIA) at BARC, Mumbai, 3 MV Tandetron, Institute of Physic (IOP), Bhubaneswar and 14 MV BARC-TIFR Pelletron facility, Mumbai. An in-situ beam current normalization approach was developed using either of Li, F and Al elements where Li or F was externally added to the target and in the case of Al, its thin foil was wrapped on the sample facing the beam. Beam current variations were monitored/normalized either by conventional RBS method (using thin Au foil) or by measuring the charge directly from the conducting sample in graphite matrix. The prompt gamma-rays were measured using high resolution gamma-ray spectrometry using HPGe detector coupled with 8k PC based multi-channel analyzer (MCA). The sensitivity (count rate per unit concentration) of in situ current normalizer was used to obtain current normalized count rate of isotope of interest in the sample and standard. The elemental concentrations were determined using relative method. Details of samples, their preparation, experimental set ups, gamma-ray spectrometry and methods for concentration calculation are given in this Chapter

2.1 Samples analyzed in the present study and their importance

Samples of barium borosilicate glass (BaBSG), lithium based ceramics (like lithium doped neodymium dititanate and lithium titanate), boron based materials (like stoichiometric boron compounds) including natural and enriched boron based compounds (like boric acid and boron carbide) and reference materials from NIST and IAEA were analyzed by PIGE

methods using proton beams. Brief details about the samples and their importance are discussed below.

Barium borosilicate glass

High level radioactive liquid waste (HLW) generated from reprocessing of spent nuclear fuel mainly contains fission products, corrosion products, minor actinides and inactive chemicals added at different stages of reprocessing. Borosilicate glass (BSG) / Barium BSG (BaBSG) is a potential matrix for immobilizing HLW before their long term disposal in geological repositories. Developmental work is being carried out using mixture of HNO_3 and HF for dissolution of (thoria based) spent nuclear fuels because of its refractory nature. In view of the corrosive nature of F^- ions, $Al(NO_3)_3$ is also added to complex excess amount of F^- ions **[48]**. Thus, F^- ions are present in significant amount in the HLW generated during reprocessing stage of spent fuel. High radiation stability, physico-chemical properties, good leaching behavior, thermal and mechanical stability of BSG, makes it better and suitable candidate for vitrification of HLW **[48-51]**. These properties of BSG can be tailored judiciously by varying the concentrations of glass modifiers like Na, Li, Al and F. Presence of fluoride ions in BaBSG affect its leaching behavior, which will increase the risk of spread of radioactivity to the surroundings from geological repositories. During vitrification of HLW, loss of glass ingredients is expected due to volatilization/carryover in the form of volatile halides of boron, silicon, and alkali metal fluorides, which can corrode and hence damage the inconel vessels of the vitrification plant. Therefore, the exact/optimum composition of such glass sample is necessary to examine retention/loss of F and fission products during vitrification. As a part of chemical quality control exercise, it is important to accurately determine concentration of F as well as the low Z elements like Li, B, Na, Al and Si as major matrix elements in different BSG samples. Determination of fluorine in this complex matrix sample using wet chemical methods is cumbersome and tedious. Therefore, a

non-destructive method is preferred over wet chemical methods for the estimation of these low Z elements in this complex matrix.

Lithium doped neodymium dititanate ($Nd_2Ti_2O_7$)

Lithium doped neodymium dititanate (NTO) is a high temperature ferroelectric material. In order to study the effect of doping of low Z element like Li on its various properties including ferroelectric behavior, NTO samples were doped with varying concentrations (600-1700 mg kg^{-1}) of Li **[52,53]**. It was necessary to estimate Li in the heat-treated samples (at 800^{o}C) for studying the ferroelectric properties with actual concentration of Li. Thus, Precursor and heat-treated Li-doped NTO samples were used for analysis.

Lithium titanate (Li_2TiO_3)

It is one of the best proposed tritium breeder blanket material for deuterium-tritium (D-T) reaction based fusion reactor. The characteristic features of lithium titanate, like good tritium release ability and mechanical strength at elevated temperatures, made it a suitable candidate to use as blanket material. Lithium titanate samples were prepared using sol-gel method of synthesis. For optimizing the synthesis route, lithium titanate samples were prepared under different set of conditions like different starting materials (like LiCl, $LiNO_3$ and 1:1 mixture of LiCl and $LiNO_3$), varying sintering temperature (500-1250 ^{o}C) and washing and no washing of final product with LiOH. Therefore, concentrations of Li, Ti and O were determined in lithium titanate samples as a part of optimization of sol-gel synthesis route **[53,54]**.

Boron based compounds

Boron and its compounds, composites and alloys find extensive applications in various

fields including nuclear technology due to its high thermal neutron absorption cross section. The mechanical properties of elemental boron are not suitable, and therefore various solid boron based materials (like boric acid, boron carbide, rare-earth and refractory metal borides) are extensively used in nuclear industry as neutron sensors, human and instrument shielding against neutrons, nuclear/neutron poison, control/shutoff rods and in nuclear material storage. Boron carbide is used as control rod material in both pressurized water reactors and boiling water reactors. Boron plays a pivotal role in controlling and ensuring the safe operation of nuclear reactors. Therefore, exact determination of total concentration along with its isotopic composition ($^{10}B/^{11}B$ atom ratio) in different boron based materials is very important for chemical quality control **[55]**.

PIGE methods using proton beams from tandem accelerators have been standardized for chemical characterization of borosilicate glass, lithium based ceramics (Li in lithium doped neodymium dititanate and lithium titanate), and, total boron as well as its isotopic composition determination. A brief introduction and discussion about tandem accelerator facilities used in the present work are given in the following section.

2.2 Tandem accelerator facilities

In the present study, proton beams from tandem accelerators at BARC and IOP as well as pelletron facility at TIFR are used. The underlying principle of these accelerators is detailed as follows. The electrostatic attraction of negative ions generated by sputtering mechanism (using Cs sputter) are accelerated to low energies (100-250 keV) in short horizontal section. These low energy ions are injected into the vertical accelerating column through an injector magnet. In the first stage, the acceleration results from the electrostatic attraction of the negative ions by the positively charged high voltage terminal. The high electric potential at the terminal is achieved by a continuous transfer of charge to the terminal by means of the chain of steel pellets. At the terminal, the ions pass through a stripper, either

a thin carbon foil or a small volume of a gas (like N_2), where they lose electrons and acquire positive charge. The average charge (q) of the ion depends upon the type of ion and the terminal voltage (V). The resulting positive ions enter the second stage of acceleration where the positive voltage of the terminal acts repulsively on the positive ions. The final energy of the ion accelerated through a potential of 'V' volts and has acquired a positive charge of 'q' units will be given by the following relation:

$$E = (q + 1)V \quad ---(2.1)$$

2.2.1 FOlded Tandem Ion Accelerator (FOTIA) facility at Mumbai

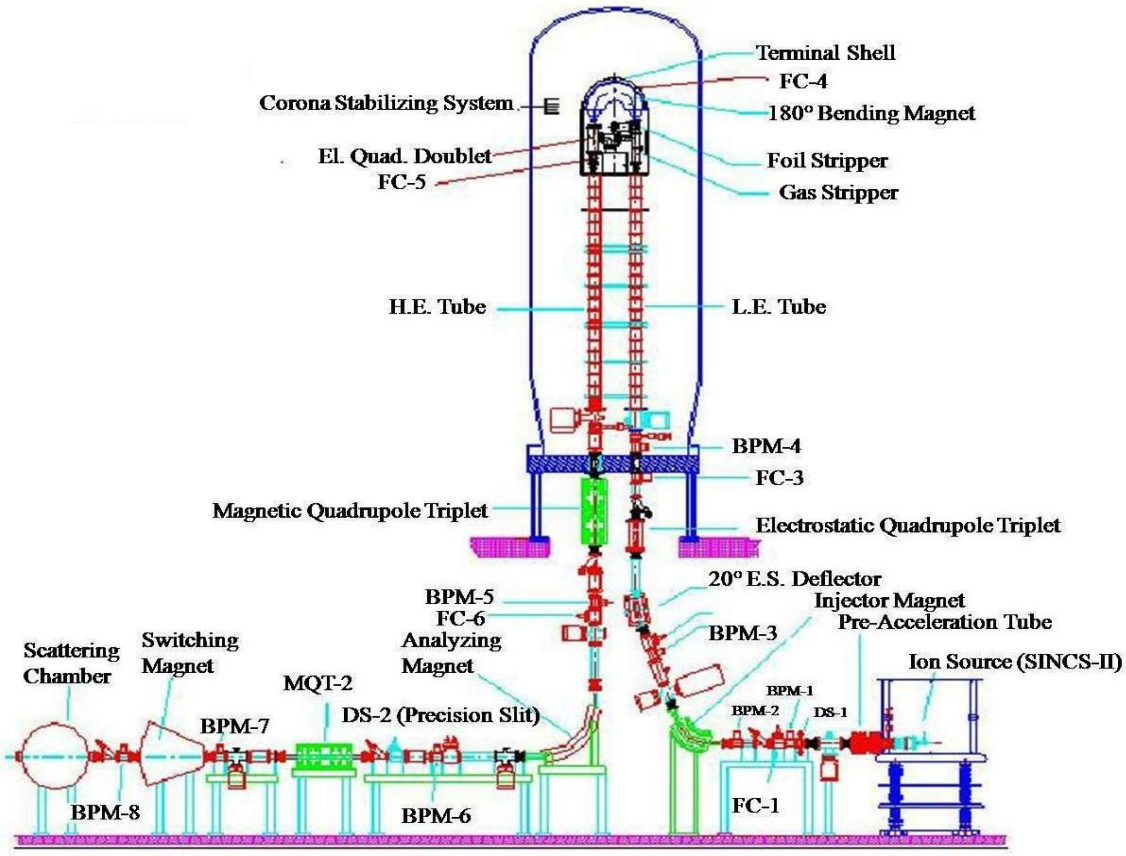

Fig.2.1: Schematic diagram of FOTIA facility at BARC, Mumbai ((*Source: BARC Newsletter-2002, p.22-32*)

The 6 MV FOlded Tandem Ion Accelerator (FOTIA) used in present work is shown in **Fig. 2.1**. It can provide accelerated heavy ion beams of up to A = 60 and energy up to 60 MeV.

The ions which can be accelerated in FOTIA are ^{1}H, ^{4}He, ^{12}C, ^{16}O, ^{24}Mg, ^{28}Si, ^{32}S, ^{37}Cl, and ^{40}Ca up to the energy of 60 MeV. FOTIA uses SNICS-II type of source for pre-acceleration of negatively charged particles (up to the energy of 150 keV). The terminal voltage of FOTIA is stable within ±2 kV. Protons can be accelerated up to 6 MeV using FOTIA, with beam currents

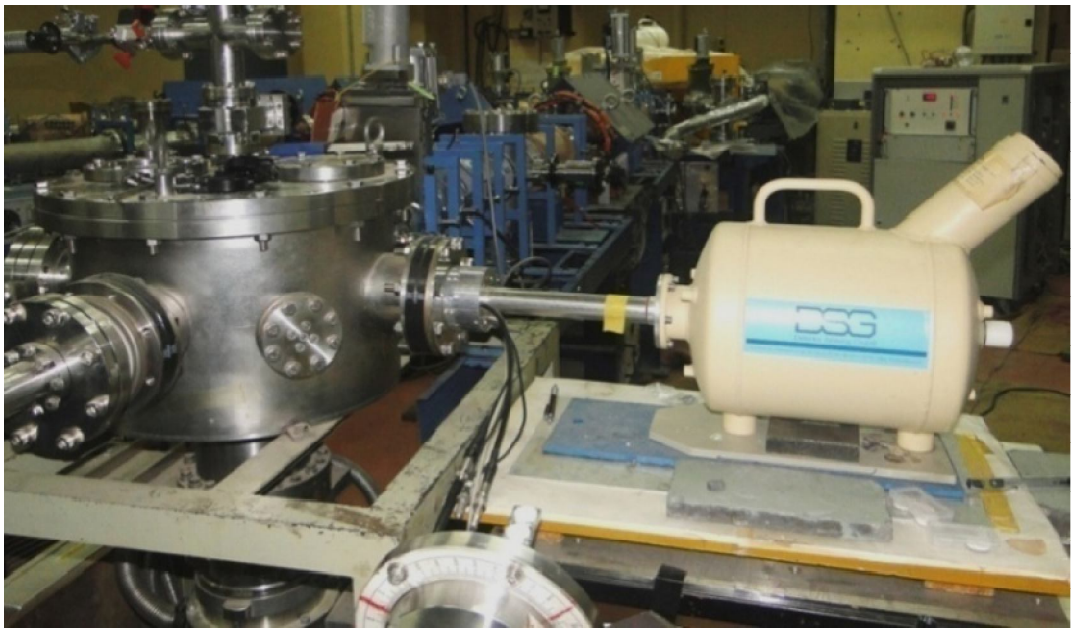

Fig. 2.2: PIGE set up at FOTIA, BARC showing beam chamber and HPGe detector system.

of few hundreds of nano-ampere. FOTIA is having three beam lines out of which one is dedicated to IBA studies and other two for nuclear physics and positron based experiments **[56]**. The PIGE facility was set up at FOTIA, BARC for concentration determination of low Z elements in various solid samples. The PIGE set up was installed in 25°S beam line dedicated for PIGE-PIXE studies. The reaction chamber is having a port, exactly at right angle to the sample/target holder, to which HPGe detector (30% relative efficiency) was fixed as shown in **Fig. 2.2.** HPGe detector was coupled to 4k/8k PC based MCA for data acquisition. The experiments were carried out under high vacuum conditions (10^{-7} torr). Seven targets were fixed on the stainless steel target holder. The **Fig. 2.3** shows the targets fixed on stainless steel ladder before irradiation with proton beam.

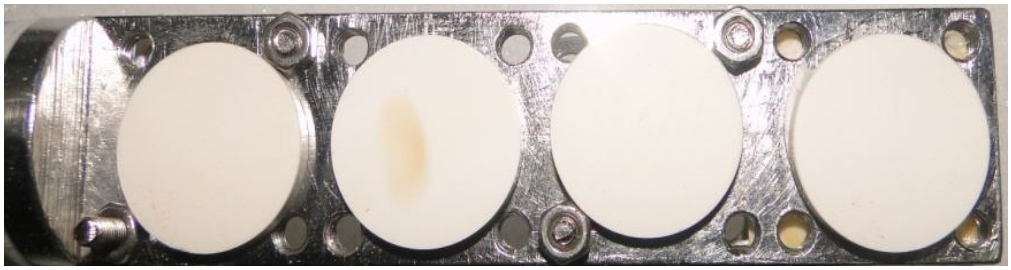

Fig. 2.3: Target ladder at FOTIA, BARC showing mounted targets.

2.2.2 Tandem accelerator at Institute of Physics

The ion beam laboratory of Institute of Physic (IOP) consists of a tandem Pelletron accelerator that can deliver positive ion beams (H, He, Li, C, Si, Ag and Au) in the energy range of 1-12 MeV. The maximum terminal voltage is 3 MV and can be set anywhere between 0.5-3.0 MV as per the requirement of user. The accelerator is equipped with two negative ion sources; Alphatross and Multi-Cathode Source of Negative Ions by Cs Sputtering (MC-SNICS). Alphatross is exclusively used for producing He^{-} ions whereas

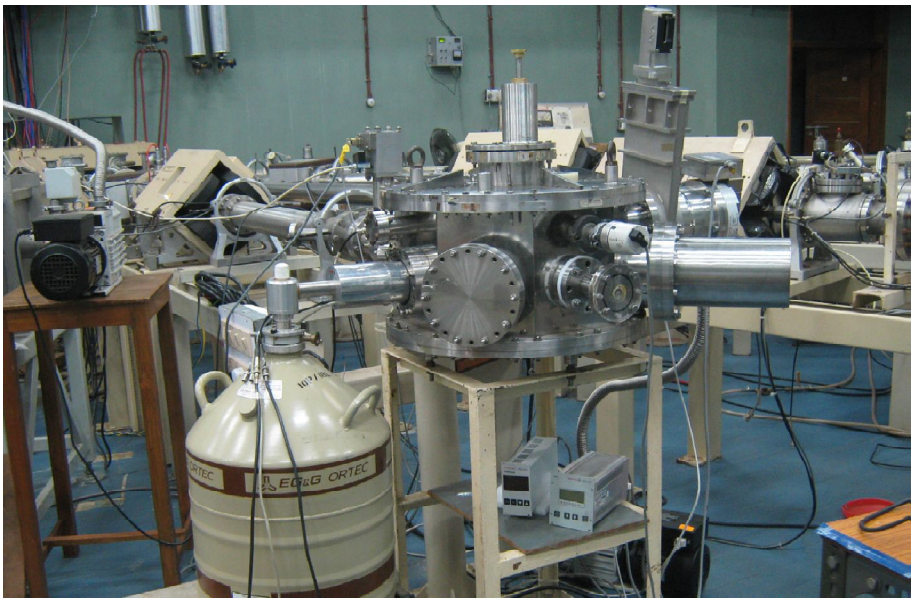

Fig. 2.4: PIGE set-up at IOP, Bhubaneswar.

MC-SNICS is used for producing all other types of negative ions. Initially the desired beam particles are converted into negative ions (~55 keV) before injection into the accelerator. For stripping of negative ions, Ar gas is used to strip off the electrons at high terminal voltage and the beam particles are ejected as positive ions with high energies depending on the terminal voltage applied. The beam currents on target range from a few nano-Amperes to a few tens of nano-Amperes. The accelerator facility is equipped with dedicated set ups for ion beam analysis (IBA) studies like RBS, ion-channeling, NRA, PIXE, PIGE and ERDA. Other than these, the facility is also being used for ion-implantation, irradiation studies and accelerator mass spectrometry of radiocarbon **[57]**.

The PIGE facility at 3 MV tandem accelerator of IOP, Bhubaneswar was also utilized in this work. The HPGe (60% relative efficiency) detector coupled to PC based 8k MCA, kept perpendicular to beam direction (to minimize Compton affect), was used to measure prompt gamma-rays emitted from the targets **[Fig. 2.4]**. Provision of mounting 40 targets on an octagon aluminum ladder is available in this facility. The target mounted ladder is aligned at an angle of 45° with respect to beam direction and HPGe detector. **Fig. 2.5** shows target ladder with mounted sample pellets on it.

Fig.2.5: Multi-target ladder with targets at IOP, Bhubaneswar

2.2.3 BARC-TIFR Pelletron facility

Fig.2.6: PIGE set up at BARC-TIFR Pelletron facility.

The BARC-TIFR Pelletron accelerator facility at TIFR is functional since 1989 **[58]**. The ion source used here for production of negative ions which accelerate with low energy (150-250 keV) is MC-SNICS. In addition to continuous beams, pulsed beams of ~1 ns width separated by about 100 ns to 1.6 ms have also been made available by installing a double harmonic buncher in the low energy section **[59]**. Five beam lines are laid in the main beam hall. The beam transport system on these lines is remotely controlled using a CAMAC system and integrated with the indigenously developed PC based control system of the main accelerator **[60]**. The beam current (for proton) of few hundreds of nano-Amperes can be delivered at the point of irradiation. This facility is generally used for Nuclear Physics and Atomic Physics experiments. Additionally the facility can be used for carrying out studies based on IBA techniques.

Fig. 2.7: Chamber showing targets mounted on a sample holder for irradiation at BARC-TIFR Pelletron facility.

A PIGE facility was also set up (15^{o} North) at BARC-TIFR Pelletron facility of at TIFR, Mumbai for simultaneous determination of Li, Ti and O in sol-gel synthesised lithium titanate samples. **Fig. 2.6** and **2.7** shows the set up of PIGE at BARC-TIFR Pelletron facility and reaction chamber showing mounted targets on sample holder. HPGe detector (30% relative efficiency) coupled to PC based 8k MCA was used for data acquisition.

2.3 Sample preparation

Solid powdered samples were ground to fine particles using agate mortar and pastel. Microcrystalline cellulose (Aldrich-Sigma) or spectroscopic grade graphite powders were used for diluting the samples as well as binder to make sample pellets. Chemicals were

handled in fume hoods with proper safety guidelines by wearing hand gloves and cloth masks. Details are given in the following:

2.3.1 Sample preparation for determination of F in glass samples

Standard pellets of fluorine were prepared by mixing varying amount of NaF (corresponding to F amount 1,000–40,000 mg kg^{-1}) using cellulose as major matrix. Synthetic samples of borosilicate glass were used for validating the PIGE method. One synthetic standard pellet was prepared by mixing stoichiometric compound LiF (~4 mg) in cellulose matrix. Four synthetic sample pellets were prepared by mixing cellulose (~600-650 mg) and base glass (~100–150 mg) with known amount of fluorine (0.3–1.8 wt%). Sample pellets of BSG containing F were prepared by mixing about 100–150 mg of BSG sample and 650–600 mg of cellulose. The powders were mixed (~30-45 min) using agate mortar and pastel to achieve homogeneity and the mixtures were pelletized by hydraulic press machine **[61]**.

2.3.2 Sample preparation for barium borosilicate glass for F and other low Z elements

Two sets of glass standards were prepared for determination of concentrations of low Z elements in several BSG samples.

Sample preparation using graphite

Two standards were prepared by mixing homogenously known amount of Li_2CO_3, NaF, H_3BO_3, SiO_2 and Al_2O_3 in graphite matrix. Two synthetic standard pellets were prepared, for validation of PIGE method, by mixing known amount of Li_2CO_3, H_3BO_3, NaF, Al_2O_3 and SiO_2 in graphite matrix. Three samples of BSG were prepared by homogenously mixing ~200 mg of borosilicate glass samples in 550 mg of graphite powder. The powders were mixed homogenously in mortar and pastel followed by pelletization of powders using hydraulic press machine **[62]**.

Sample preparation using cellulose

Standards for this set of glass samples were prepared by mixing homogenously H_3BO_3, NaF, Al_2O_3 and SiO_2 with cellulose as matrix. BSG samples (~200 mg) were mixed in cellulose (~530 mg) with constant amount of Li_2CO_3 (~20 mg) to every standard and sample pellet. The method was validated by analyzing two synthetic standards from NIST (NBS SRM 1633a and NBS SRM 1645). The synthetic samples were also prepared by mixing homogenously (~30-45 minutes) the reference materials (RMs) (~200 mg each) in cellulose matrix (~530 mg) with constant amount of Li_2CO_3 (~20 mg) using agate mortar pastel **[62]**.

2.3.3 Sample preparation for determination of Li in Li based ceramics (Li doped $Nd_2Ti_2O_7$ (NTO) and Li_2TiO_3)

(i) For quantification of Li in Li doped NTO, Li standards with varying amounts (~500–7,000 mg-kg^{-1}) of Li were prepared by mixing $Li_2SO_4.H_2O$ (~3–50 mg) with constant amount of NaF (5 mg) in cellulose matrix. Four synthetic sample pellets were prepared by mixing ~200 mg of $Nd_2Ti_2O_7$ (without any Li) with constant amount of NaF and varying amounts (~500–6,000 mg kg^{-1}) of Li in cellulose matrix. The sample pellets were prepared in similar way to that of synthetic samples Li doped NTO ceramic sample (~200 mg) were homogeneously mixed with fixed amount of NaF in cellulose matrix. The net mass of each pellet was kept at 750 mg. After homogeneous mixing of samples using agate mortar and pastel, the pellets were prepared by pressing homogenously mixed powders using hydraulic press **[63]**.

(ii) In sol-gel synthesized Li_2TiO_3, Li was quantified using *in situ* PIGE method and Ti by instrumental neutron activation analysis (INAA). For PIGE, Standards of lithium were prepared by homogeneously mixing varying amounts of lithium sulphate with constant amount of CaF_2 (~20 mg) in cellulose matrix using agate mortar and pastel. For method validation, eight synthetic samples of Li were prepared. One synthetic standard pellet was

prepared by mixing constant amount of CaF_2 (~20 mg) and Li_2CO_3 (~50 mg) in cellulose matrix, and, rest seven pellets were prepared by mixing cellulose, constant amount of CaF_2 (~20 mg) and titanium dioxide (TiO_2, ~50 mg) with known lithium content (3–19 wt% of Li). The sample pellets of were prepared by homogeneously mixing lithium titanate sample powders (~ 100 mg) with fixed amount of CaF_2 (~20 mg) in cellulose matrix. The total mass samples, synthetic samples, and standard pellets were nearly identical ~1 g. Target pellets were prepared by pressing homogenously mixed powders using hydraulic press **[53]**.

(iii) Sample preparation for INAA

For instrumental neutron activation analysis (INAA) method titanium standards were prepared by homogeneously mixing known amount of TiO_2 (30–100 mg) with cellulose matrix. Similarly, synthetic samples for titanium were prepared by mixing varying amount of TiO_2 and lithium sulphate in cellulose matrix. From these mixtures of sample, standard and synthetic samples, ~10 mg of each were packed separately in polyethylene sheets followed by irradiation with neutrons at pneumatic carrier facility of Dhruva reactor at BARC, Mumbai for 1 minute **[53]**.

For simultaneous determination of Li, Ti and O in Li_2TiO_3, standard pellet (~650 mg) of Li, Ti and O was prepared by mixing homogenously known amount of Li_2CO_3 (~50 mg) and TiO_2 (~50 mg) in graphite matrix (~550 mg). Synthetic samples of lithium titanate were prepared by mixing homogenously lithium sulphate and TiO_2 in graphite matrix. Four samples of sol-gel synthesized lithium titanate (~100 mg) were mixed homogeneously with graphite (~550 mg) as matrix. All homogenously mixed samples were palletized using hydraulic press machine as described earlier **[54]**.

2.3.4 Preparations of boron based stoichiometric compounds and samples

Boric acid standard and different samples were prepared in pellet form in cellulose

matrix for the PIGE experiment. Boron standard pellets were prepared by homogeneously mixing varying amounts of boric acid (~25−250 mg with effective B mass ~4.4−44 mg) with a fixed amount of CaF_2 (~25 mg) in cellulose matrix. Targets of stoichiometric compounds, namely lithium metaborate ($LiBO_2$), borax ($Na_2B_4O_7.10H_2O$), borazine ($B_3N_3H_6$), and samples (boric acid and boron carbide enriched with ^{10}B, natural boron carbide, carborane, elemental boron, and borosilicate glass) were prepared by homogeneously mixing known amounts (~50−100 mg) of samples and CaF_2 (~25 mg) in cellulose matrix. Another set of samples, namely boron carbide (natural and enriched with ^{10}B) and boric acid (enriched with ^{10}B), were prepared by wrapping the pellets with thin aluminum foil (~1.5mg cm^{-2}), instead of mixing F. Synthetic samples of B_4C were also prepared by mixing different amounts of enriched and natural boron carbide for isotopic composition studies **[55]**.

2.4 Irradiation details

The targets in pellet form were mounted on target ladder are shown in **Fig. 2.3, 2.5** and **2.7** respectively. The targets were kept under vacuum (~10^{-6} Torr) inside a small scattering chamber for irradiation. The set up of PIGE facility at FOTIA, IOP and TIFR are shown in **Figs. 2.2**, **2.4** and **2.6**. The target pellets, placed at 45° to the beam direction, were irradiated using a 4 MeV or 8 MeV proton beam (current 10−15 nA) from tandem accelerators (**Section 2.3**). The irradiation time was varied from 15-60 minute depending on the concentrations of analyte in the target. HPGe detector was placed perpendicular to the beam direction at a fixed distance of 7 to 15 cm from the target ladder to measure gamma-rays. Replicate sample analyses were carried out to evaluate the reproducibility of PIGE measurements. Gamma-rays which were measured in present study are detailed in **Table 2.1.** The dead time of the detector was maintained below 5%. During experiments, personal exposure from proton and gamma-rays was avoided, as the counting systems were kept outside the beam hall.

Gamma-ray spectra were analyzed using peak-fit software called Pulse Height Analysis SofTware (PHAST) for peak area determination. In order to ensure lower counting statistical errors, accumulated counts under the gamma-ray peaks of interest of boron in samples were kept in the range of 20,000−1,00,000 whereas, for *in situ* current normalizers (like Li, F or Al), the counts were in the range of 80,000−5,00,000.

Table 2.1: Nuclear reaction and gamma-ray energies used in PIGE work

Element	Reaction	Energy (keV)
Lithium	$^{7}Li(p, p'\gamma)^{7}Li$ $^{7}Li(p,m\gamma)^{7}Be$	478 429
Boron	$^{10}B(p, \alpha\gamma)^{7}Be$ $^{10}B(p, p'\gamma)^{10}B$ $^{11}B(p, p'\gamma)^{11}B$	429 718 2125
Oxygen	$^{16}O(p, p'\gamma)^{16}O$	6129
Fluorine	$^{19}F(p, p'\gamma)^{19}F$	110, 197, 1236
Sodium	$^{23}Na(p, p'\gamma)^{23}Na$	440
Aluminum	$^{27}Al(p, p'\gamma)^{27}Al$	844, 1014
Silicon	$^{28}Si(p, p'\gamma)^{28}Si$	1263, 1779
Titanium	$^{48}Ti(p, p'\gamma)^{48}Ti$	985

2.5 Concentration calculation in PIGE and current measurement/ normalization

The activity (*A*) for a given gamma-ray of interest of an isotope produced in a thick target by a proton beam of energy *E* having range *x* is given by **Eq. 2.2**,

$$A = NI_o \int_0^x \sigma(E)dx \qquad (2.2)$$

$$= NI_o \int_{E_o}^{0} \frac{\sigma(E)dx}{\left(dE/dx\right)_E}$$

where *N* is number of target atoms/cm^3, I_o is the beam current, $\sigma(E)$ is the energy dependent gamma-ray production cross-section for a particular nuclear process and $(dE/dx)_E$ stopping

power of the matrix. The count rate R (in terms of counts per second, cps) of gamma-rays of interest emitted in bombardment of a thick target by a proton beam of energy (E_{max}) is given by

$$R(cps) = \left[\frac{\rho.N_A.\theta.C}{M}\right].I_o.\varepsilon_r.\int_{E_{max}}^{0}\frac{\sigma(E)dE}{\left(dE/dx\right)_E} \qquad (2.3)$$

where N_A is the Avogadro number, M is the atomic mass, ρ is elemental density (in g cm^{-3}), ε_r is the detector efficiency, θ is isotopic abundance of analyte, $(dE/dx)_E$ is the stopping power of target at beam energy E and C is the concentration (wt% or mg kg^{-1}) of analyte in the pellet. The major matrix used for preparing the sample and standards throughout the work was either cellulose or graphite which was in the range of ~90-95%. Thus, for such diluted samples, the stopping powers of sample and standard pellets for proton beam were mainly due to the matrix and thus it doesn't require stopping power correction. The **Eq. 2.3** in relative PIGE method can be expressed as follows for a sample and standard (reference):

$$\frac{R_{Sam}}{R_{Ref}} = \frac{C_{x,Sam}}{C_{x,Ref}} \times \frac{(I_o)_{Sam}}{(I_o)_{Ref}} \qquad (2.4)$$

As clear from **Eq. 2.4,** it is important to know the value of beam current ratio [$(I_o)_{Sam}/(I_o)_{Ref}$] As PIGE involves online measurement of gamma-rays emitted from the target, current measuring/normalization is an important aspect of accelerator based experiments. Therefore it is very important to measure/normalize beam current fluctuations during the experiment. Depending on the type of sample there are different approaches for measuring/normalizing the effects of beam currents during the experiment:

2.5.1 Thick and conducting sample

In case of thick and conducting samples beam current can be measured directly from the target. In this approach, the beam current variations are normalized by measuring the beam current and hence the total charge falling on the target. The target ladder is generally fixed with an electron suppressor for accurate measurement of charge. The electron

suppressor is floated with negative potential which will suppress the detection of emitted secondary electrons from the target. In this way it will help in measuring the charge correctly. In the present study the non-conducting sample targets were made conducting by using high purity graphite as matrix. The gamma-ray count rates (R) of interest from sample and standard were normalized by charge (Q *in* μC) falling on sample and standard which are irradiated separately. The charge normalized sensitivity of standard ($S_{Std,\ x})_N$ is arrived at using the following relation:

$$(S_{Std,x})_N = \frac{(R_x)_{Std}}{Q_{Std} \times C_{Std,x}} \qquad (2.5)$$

where $(R_x)_{Std}$, Q_{Std} and $C_{Std,x}$ are the count rate of gamma-ray of interest measured from standard, charge falling on the standard and the concentration of analyte 'x' (mg kg^{-1}) in the standard pellet, respectively. Similarly charge normalized count rates were obtained for the sample which can be used for determination of concentration of analyte simply by comparing with charge normalized count rate of standard. For concentration calculation of analyte in sample, the charge normalized count rate of sample is compared with sensitivity of standard using the following equation:

$$C_{Sam,x} = \frac{(R_x)_{Sam}}{Q_{Sam} \times (S_{Std,x})_N} \qquad (2.6)$$

where, $(R_x)_{Sam}$, Q_{Sam} and $C_{Sam,x}$ are the count rate of gamma-ray of interest measured from sample, charge falling on the sample and the concentration of analyte 'x' (mg kg^{-1}) in the sample pellet, respectively **[53-55,61]**.

2.5.2 Thick and non-conducting sample

In thick and non-conducting samples the beam gets completely stopped in the sample itself and measurement of beam current becomes difficult. For such samples, the current normalization is usually done by Rutherford backscattering spectroscopy (RBS) using a thin and mono-isotopic metallic foil of high Z element (e.g., Au, Ag or any other element) placed

before the targets **[46]**. In this method, the scattered beam particles are measured using solid Si based surface barrier detector, fixed at specific backward angles with respect to the beam. These backscattered particles can directly give the measure of charge fallen on the target. After irradiation, the count rate of the gamma-ray of interest from the sample is normalized by the count rate of the backscattered particles. Here the ratio of $(I_o)_{Sam}/(I_o)_{Ref}$ can be obtained from the ratio of RBS count rates of sample and standard since they are proportional to the RBS count rate obtained from backscattered particles from the standard and sample. The RBS normalized count rate of standard is obtained using following equation:

$$(S_{Std,x})_N = \frac{(R_x)_{Std}}{(RBS_{CPS})_{Std} \times C_{Std,x}} \qquad (2.7)$$

where $(R_x)_{Std}$, $(RBS_{CPS})_{Std}$ and $C_{Std,x}$ are the count rate of gamma-ray of interest measured from standard, RBS count rate for standard and the concentration of analyte '*x*' (mg kg^{-1}) in the standard pellet, respectively. Similarly charge normalized count rates were obtained for the sample which can be used for determination of concentration of analyte simply by comparing with charge normalized count rate of standard. For concentration calculation of analyte in sample the charge normalized count rate of sample is simply compared with sensitivity of standard using the following equation:

$$C_{Sam,x} = \frac{(R_x)_{Sam}}{(RBS_{CPS})_{Sam} \times (S_{Std,x})_N} \qquad (2.8)$$

where, $(R_x)_{Sam}$, $(RBS_{CPS})_{Sam}$ and $C_{Sam,x}$ are the count rate of gamma-ray of interest measured from sample, RBS count rate for sample and the concentration of analyte '*x*' (mg kg^{-1}) in the sample pellet, respectively.

2.5.3 In situ current normalization approach for thick sample

In case of thick and or non-conducting targets, instead of RBS approach, current normalization can be done through an *in situ* approach. In this approach a known amount of an element having good analytical sensitivity towards PIGE, (like Li, F or Al) which is not

present in the matrix, is added externally to the sample during target preparation. The count rate (counts per second, CPS) of the gamma-ray of interest is normalized with the sensitivity (S = CPS per unit mass or concentration) of the added element to account for the current variations, if any, during the experiment. The current normalized count rate of element of interest is referred as normalized count rate or normalized CPS in the rest of the thesis. This normalization procedure makes the analysis independent of any fluctuation in beam current during irradiation as the count rate of the current normalizing standard as well as the element of interest changes proportionally with the beam current.

$$(S_{Std,x})_N = \frac{(R_x)_{Std}}{(S_{IS})_{Std} \times C_{Std,x}} \qquad (2.9)$$

where $(S_{std,x})_N$ $(R_x)_{Std}$, $(S_{IS})_{Std}$ and $C_{Std,x}$ are current normalized sensitivity of elemental standard, the count rate of gamma-ray of interest measured from standard, sensitivity of internal standard for standard pellet and the concentration of analyte 'x' (mg kg^{-1}) in the standard pellet, respectively. For concentration calculation of analyte in sample, the *in situ* current normalized count rate of sample is simply compared with beam current normalized sensitivity of standard using the following relation:

$$C_{Sam,x} = \frac{(R_x)_{Sam}}{(S_{IS})_{Sam} \times (S_{Std,x})_N} \qquad (2.10)$$

where, $C_{Sam,x}$, $(R_x)_{Sam}$ and $(S_{IS})_{Sam}$ are the concentration of analyte 'x' (mg kg^{-1}) in the standard pellet, count rate of gamma-ray of interest of analyte in sample and sensitivity of internal standard for sample pellet, respectively.

2.6 Determination of isotopic composition

Isotopic composition of an element in a sample can be determined simultaneously with its total concentration using PIGE method. The isotopes of an element must have suitable gamma-rays and high sensitivity towards PIGE. Isotopic composition (IC) can be determined using PIGE method by comparing the peak area ratios of gamma-rays of two isotopes of an

element. The atom ratio of two isotopes of X, ($^{a}X/^{b}X$) can directly be obtained from peak areas under the γ-rays of isotopes of X (in standard and sample) as given below:

$$(^{a}X/^{b}X)_{Atom\ Ratio} = \left[\frac{\left(\frac{PA\ (^{a}X)}{PA\ (^{b}X)}\right)_{Sam}}{\left(\frac{PA\ (^{a}X)}{PA\ (^{b}X)}\right)_{Ref}}\right] \times \left[\frac{\theta\ (^{a}X)}{\theta\ (^{b}X)}\right]_{Ref} \qquad (2.11)$$

where $[\theta(^{a}X)/\ \theta(^{b}X)]_{Ref}$ is IC of X in standard. Using the atom ratio calculated using **Eq .2.11**, the atom % of ^{a}X can be calculated using following expression:

$$^{a}X\ (Atom\ \%) = \frac{(^{a}X/^{b}X)_{Atom\ Ratio}}{(^{a}X/^{b}X)_{Atom\ Ratio} + 1} \times 100 \qquad (2.12)$$

This approach was applied for determination of enrichment percent of boron with respect to ^{10}B described in **Chapter 5 [55]**. In the specific case of boron the above equation becomes as follows:

$$(^{10}B/^{11}B)_{Atom\ Ratio} = \frac{\left(\frac{PA(^{10}B)}{PA(^{11}B)}\right)_{Sam}}{\left(\frac{PA(^{10}B)}{PA(^{11}B)}\right)_{Ref}} \times \left(\frac{\theta(^{10}B)}{\theta(^{11}B)}\right)_{Ref} \qquad (2.13)$$

The $^{10}B/^{11}B$ atom ratio can directly be obtained from peak areas under the γ-rays of boron isotopes, where $[\theta(^{10}B)/\theta(^{11}B)]_{ref}$ for natural boron composition is 0.247. Then the atom % of ^{10}B can be calculated using the following expression:

$$^{10}B(Atom\%) = \frac{(^{10}B/^{11}B)_{\ Atom\ Ratio}}{(^{10}B/^{11}B)_{\ Atom\ Ratio}} \times 100 \qquad (2.14)$$

2.7 Experimental work on neutron activation analysis

In NAA method, a sample is irradiated in a flux of neutrons (from neutron sources like nuclear reactor and neutron generator) and subsequent counting of the induced radioactivity (β,γ) to determine the concentration of an analyte of interest, present in the sample. The nuclear reaction involving absorption of a neutron forming a compound nucleus in excited state that de-excites by the emission of prompt gamma-rays (PGNAA) and radiations like

alpha and beta. The emitted alpha and beta rays left the nucleus in excited state which de-excites via emitting gamma-rays (NAA) which are used for determining the concentration of analyte in a sample. NAA facility, Dhruva reactor at BARC was used for determination of Ti concentrations in sol-gel synthesized samples of lithium titanate. This is a 100 MW uranium metal fuelled reactor and neutron flux is ~1.8 x 10^{14} $cm^{-2}s^{-1}$. Cadmium absorbers are used as shut off rods. Long as well as short time irradiation facilities are available at Dhruva reactor at tray rod position and PCF respectively. Tray rod position and PCF were used for sample irradiations. The thermal neutron fluxes at tray rod position and PCF position were of the order of $3x10^{11}$ $cm^{-2}s^{-1}$ and 5×10^{13} $cm^{-2}s^{-1}$ respectively **[70]**.

2.7.1 Pneumatic carrier facility (PCF)

PCF is useful for short-lived activation products having half-lives in the range of seconds to minutes. Target material placed inside a carrier container, called rabbit, is pneumatically sent to the irradiation site. A clock starts the moment rabbit reaches the irradiation site and after a pre set time of exposure of the rabbit to neutrons in the reactor, it is retrieved pneumatically to the laboratory. Rabbit travels through a pipe that is very selective to the reactor facility and the diameter of the pipe depends on the size of the rabbit (2.5 cm). Since the distance between the rabbit shooting/retrieval site and irradiation site is fixed, the time taken for retrieval depends exclusively on the pressure of the gas used to carry the rabbit. The transport time varies between 2 to 3 s **[71]**.

2.7.2 INAA for Ti determination in lithium titanate

Titanium standards were prepared by homogeneously mixing known amount of TiO_2 (30–100 mg) with cellulose matrix. Similarly, synthetic samples for titanium were prepared by mixing varying amount of TiO_2 and lithium sulphate in cellulose matrix. Out of 1 g of homogeneously mixed powder, three samples of ~10 mg were sealed in polyethylene sheet

for irradiation. Sample, standard and synthetic samples, sealed in polyethylene, enclosed in polypropylene capsule were irradiated for 1 min at pneumatic carrier facility (PCF) of Dhruva reactor, BARC. The gamma-ray of 320 keV from ^{51}Ti ($t_{1/2}$ = 5.76 min) was measured by high resolution gamma-ray spectrometry using a 40 % relative efficiency HPGe detector coupled to PC based 8k MCA **[53]**. The concentrations of Ti in lithium titanate samples were determined using relative INAA method.

2.7.3 Concentration calculations in NAA

The following relation was used for determining the concentrations of Ti in various lithium titanate samples:

$$(C_i)_{Sam} = \frac{(R_i)_{Sam}}{(R_i)_{Std}} \times \frac{(m_i)_{Std}}{W_{Sam}} \times \frac{D_{Std}}{D_{Sam}} \qquad (2.25)$$

where, $(C_i)_{Sam}$ is the concentration of sample (usually in mg kg^{-1}), $(R_i)_{Sam}$ and $(R_i)_{Std}$ are count rate of analyte in sample and standard, respectively, $(m_i)_{Std}$ is the mass of the analyte in standard, W_{Sam} is the mass sample (in g) and D_{Sam} and D_{Std} are decay correction factors ($e^{-\lambda t_d}$) for activation products of sample and standard, respectively, where t_d is the decay period.

2.8 QA/QC in measurements

The quality of analytical data is reflected from various parameters under quality assurance (QA) programme. Quality control (QC) is a sub-set of QA which is carried out by analyzing primary standard or certified reference materials (RMs) or synthetic samples and evaluating accuracy of the method. In other words, this is referred as method validation. QA is carried out by performing the following:

(i) Analysis of QC samples for evaluating the accuracy of method

(ii) Analysis of samples using other reference methods

(iii) Evaluation of precision of method by replicate sample analysis

(iv) Evaluation of uncertainty

(v) Blank/background measurement and evaluation of detection limits

The first step of QA is to evaluate the accuracy of the method used. As described before, it is carried out using certified reference materials (RMs) obtained from various certifying bodies like NIST, IAEA and USGS. In the case of non-availability of RMs which is generally experienced in the cases of nuclear technology materials, synthetic samples as well as stoichiometric compounds (solid or solution) are used. To evaluate the accuracy of PIGE methods used, calibration plots were obtained by plotting current normalized count rate of analyte of interest in the standards against the varying concentrations in standard pellets. Since in most of the cases reference materials are not available, synthetic standards or synthetic samples were prepared in similar way to that of samples and analyzed. Wherever available, the reference materials were analyzed for validation of PIGE methods. For example; for Si, Al and Na, NIST and IAEA reference materials and for F, NIST 1645 (river sediment) were analyzed.

To validate the results, one or more other reference methods are also recommended. The reference methods could be atomic spectroscopic methods, mass spectrometric methods, classical methods and radio/nuclear analytical methods. The choice of reference technique is based on their principle as well as how they are practised like whether they are destructive or non-destructive in their approach. This approach of using a different technique will help in giving results without any bias which is expected if the sample is analyzed by same technique in different laboratories. The quality of the results are judged by the uncertainties or precision reported for the mean concentration values. The precision of the results is obtained by analyzing replicate samples in identical ways and it is evaluated from standard deviation ($\pm 1\sigma$ or $\pm 2\sigma$) of concentration values. Though this gives a measure of overall uncertainty from all independent parameters, the total uncertainty is obtained by error propagation of

individual uncertainty as given below (Eq. 2.16).Concentration calculation using relative method follows the simple equation,

$$Y = \frac{A \times B}{C} \qquad (2.15)$$

and the uncertainty on Y value is evaluated using following equation:

$$\left(\frac{\sigma_Y}{Y}\right)^2 = \left(\frac{\sigma_A}{A}\right)^2 + \left(\frac{\sigma_B}{B}\right)^2 + \left(\frac{\sigma_C}{C}\right)^2 \qquad (2.16)$$

$$(\sigma_Y\%) = \sqrt{(\sigma_A\%)^2 + (\sigma_B\%)^2 + (\sigma_C\%)^2} \qquad (2.17)$$

In the present case propagated uncertainty values were arrived at from the (i) counting statistics of samples ($\sigma_{CSE,Sam}$), standard ($\sigma_{CSE,Std}$), *in situ* current normalizer ($\sigma_{CSE,CN}$), (ii) uncertainties on their corresponding masses of sample ($\sigma_{m,Sam}$), standard ($\sigma_{m,Std}$) and *in situ* current normalizer ($\sigma_{m,CN}$) and (iii) uncertainty on the concentration of standard ($\sigma_{C,Std}$). The overall uncertainty in the result of concentrations of analyte can be obtained using following equation:

$$(\sigma\%) = \sqrt{(\sigma_{CSE,CN}\%)^2 + (\sigma_{CSE,Std}\%)^2 + (\sigma CSE_{,CN}\%)^2 + (\sigma_{m,Sam}\%)^2 + (\sigma_{m,Std}\%)^2 + (\sigma_{m,CN}\%)^2 + (\sigma_{C,Std}\%)^2} \quad (2.17)$$

If RBS method is used instead of *in situ* current normalizing method than uncertainty on RBS count rate and mass of the foil are considered instead of current normalizing (CN) element. Measurement of blank or background is an important aspect in gamma-ray spectrometry. Gamma-ray spectra in PIGE is relatively simpler and are not affected by ambient background coming from natural decay series and from ^{60}Co, ^{137}Cs and ^{40}K because the characteristic gamma-rays of low Z elements are different (**Chapter 1**, **Table 1**). For evaluation of detection limits, background counts under the gamma-rays of interest are used as input parameters (**Chapter 1, Equation 1.14**) along with elemental sensitivity. This indicates that the lower is the background count rate, better is the detection limit. If an isotope of interest has multiple gamma-ray peaks, the gamma-ray peak with higher yield and lower background will be preferred to achieve better (lower) detection limit. Further background details are given in **Chapter 1**, **Section 1.9**.

2.9 High resolution gamma-ray spectrometry

Prompt gamma-rays emitted during PIGE experiment and delayed gamma-ray in INAA, the irradiation were assayed using high resolution gamma-ray spectrometry using HPGe based detection system. This section gives a brief description about interaction or gamma-rays with matter, gamma-ray detection system and its electronics **[65-67]**.

2.9.1 Interaction of Gamma-rays with Matter

Gamma-rays interact with matter by more than 20 ways **[65]** but three of them play a major and important role: photoelectric absorption, pair production and Compton scattering. In the first two processes the entire energy of photon is transferred to the medium but in the latter process energy is deposited partially in the medium. These interaction processes are shown in the **Fig.2.8**:

(a) Photoelectric absorption (PEA)

When a gamma-ray interacts with an atom, the gamma-ray photon is absorbed by atom which results in ejection of an electron from the atom. The energy of an emitted electron is (E_e-) is equal to the difference between incident energy of gamma-ray (E_γ) and the binding energy of electron (E_b), expressed as below:

$$E_{e^-} = E_\gamma - E_b \qquad (2.13)$$

The ejected electron interacts with the medium resulting in ionization and excitation processes in the detector's material. The vacancy created due to ionization of electrons is quickly filled either through capture of a free electron from the medium or through any electronic rearrangement of electrons from other shells. In the process of rearrangement, the energy difference of two orbital is equal to the energy of emitted X-ray or Auger electron or summation of both. About 80% of interactions occur with K-shell electrons and the other 20% with L-shell electrons. The ionization produced is proportional to the gamma-ray energy

and hence the resulting signal is called full energy signal (peak) and the observed corresponding peak in the spectrum as photo peak. The photoelectric cross-section is given by the following relation:

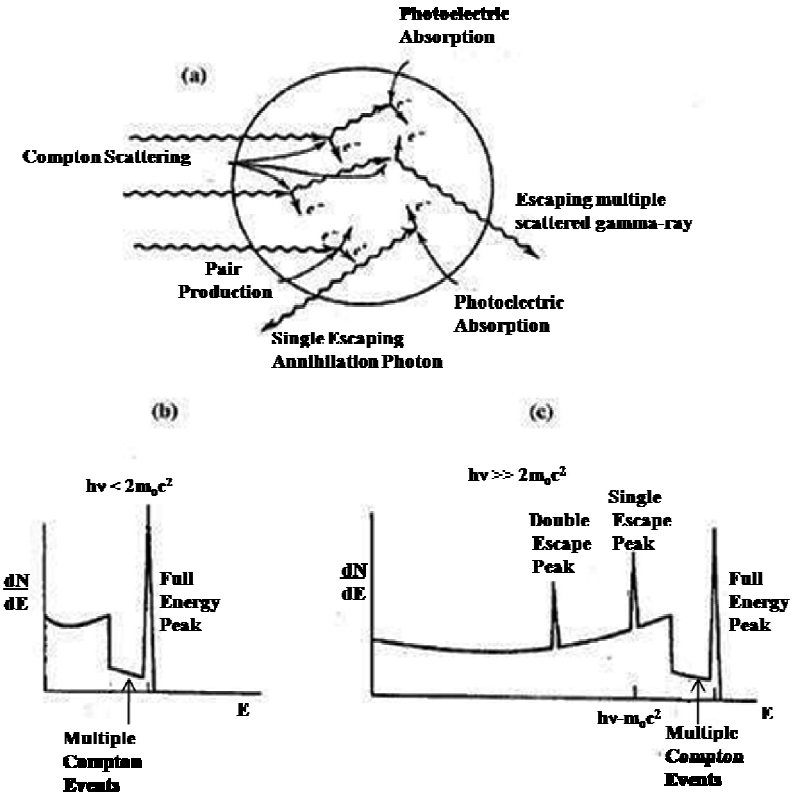

Fig.2.8: (a) Different interaction processes in HPGe detector
(b) Full energy peak with multiple Compton events
(c) Full energy peak and multiple Compton events with Ist and IInd escape peaks **[66]**

The exponent '*n*' varies between 4 and 5 over the gamma-ray energy region of interest **[65]**. The probability of the process increases sharply with the Z (atomic number) of the medium and decreases fast with the gamma-ray energy. The photoelectric process is the main mode of interaction for relatively low energy (< 1 MeV) of gamma rays and the absorber material of high atomic number. Due to this property, lead (Z=82) is used as common shielding material for gamma rays.

(b) Compton scattering

In this process, a photon of energy $E = h\upsilon$ is scattered by weakly bound/valence shell electrons of the medium. The scattered gamma-ray photon with a reduced energy of $h\upsilon'$ and the ejected electrons with kinetic energy of $h(\upsilon-\upsilon')$, move in the medium. The collision between stationary and free electron and photon is treated as elastic collision and hence the energy of scattered photon is given by the following equation:

$$h\nu' = \frac{h\nu}{1 + \frac{h\nu}{m_0 c^2}(1 - cos\theta)} \qquad (2.15)$$

where, $h\upsilon$ is the energy of incident photon, m_0c^2 is rest mass of the electron in the unit of energy, and θ is the angle of incidence between photon and scattered photon of gamma-ray. The energy of scattered electron extends from zero ($\theta = 0$) to a maximum value $\geq E_\gamma - m_0c^2/2$ at $\theta = 180°$. The Compton scattered electrons interact with detector material and results in a continuum in the gamma-ray spectrum from zero to a value which is roughly equal E_γ - *0.255 MeV*, if E >> 0.255 MeV. It is seen from the **Eq.2.15,** that energy lost is zero for $\theta = 0°$ and is maximum for photon scattered at $\theta = 180°$. Thus a Compton scattered photon never loses its entire energy in a single collision. The Compton process cross-section is given by following relation:

$$\sigma_C \, \alpha \, \frac{Z}{E_\gamma} \qquad (2.16)$$

Compton scattering is much significant for photons with energies range 1-5 MeV, for high Z materials and over a wide range of energies in the low Z materials.

(c) Pair Production

When energy of gamma-ray photon is more than $2m_0c^2$, it may produce a pair of electron and positron in the field of nucleus. The remaining energy of gamma-ray photon (E_γ-$2m_0c^2$) is shared by electron and positron as their kinetic energy. The electron and positron

lose their energy by interaction (ionization and excitation of the medium) with detector material. Positron, after thermalization under goes annihilation with electrons and produces two gamma-rays with 511 keV. These annihilation gamma rays move in opposite direction. They may interact with the medium or escape. If both the gamma rays of 511 keV are absorbed in the gamma ray detector, then it corresponds to the full energy deposition in the detector. On the other hand if one or both annihilation gamma rays escape then the energy deposited accordingly is either (E_γ-m_0c^2) or (E_γ-$2m_0c^2$). The cross-section for pair production phenomena is given by the following equation:

$$\sigma_P \, \alpha \, Z^2 \, ln(E_\gamma - 1.022) \qquad (2.17)$$

This interaction becomes very important when the energy is in the region of 5 MeV and above. The cross-sections for all these three processes are shown in **Fig. 2.9** as follows:

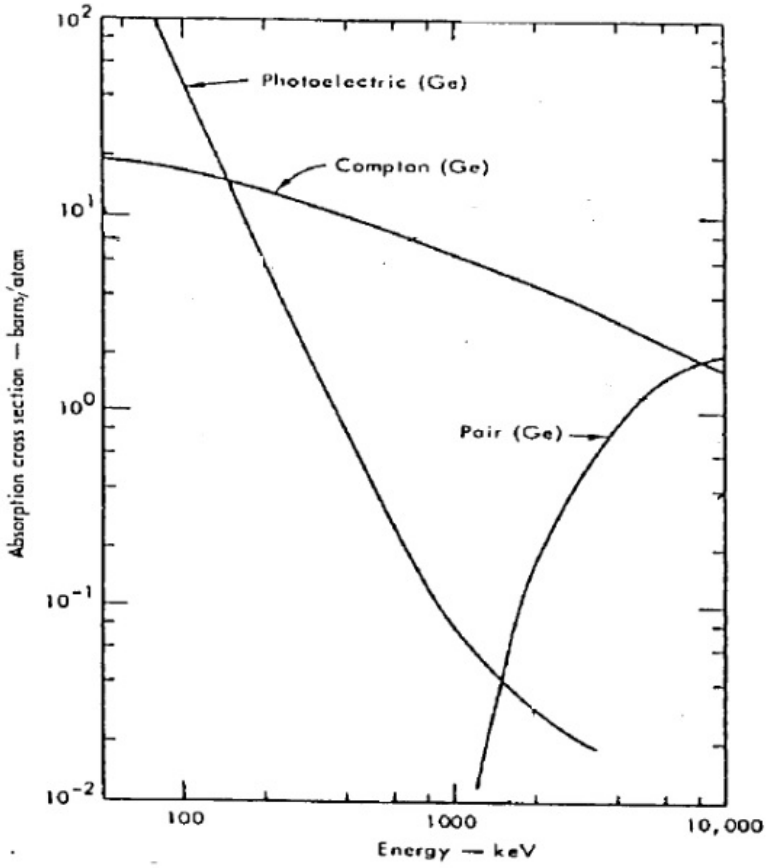

Fig. 2.9: Gamma-ray interaction cross-section in different processes namely photoelectric effect, Compton scattering and pair production in Ge targets **[66]**.

2.9.2 Gamma-ray detection system

A spectrometer receives gamma-ray pulses from the detector and sorts them according to their pulse height which is proportional to the energy of gamma-ray. Two types of detectors are used for detection of gamma-rays from the source: sodium iodide (thallium) (NaI(Tl)) and high purity germanium (HPGe) detectors. The inorganic scintillation NaI(Tl) detector, because of its high efficiency, availability in desired size and low price, is still useful in routine low-level measurements compromising on the spectral resolution. The HPGe detectors play a pivotal role in gamma-ray spectrometry because of their superior resolution and availability in higher relative efficiency. HPGe detectors have been used in the present study and will be discussed briefly here.

The high resolution gamma-ray spectrometer system consists of components like HPGe detector, high voltage (HV) unit, amplification system, analogue to digital convertor (ADC) and multi-channel analyser MCA **[66]**.

(a) HPGe Detector

Until 1970s the germanium crystals were not of high purity and were doped with Li to compensate for the p-type impurities to create intrinsic region. These detectors were called as Ge(Li) detectors **[67,68]**. With the advancement of technology, high purity Ge (concentration of defects $\leq 10^9$ cm^{-3}) crystals of practical sizes have been grown which leads to improve in their resistivity and make them to be used as a detector. These are called high purity germanium detectors (HPGe). There are two types of HPGe detector configurations: (a) n-type HPGe (uses Ge crystal formed by diffusing lithium or phosphorous ions) and (b) p-type HPGe (uses Ge crystal surface formed by implantation of boron ions) detectors. The p-type HPGe detectors used for gamma-ray spectrometry have relative efficiency in the range of 10 % to more than 100%. This relative efficiency is defined with respect to the efficiency of 3"x 3" NaI(Tl) detector at a detector to source distance of 25 cm for 1332 keV gamma ray of ^{60}Co

[69]. A schematic diagram of PIGE set up with HPGe detector is shown in **Fig.2.2.** The resolution which depends on the full width at half maximum i.e., FWHM is in the range of 1.8 to 2.1 keV at 1332 keV and peak to Compton ratio (P/C) is in the range of 40 to 50 **[66]**. High efficiency n-type detector with thin Al or Be window is available for high resolution gamma-ray spectrometry from low (10 keV) to high gamma-ray energy range and, the resolution and other properties are same as p-type detector. The Ge crystal of HPGe detector has to be cooled to liquid nitrogen (LN_2) temperature to minimize the leakage current and hence the system will be always attached to a LN_2 dewar via Cu rod.

(b) High Voltage Supply

The semiconductor detectors are operated in totally depleted condition with a sufficient over voltage so that high electric field is achieved throughout the detector that collects the charge generated in it. The bias supply is required only to operate the detector and it does not contribute any signal processing mechanism. High voltage/bias supplies for Ge detectors range is ±1500 V to ±5000 V with current capacities of 100 A. There will be provision to set the polarity (switch) and voltage (helipot with dial). The polarity and voltage as specified by the manufacturer is given to the detector.

(c) Preamplifier

Preamplifier is the most important part of the detector for optimum resolution. It collects the charges generated in the active region of the detector due to gamma-rays interaction and develops a tail pulse with a height proportional to the number of charges which in turn is proportional to the gamma-ray energy. The preamplifier is in close proximity to the detector and it provides an optimal coupling by minimizing the low voltage noise before its reaching the amplifier. As the resolution depends on the noise generated here, some components (like resistor) are cooled and kept under vacuum along with the detector crystal.

The remaining part is mounted just outside this vacuum assembly. The output tail pulse will have a height of few mV and decay time typically 50-100 μs.

(d) Amplifier

The pulses from preamplifier are amplified and shaped by the spectroscopic amplifier. The height of the pulse (normally in mV) is proportional to the incident gamma-ray energy. The tail pulse from pre-amplifier is fed to the amplifier where it is shaped (semi Gaussian shape) and amplified to get output in volts. The gain is adjusted to cover the energy range of interest; the highest energy peak should be within the ADC input range (normally 0-10 V). The Gaussian peak shape has two advantages; the signal to noise ratio is better for individual pulses and secondly the pulses return to the base line faster. Pole zero circuit maintains a stable baseline and the pileup rejection circuit improve performance of the amplifier during high count rate measurements. Normally unipolar output of amplifier is connected to the MCA.

(e) Multi channel analyzer

The pulse height analysis (PHA) of gamma-ray pulses coming from the main amplifier is carried out in MCA. The most important function of MCA is to convert the pulse height of the input pulses into a digital value and save the count in the appropriate counter that corresponds to digitized channel height. This is achieved by analogue to digital converter (ADC). Generally an ADC of 4k (12 bit-4096 channels) or 8k (12 bit-8192 channels) is used in gamma-ray detection system. In other words, a 4k ADC can sort the heights of the input pulses into 4096 discrete energy values and save into their memory. The other function of the MCA is to analyze the acquired data. This includes display of the differential spectrum (pulse height that is energy on X-axis and counts on Y-axis), calibration of the X-axis in terms of

energy, identification of the peaks, area integration of the peaks and calculation of FWHM of the peaks.

2.9.3 Energy and efficiency calibration

(a) Energy calibration

The energy calibration involves the relation between the pulse amplitude of a photo peak and channel number of MCA. This involves location of channel number of peak positions of gamma rays of different energies, covering the entire range of interest and fitting these channel number and energy of the gamma -ray to a linear equation. Standard sources such as ^{241}Am, ^{57}Co, ^{60}Co and ^{152}Eu are used for this purpose. The MCA is calibrated to 2.6 MeV where the slope is about 0.31 keV per channel. Depending on the requirement the conversion gain can be changed and so also the energy calibration. One has to note that, the multi-gamma source encompasses the energy range of interest. The energy calibration may deviate when energy range of interest is below or above the energies used for the calibration. This can be done by using standard multi-gamma source with known energies. Now-a-days use of multi-gamma sources such as ^{152}Eu has become routine in gamma ray spectrometry. The functional form of energy calibration is,

$$E = a + bx + cx^2 \qquad (2.18)$$

where, E is the gamma-ray energy, x is the channel number and a, b and c are the arbitrary constants that can be used for further calculations.

(b) Shape calibration

Once the peak is located and energy is assigned, shape calibration is done. For fitting the assumptions are: Gaussian peak with left tailing and polynomial background. For this FWHM is fitted into a polynomial of the form:

$$FWHM = p + qx + rx^2 \qquad (2.19)$$

The arbitrary constants p, q and r stored in the computer memory and used for subsequent analysis. The shape calibration helps in deconvoluting doublets or triplets from singlet due to their higher peak width (FWHM) than the assumed one. However, if the peak is naturally broad like in the case of Doppler broadened peak, the peak area is evaluated manually using linear subtraction of the Compton background.

(c) Resolution of detector

Generally the resolution of HPGe detector is sufficiently good to avoid interference of other peaks. The sensitivity of the system improves with the resolution of the detector. Since, the spectral line width is less; fewer background counts are obtained in doing peak integration. Resolution of the detector is measured using the following equation:

$$Resolution\ \% = \frac{FWHM\ (in\ keV)}{Peak\ Position, E_0\ (in\ keV)}\ x\ 100 \qquad (2.20)$$

The calculation of energy resolution for a detector is shown in **Fig. 2.10**. For checking true Gaussian nature, ratios such as full width at tenth maximum (FWTM) to FWHM (FWTM/FWHM = 1.82) and FW at fiftieth maximum (FWFM) to FWHM (FWFM/FWHM = 2.38) are measured and compared with standard values.

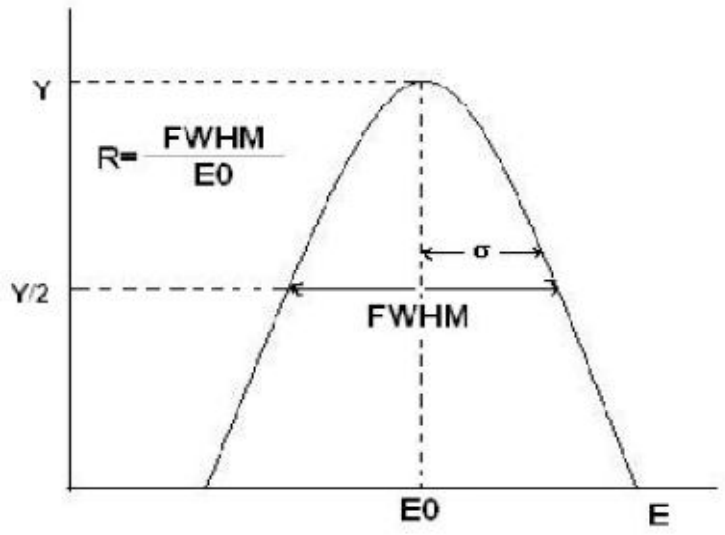

Fig. 2.10: Determination of resolution of detector from FWHM.

(d) Efficiency calibration

It is very important aspect of gamma-ray spectrometry for absolute quantification of the measured activity. The absolute full-energy peak efficiency of full energy peak/absolute photon detection efficiency (ε_{abs}) can be expressed as:

$$\varepsilon_{abs} = \frac{Total\ number\ of\ photon\ detected\ in\ full\ energy\ peak}{Total\ number\ of\ photons\ emitted\ by\ source} \qquad (2.21)$$

The detection efficiency depends on the sample-to-detector distance, the detector characteristics as well as the gamma-ray energy. It is determined as a function of energy by measuring the efficiency at a number of energies and fitting the experimental efficiency with an appropriate function. The following relation can be used for determining the absolute efficiency manually:

$$\varepsilon = \frac{CPS}{DPS \times a_\gamma} \qquad (2.22)$$

where, *DPS* is disintegrate per second of the known source. For a fixed detector to source geometry, absolute efficiencies (ε) are calculated using above equation for different energies using different sources and a graph is plotted between efficiency (log scale) and energy. A curve is obtained by fitting the data points by least square method using following equation. The peak efficiency (ε_p) depends on gamma-ray energy (E_γ) is usually formulated for calculation using a polynomial equation:

$$\ln(\varepsilon_p) = a + b.(lnE_\gamma) + c.(lnE_\gamma)^2 + \cdots \qquad (2.23)$$

The parameters (a, b, c…) are calculated by fitting procedure with the least squares method for experimental values of ε_p. The detection efficiency depends on sample geometry, matrix, distance from the the detector and active volume of detector or %relative efficiency.

Chapter 3

Applications of *In situ* Current Normalized PIGE Methods for Compositional Characterization of Barium Borosilicate Glass Samples by Determining Low Z Elements

Borosilicate glass (BSG) is a promising matrix for vitrification of nuclear waste generated from the spent nuclear fuel. Various Barium BSG samples were prepared using glass forming elements (like Si, B and O) glass modifiers (Li, Al, Ti, Ba etc.) along with NaF. Presence of F is expected mainly in dissolver solution of thoria based nuclear waste. Thus, chemical characterization of the vitrified glass is required as a part of chemical quality control as well as to estimate the retention percentage of F in these glasses. Two in situ current normalized particle induced gamma-ray emission (PIGE) methods were standardized using 4 MeV proton beam for compositional characterization of these BSG samples by determining the concentrations of F as well as other low Z elements like Si, B, Na, Al and Li. Sample and standard pellets were prepared either in cellulose and/or in high purity graphite matrix. Current normalization was carried out by in situ methods using Li as current normalizer or collecting charge from the target prepared in graphite matrix. For validating the PIGE methods, synthetic samples as well as reference materials were analyzed. The methods standardized are capable of non-destructive determination of low Z elements simultaneously.

3.1 Preparation of borosilicate glass and its composition

Borosilicate glass samples were prepared by mixing appropriate stoichiometric amounts of different chemicals of high purity grade like silica (~38-46 wt%), boric acid (equivalent to B_2O_3 ~21-26 wt%), barium nitrate (~ 9-11.5 wt%), sodium nitrate (equivalent to $NaNO_3$ ~11-14 wt%), sodium fluoride (~0.5-4.0 wt %) and corresponding salts of all other elements expected in the nuclear waste for 100 gm batch size scale transferred into a sillimanite crucible. The crucibles were heated gradually under static air using a resistance furnace (with a temperature controller to maintain the temperature within ±5 ^{o}C) and heated at 700 ^{o}C for 4 hours to complete the calcination process. Subsequently, the mixture was crushed to fine

powder using agate mortar and again heated in fireclay crucible. This was repeated for three times and finally the calcined product was transferred into a platinum crucible kept inside a furnace. The temperature of the furnace was increased in step-wise fashion with an interval of 50 ^{o}C and kept for 1 hour at corresponding temperature. The glass melt was then poured directly on clean stainless steel plate maintained at room temperature.

3.2 Role of low Z elements in borosilicate glass

In the present section the role of different low Z elements like Li, B, F, Na, Al and Si in defining the properties of BSG are discussed briefly. In borosilicate glasses, boron and silicon are known as main glass matrix formers. They form tetrahedral structural units with bridging and non-bridging oxygen atom e.g. Si form Q^4 and B form Q^3 structural units, respectively, in borosilicate glass (Q^i = non-bridging O atoms generated per tetrahedra, *i* represent number of non-bridging O atoms). Al creates Q^3 units at the expense of Q^4 and Q^2 units in silicate glasses. Al improves mechanical and chemical resistance and reduces the tendency for remixing. Al acts as a network former in low concentrations and occurs as AlO_4 tetrahedra in the glass structure. This structural unit improves the glass stability and hence the chemical durability. Alkali metals (like Na) are located near AlO_4 tetrahedra and balance their negative charge so that alkalis (Na) no longer act as modifiers in the silicate network. Being strongly bonded to AlO_4 tetrahedra, these alkali cations are not readily leached compared to alkalis which are more weakly bonded to non-bridging oxygen (NBO). This is true if the content of Al is relatively small as it also improves glass durability. However, addition of too much Al_2O_3 may be deleterious to the processing efficiency as higher processing temperatures are required. In practice, partial replacement of SiO_2 by Al_2O_3 from 3 to 10% is considered for significant improvement in the stability of the glasses in water and hence the leaching property.

Titanium is a network former in silicate glasses as the TiO_4 tetrahedra form glass structural units and like Al, Ti increases the viscosity and stabilizes the glass. Ti is unique among cations as it readily takes up fourfold, fivefold or six fold coordination in glasses and crystals. Five coordinated Ti is the dominant species in glasses rich in TiO_2 at concentrations exceeding 16 wt%. It behaves simultaneously as a network former and network modifier although dominant in the former role. Five-coordinated Ti is likely to bond to both NBO and bridging oxygen, acting as a new Q^4 species with one additional NBO. Lithium is usually added to improve glass properties. Other modifiers, particularly sodium, can be present in the waste. Sodium is a network modifier that tends to increase the number of NBO and apparently increases glass alterability by destabilizing its structure. A similar adverse effect on the initial alteration rate is observed for all the alkali metals but over quite different composition ranges.

Thoria containing spent fuels offer resistance with respect to dissolution because of its refractory nature. Developmental work carried out by several researchers **[72]**, envisages use of mixture of HNO_3 and HF for dissolution. In view of the corrosive nature of fluoride ions, $Al(NO_3)_3$ is also added to complex excess amount of fluoride ions. Thus, fluoride ions are present in significant amount in the nuclear waste generated during reprocessing stage of spent fuel. Nuclear waste needs to be immobilized in a suitable inert matrix like borosilicate glass, before their long term disposal in geological repositories **[73**]. It is reported that barium based BSG can accommodate up to 16 wt.% of ThO_2 without any phase separation [**74,75**]. Also, it has been reported that barium based BSG can contain fluoride ions up to 4 wt.% and fluoride ions exists as $F–Na_{(x)}Ba_{(y)}$ structural units. Only negligible amount of fluoride ions form Si–F linkages in the glass [**76**]. Presence of fluoride ions in glass is likely to affect physico-chemical properties of glass namely melt temperature, glass transition temperature, viscosity, coefficient of thermal expansion and chemical durability. Therefore, it is very important to understand the behavior of fluoride ions during vitrification of nuclear waste.

Vitrification process of nuclear waste using BSG is carried out at high temperature (~1,000 °C). Vitrification includes many steps like evaporation, calcinations, fusion and soaking, which are main events of this process. Retention of fluoride in the glass, therefore, becomes important to ascertain the extent of loss, if any, as they corrode the inconel containers used for the vitrification of nuclear waste. Therefore, it is important to quantify accurately the concentrations of these low Z elements including F in these glass samples with a suitable analytical method [**77-79**].

3.3 Chemical characterization of barium borosilicate glass

Chemical characterization of BSG is the most important step under chemical quality control (CQC) exercise. CQC helps in ensuring the quality of the prepared BSG with respect to the required chemical specifications before and after vitrification of simulated inactive nuclear waste. It involves quantitative analysis of major, minor and trace elements present in the finished borosilicate glass samples. Quantification of low Z elements is difficult by conventional analytical methods like AAS, ICP-MS and ICP-OES. However, laser microprobe inductively coupled plasma mass spectroscopy (LM-ICP-MS) has been employed, for example, to provide direct chemical analysis of vitrified glass samples both in their as-cast and leached states [**80**]**.** As borosilicate glass is a complex matrix, it requires high temperature and strongly acidic medium for dissolution of glass samples. Under these conditions, the volatile compounds like fluorides of alkali metals (like NaF and LiF), SiF_4, AlF_3 and BF_3 may escape from the solution, that may leads to underestimation of the contents actually present in the glass. For complex matrix sample, non-destructive methods like neutron activation analysis (NAA), prompt gamma-ray NAA (PGNAA), X-ray fluorescence (XRF) and particle induced X-ray emission (PIXE) and PIGE methods are preferred. X-ray based techniques (e.g., PIXE, and XRF) are not used for low Z elements due to self

attenuation of X-rays by the sample itself. In NAA, the neutron activation products of ^{27}Al (^{28}Al; $t_{1/2}$ = 2.24 min; 1,779 keV) and ^{23}Na (^{24}Na; $t_{1/2}$ = 15 h; 1368.5 keV; 2,754 keV) give high dead time and Compton background during gamma ray spectrometry. ^{23}Na also undergoes (n,αγ) threshold reaction with fast/high energy neutrons in reactor and produces ^{20}F ($t_{1/2}$ ~11.6 s), which is an interfering reaction for F present in the BaBSG matrix. In PGNAA presence of B in borosilicate glass matrix also reduces the neutron flux as B is a neutron poison leading to underestimation of the constituents. Therefore, NAA is not suitable to estimate low Z elements including fluorine in BSG samples. A suitable alternative is PIGE for non-destructive and simultaneous determination of low Z elements namely Li, B, F, Na, Al and Si **[36,39,61,62,81-83]**.

3.4 PIGE methods for simultaneous quantification of low Z elements including fluorine

PIGE technique utilizes measurement of prompt gamma-rays and it is capable of non-destructive determination of various low Z elements. It also requires minimal sample preparations for analysis. Details of nuclear reactions, gamma-rays of interest are given in **Chapter 1**, **Section 1.8**. Therefore, PIGE method was adopted for simultaneous determination of these low Z elements including F in various borosilicate glass samples. The following three approaches have been standardized for determination of F and other low Z elements in borosilicate glass samples following approaches

(i) PIGE method using RBS approach

In RBS method, current normalization is carried out by measuring backscattered ions from thin foils of mono-isotopic high Z metals like Au, Ag and W placed just before the sample. The backscattered particles (of ion beam) can be measured using a solid Si based

surface barrier detector kept at a fixed backward angle with respect to the ion beam. In this method, gamma-ray counts from the isotope of the element of interest are normalized by the RBS counts of protons. This method was used for non-destructive determination of fluorine concentrations in BSG samples. The standards of fluorine using NaF in varying amount (that corresponds to F concentrations in the range of 1000-40000 mg kg^{-1}) were prepared by homogenously mixing in cellulose as matrix. The method was validated by determining the concentrations of F in synthetic BSG samples (having F in the range of 600-4000 mg kg^{-1}) that were also prepared in cellulose matrix. The beam current variations were normalized by measuring the backscattered protons from thin (1.6 mg cm^{-2}) ^{197}Au foil **[61]**. A typical RBS spectrum is shown in **figure 3.8**

(ii) In situ current normalized PIGE method using lithium

In accelerator based experiments, current fluctuations can also be measured by an *in situ* method, where an element that is not present in the sample and has high sensitivity towards PIGE, in constant amount is added externally to the standard and samples. In this approach the gamma-ray counts from the isotope of the element of interest are normalized by sensitivity of internal standard. For determining the concentrations of F in BSG samples, Li was used as an *in situ* current normalizer. Standards, synthetic samples and samples were prepared in cellulose matrix with constant amount of Li in the form of lithium sulphate. The method was validated by calculating the concentrations of F, B, Al, Na and Si in synthetic samples **[61,62]**.

(iii) In situ charge/current normalized PIGE method using target in graphite matrix

In this method the gamma-ray counts from isotope of the element of interest were normalized by the total charge measured from thick conducting target. This PIGE approach was standardized for determination of Li, F, B, Na, Al and Si in three BSG samples. The

standard and samples were prepared in high purity graphite matrix. The method was validated by determining the concentrations of Na, Al and Si in NBS or NIST reference materials (RMs) **[46]**.

3.5 Results and discussion

3.5.1 Determination of Fluorine in Borosilicate Glass Samples

(i) PIGE Method using RBS Approach for Current Normalization

The calibration plot (**Fig. 3.1**) for F was obtained by plotting RBS normalized count rate (of197 keV gamma-ray of F) against the concentration of F (500-40000 mg kg^{-1}).

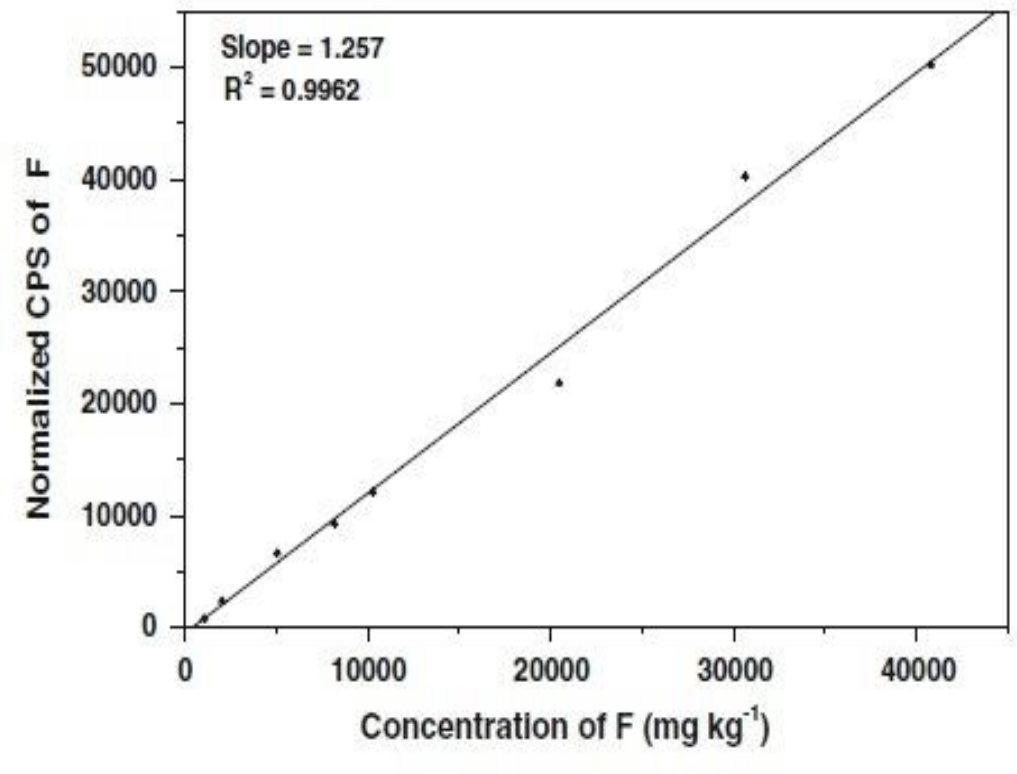

Fig. 3.1: RBS normalized count rate (CPS) of F with concentration of F.

Fig. 3.2 shows a typical gamma-ray spectrum of BSG sample. In order to validate the PIGE method, F contents were determined in four synthetic samples of BSG and also in one LiF

synthetic standard. The concentrations of F, determined in these five targets were in the range of 600-4000 mg kg^{-1}. The comparisons of expected and experimentally obtained values of fluorine

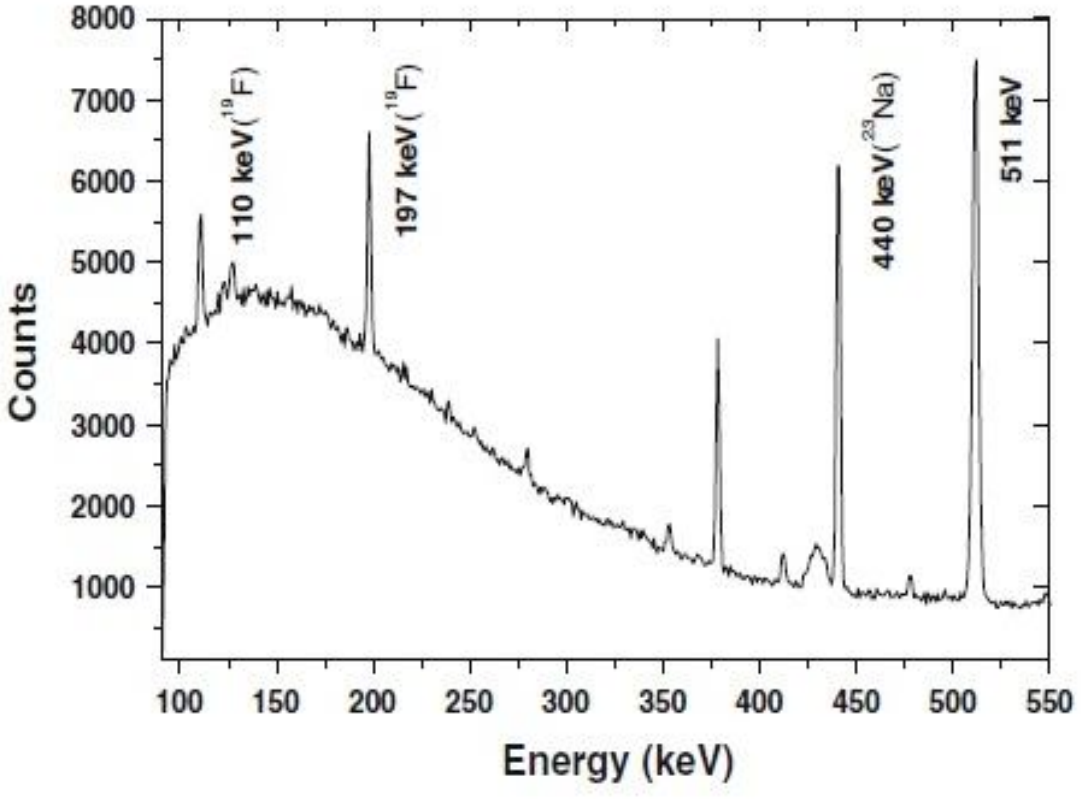

Fig. 3.2: Proton induced gamma-ray spectrum of a BaBSG sample (without Li).

concentrations in these synthetic targets are shown in **Fig. 3.3** which clearly shows a good agreement between experimentally determined concentrations of F against the expected values (within ±5%). The method was applied to five BSG samples and fluorine concentrations were determined which was in the range on 700-5000 mg kg^{-1} in BSG pellets that corresponds to 0.36-3.76 wt% of F in BSG samples (**Table 3.1**). The total propagated uncertainties in the results of F contents in synthetic targets of F and in the BSG samples were in the range of 1.0-4.0% which is mainly due to the counting statistics and peak fitting

errors. The other contributing factors to total uncertainty include masses of sample and standards (0.05-1.0%) and RBS counting statistics (0.1%) **[61]**.

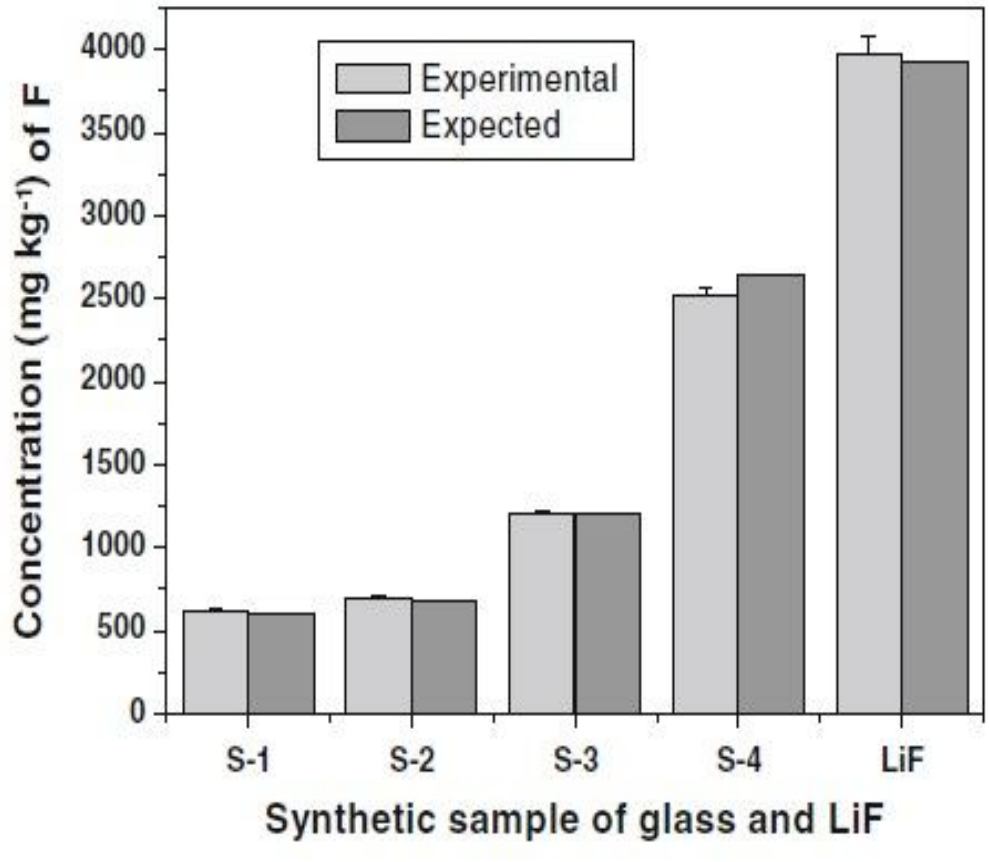

Fig. 3.3: Validation of PIGE method using RBS approach: Comparison between expected and experimental values of F.

Table 3.1: Results of F content in BaBSG samples using PIGE method RBS approach.

Sample-ID	F (mg kg^{-1}) obtained w.r.t. pellet mass	F (wt%) obtained w.r.t. actual sample mass
BSG-1	718 ± 27	0.36 ± 0.01
BSG-2	1622 ± 22	1.22 ± 0.02
BSG-3	3620 ± 65	2.72 ± 0.05
BSG-4	3760 ± 75	2.82 ± 0.06

BSG-5	5010 ± 60	3.76 ± 0.04

(ii) Determination of fluorine concentration using in situ PIGE method

The *in situ* current normalized sensitivity of F was obtained from calibration plot (**Fig. 3.4**) which was obtained by plotting the Li sensitivity (count rate of 478 keV gamma-rays per mg kg^{-1}) normalized CPS of 197 keV of F against the concentration of F (1000-40000 mg kg^{-1}) in standard pellets. The plot shows linearity for F concentration in the range 1,000–40,000 mg kg^{-1}. The sensitivity of F relative to Li is obtained by plotting a calibration plot between Li normalized 197 keV gamma-ray count rate of F against the concentration of F in standards

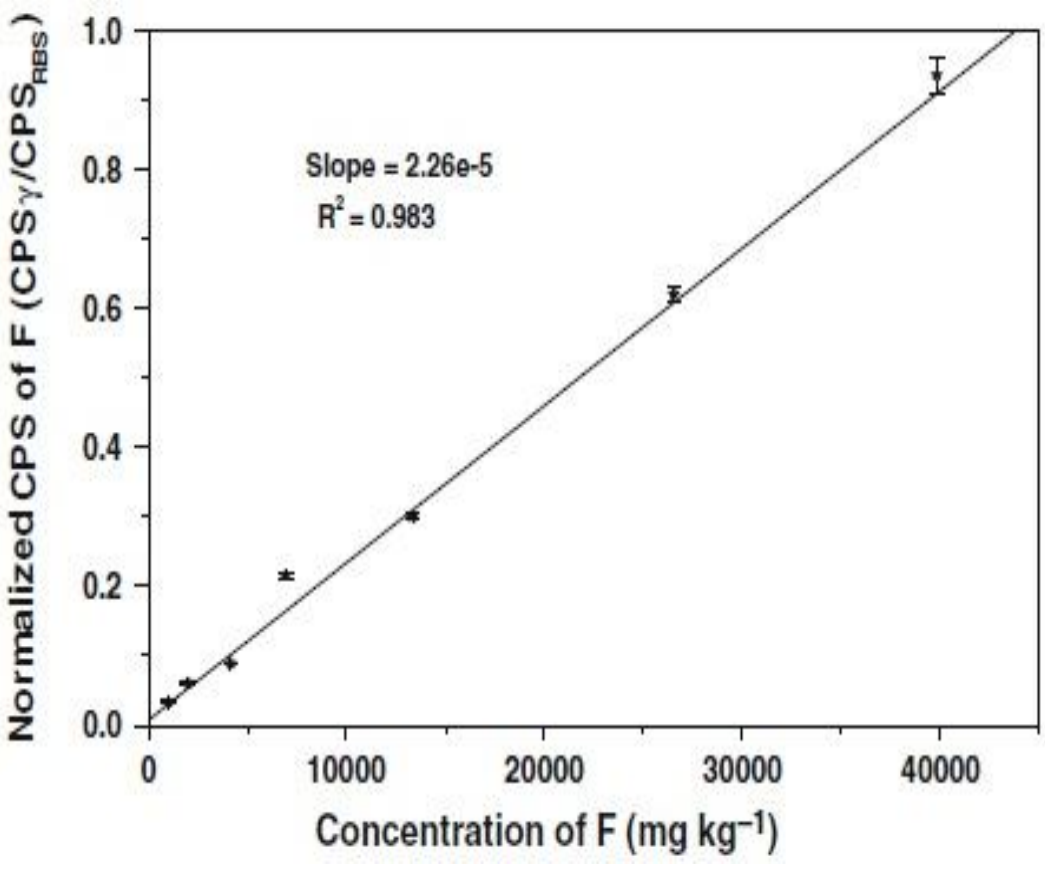

Fig. 3.4: *In situ* current normalized (using Li) count rate at 197 keV of ^{19}F with concentration of F.

Typical *in situ* PIGE gamma-ray spectrum of BSG sample containing Li as *in situ* current normalizer is shown **Fig. 3.5.** For method validation, concentrations of F in five synthetic borosilicate glass samples were determined. Control glass samples were also irradiated in

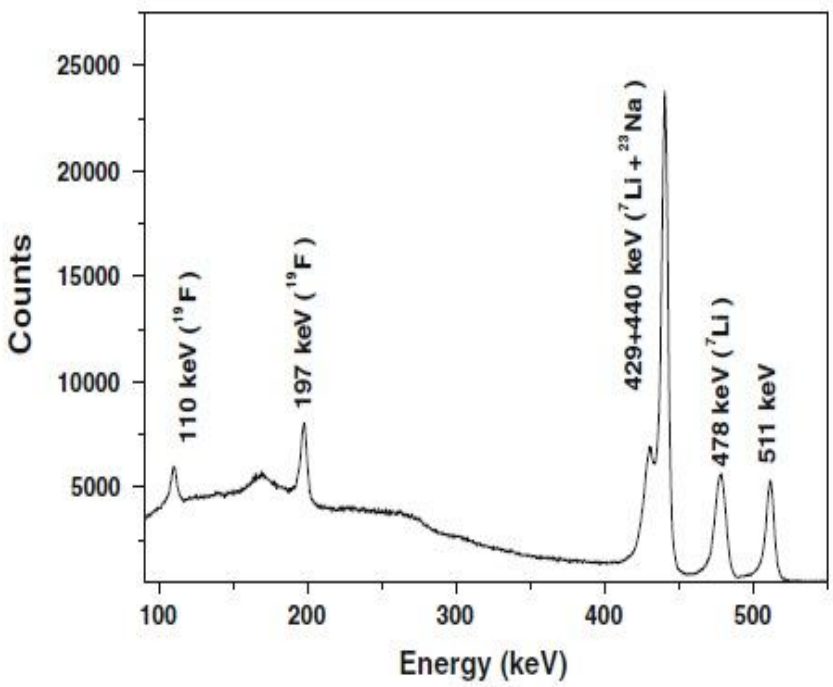

Fig. 3.5: Proton induced γ-ray spectrum of BSG sample (with Li) showing γ-rays of F and Li.

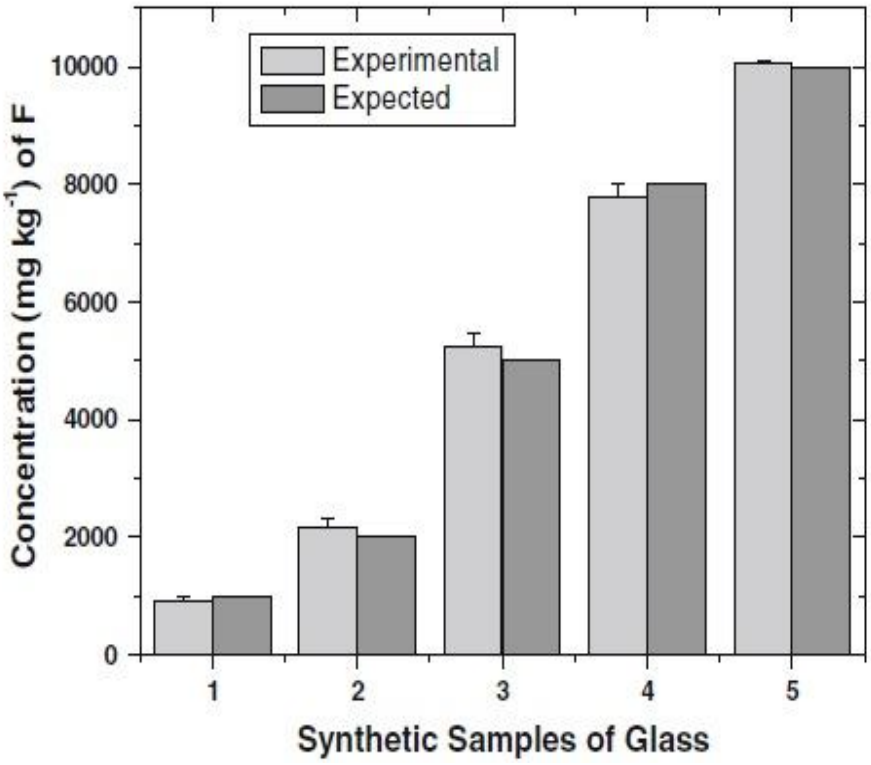

Fig. 3.6: Comparison of expected and experimentally determined concentration of F in synthetic samples using *in situ* approach.

order to ensure that Li can be used as *in situ* current normalizer for beam current normalization. The results of F concentrations in synthetic samples are shown in **Fig. 3.6**. The percentage deviations of F determined in synthetic samples which were in the range of ± 0.5–5% with respect to the expected values. The method was applied to two borosilicate glass

Table 3.2: Results of F content in BSG samples by PIGE method using Li as *in situ* current normalizer.

Sample-ID	F (mg kg^{-1}) obtained w.r.t. in pellet	F (wt%) in actual sample
BSG-1a	1722 ± 65	1.72 ± 0.07
BSG-2a	1487 ± 34	1.49 ± 0.03

samples results of which are shown in shown in **Table 3.2.** The uncertainties in the results of F concentrations determined in two borosilicate glass samples were less than ±4.0%. The 3σ detection limit (L_D) for F in seven BSG samples was calculated for both the methods using following equation (**Eq. 3.1**):

$$L_D = \frac{3\sqrt{C_b}}{LT \times S_F} \qquad (3.1)$$

where, C_b is background counts under 197 keV peak of F in sample spectrum, LT is live time of counting using HPGe detector and S_F is the sensitivity of F defined as follows:

$$S_F = \frac{Count\ Rate\ of\ F}{Concentration\ of\ F\ (in\ mg\ kg^{-1})} \qquad (3.2)$$

The detection limits achieved for F, using both the PIGE methods were in the range of 16–19 mg kg^{-1}. Due to variation in the background counts we obtained a range in L_D values of F **[61]**.

3.5.2 Applications of in situ current normalized PIGE method for analysis of borosilicate glass samples

Besides fluorine, the other low Z elements namely Li, B, Na, Al and Si were determined in various BSG samples using *in situ* current normalized PIGE methods.

Method 1: In situ PIGE method using Li as current normalizer

Method validation

The *in situ* current normalized PIGE method was validated by determining fluorine in NIST SRM 1645 and Na, Al and Si in two NBS SRMs 1633a and 1645a samples. Li was used as *in situ* current normalizer. The *in situ* current normalized count rate of the gamma-ray of interest from the sample and standard were used for concentration calculations (**Chapter 2, Section 2.6, Eq. 2.9 & 2.10**). The results of F, Na, Al and Si for three reference materials

are shown in **Table 3.3**. The percentage deviations in the results RMs were within 10% (≤ 6% for F, ≤ 8 for Na, ≤ 5% for Al and ≤ 8% for Si). The propagated uncertainties due to counting statistics, peak fitting and sample and standard masses in the results of these RMs is less than 3% (**Table 3.3**) [62].

Results from PIGE analysis of borosilicate glass samples

Concentrations of different low Z elements (B, F, Na and Si) in ten BSG samples were determined using *in situ* PIGE method. The typical PIGE spectrum of one of the glass samples is shown in **Fig. 3.7**. Lithium was used as *in situ* current normalizer. The sensitivity of Li obtained from gamma-ray of 478 keV energy from $^{7}Li(p, p'\gamma)^{7}Li$ nuclear reaction was used for obtaining the current normalized sensitivities of different low Z elements. The sensitivities for different low Z elements (**Chapter 2, Section 2.6, Eq. 2.9**) thus obtained were used for determining their concentrations in BSG samples (**Chapter 2, Section 2.6, Eq. 2.10**). The results of concentrations of different low Z elements in ten borosilicate glass samples are presented in **Table 3.4**. The concentrations of F, Na and Si were in the range of 0.19-3.59 wt%, 8.24-11.58 wt% and 16.24-18.00 wt%, respectively.

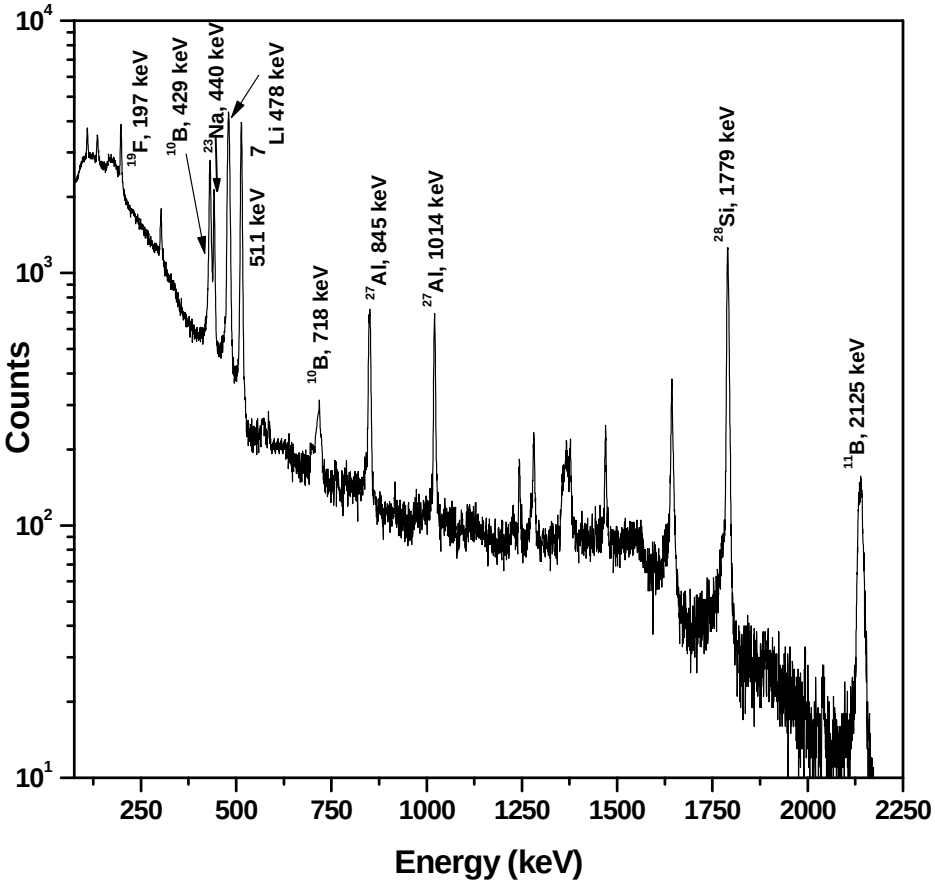

Fig. 3.7: Typical PIGE spectrum for one of the borosilicate glass sample prepared in high purity graphite matrix.

Boron concentrations were determined using 718 keV and 2125 keV of gamma-rays which are in the range of 4.28-9.34 wt% and 4.53-9.23wt%, respectively. The propagated uncertainties in the results were due to the counting statistics, peak fitting errors, masses of samples, standards and *in situ* current normalizer. The uncertainties due to counting statistics and peak fitting is ≤ 1.0% for F, ≤ 1.1% for Na and Si, and < 3.0% for B (using 718 keV) and < 2.0% for B (using 2125 keV), respectively. The uncertainties due to masses of sample, standard and in situ standard are less than 0.05, 0.1 and 0.5, respectively (**Table 3.4**) **[62]**.

Table.3.3: Elemental concentrations (in wt% unless indicated) determined by PIGE in various NIST reference materials.

Element	NIST RM 1633a	
	Certified Value	Experimental Value
Na*	1700 ± 100	1739 ± 72
Al	14.30 ± 0.8	14.79 ± 0.5
Si	22.8 ± 0.8	23.8 ± 1.5
Element	NIST RM 1645a	
	Certified Value	Experimental Value
Na*	5005 ± 90	5400 ± 100
Al	2.36 ± 0.04	2.26 ± 0.04
Si	20.44 ± 0.31	23.3 ± 2.7
Element	NIST RM 1645	
F*	900 ± 13**	950 ± 21

*The Concentrations are mg kg^{-1}
**Information value

Table 3.4: Results of BSG samples analyzed by *in situ* current normalized PIGE method (% uncertainties are given in parenthesis)

Sam-Id	**B(wt%) by 718 keV**	**B (wt%) by 2125 keV**	**F (wt%)**	**Na (wt%)**	**Si (wt%)**
Sam-1	5.74 (2.6)	6.16 (1.5)	0.40 (0.8)	9.52 (1.1)	16.24 (1.1)
Sam-2	6.29 (2.5)	5.82 (1.5)	0.68 (0.7)	10.36 (1.1)	16.60 (1.1)
Sam-3	5.29 (2.7)	5.38 (1.5)	ND	13.26 (1.1)	17.94 (1.1)
Sam-4	4.28 (2.8)	4.53 (1.6)	0.32 (1.0)	10.88 (1.1)	16.48 (1.1)
Sam-5	9.34 (2.4)	9.14 (1.4)	0.19 (1.0)	10.54 (1.1)	18.00 (1.1)
Sam-6	9.07 (2.5)	9.23 (1.4)	0.40 (0.8)	11.58 (1.1)	17.84 (1.1)
Sam-7	8.51 (2.4)	8.70 (1.4)	0.81 (0.7)	9.44 (1.1)	17.19 (1.1)
Sam-8	8.71 (2.4)	8.81 (1.4)	1.71 (0.6)	9.16 (1.1)	16.67 (1.1)
Sam-9	6.60 (2.5)	6.47 (1.5)	3.33 (0.6)	8.24 (1.1)	16.40 (1.1)
Sam-10	6.26 (2.6)	6.11 (1.5)	3.59 (0.6)	9.02 (1.1)	16.50 (1.1)

ND – not detected

Method 2: In situ PIGE method using targets in graphite matrix

Method validation

In this method the beam current variations were normalized by dividing the count rate of gamma-ray of interest with total charge fallen on the target during irradiation. For measuring the charge from the target, the standard, sample and synthetic standards were prepared in graphite matrix for making them conducting. The concentrations of different low Z elements like F, Li, B, Na, Si and Al were calculated (**Chapter 2, Section 2.6, Eq. 2.6**). The method was validated by analyzing the concentrations of F, Li, Al, Na, B and Si in two synthetic samples (**Table 3.5**). The results obtained for two synthetic standards are in good agreement with the expected values (**Table 3.5**). The total propagated uncertainties in the results of synthetic standards due to the counting statistics, peak fitting errors as well as masses of sample and standards. The measured total uncertainties in the results of synthetic standards were less than 1% for Li (using 478 keV), Si (using 1779 keV), Al (using 1014 keV) and for B (using 2125 keV); ≤ 1.5% for B (using 718 keV), ≤ 0.5% for F (using 197 keV) and Na (using 440 keV) (**Table 3.5**).

Results from PIGE analysis of borosilicate glass samples

The charge normalized PIGE method was applied to three borosilicate glass samples. The total elemental concentrations of low Z elements obtained for three BSG samples, using charged normalized PIGE method, were in the range of 0.75-0.96 wt% for Li, 4.10-4.80 wt% for B (using 718 keV) and 4.04-5.02 wt% for B (using 2125 keV), 1.03-1.43 wt% for F, 9.61-10.74 wt% for Na, 1.84-2.88 wt% for Al and 16.35-18.17 wt% for Si, respectively (**Table 3.6**). The total propagated uncertainties reported in the results of Li, B, F, Na, Al and Si estimation were less than < 2%. The propagated uncertainties are due to the mass of sample and standards, counting statistics and peak fitting errors **[62]**.

Table 3.5: Validation of *in situ*-PIGE method using Li as *in situ* current normalizer

Sam Id	Li wt%		B wt%			F wt%		Na wt%		Al wt%		Si wt%	
	Expected	Obtained	Expected	Obtained 718 keV	Obtained 2125 keV	Expected	Obtained	Expected	Obtained	Expected	Obtained	Expected	Obtained
Syn-1	1.53	1.52(0.6)	3.58	3.61 (1.3)	3.60 (0.7)	7.68	7.49 (0.3)	10.03	10.08 (0.3)	13.24	13.24 (0.5)	14.05	14.02 (0.7)
Syn-2	3.78	3.76 (0.5)	8.75	8.70 (1.2)	8.74 (0.7)	17.11	17.43 (0.3)	21.76	21.77 (0.3)	21.56	21.59 (0.6)	23.47	23.54 (0.7)

Table 3.6: PIGE results of borosilicate glass samples containing waste (% uncertainty in results is given in parenthesis)

Sample Id	F wt%	Li wt%	B wt% 718	B wt% 2125	Na wt%	Al wt%	Si wt%
Sam-1	1.03 (0.7)	0.96 (0.7)	4.80 (1.5)	5.02 (1.0)	10.74 (0.3)	1.84 (1.3)	18.17 (1.0)
Sam-2	1.19 (0.7)	0.83 (0.7)	4.30 (1.5)	4.41 (1.0)	9.95 (0.3)	2.25 (1.2)	16.61 (1.0)
Sam-3	1.43 (0.6)	0.75 (0.8)	4.10 (1.5)	4.04 (1.0)	9.61 (0.3)	2.88 (1.1)	16.35 (1.0)

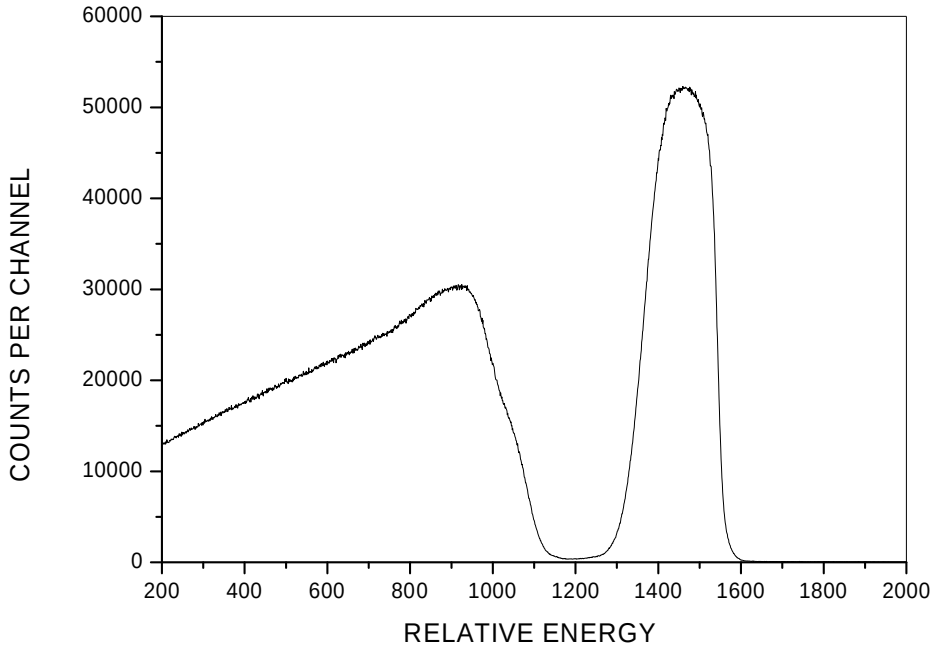

Fig. 3.8: A typical RBS spectrum of thin Au foil recorded from 4 MeV backscattered proton.

Conclusions

Three PIGE methods were standardized for determination of low Z elements in barium borosilicate glass samples. These PIGE methods are non-destructive in nature and are capable of giving results of various low Z elements like Si, B, F, Na, Al and Li simultaneously. The results of F concentrations will be helpful in estimating the retention/loss of F contents in vitrified barium borosilicate glass samples. The methods were free from interferences as far as the concentration determination is concerned since no gamma-ray interferences were observed for these elements.

Chapter 4

Application of PIGE Methods for Lithium Based Ceramics: (i) Li Doped Neodymium Dititanate and (ii) Lithium Titanate

In the present work two types of Li based ceramics namely Li doped neodymium dititanate and lithium titanate, were analyzed by PIGE methods. In situ current normalized PIGE method using 4 MeV proton beam was standardized for determination of major to trace concentrations of Li using 478 keV gamma-ray from $^{7}Li(p,p'\gamma)^{7}Li$. Since concentrations of Ti and O could not be determined by PIGE using 4 MeV proton beam, a method using 8 MeV proton beam was standardized for simultaneous determination of Li, Ti and O in lithium titanate samples.

Lithium doped $Nd_2Ti_2O_7$ (NTO) is a high temperature ferroelectric material, whose behavior can be tailored by doping varying amount of Li. The main objective of this study was to estimate the loss of Li from Li doped $Nd_2Ti_2O_7$ after heat treatment (800 °C, 10 h). Characteristic gamma-rays of 478 and 197 keV from ^{7}Li and ^{19}F were measured using high resolution gamma-ray spectrometry. The Li concentrations obtained in precursor and heat treated samples of Li doped NTO were in the range of 0.31–0.85 wt% and 0.29–0.55 wt%, respectively.

Lithium titanate (Li_2TiO_3), a tritium breeding material for D–T reaction based fusion reactor (under ITER programme), was synthesized through sol–gel route. For chemical quality control and optimization of its synthetic route, PIGE and instrumental neutron activation analysis (INAA) methods were standardized for the determination of Li and Ti concentrations in the finished lithium titanate samples. Concentrations of lithium and titanium and Li/Ti mole ratios were determined and compared with the stoichiometric concentration of Li_2TiO_3. A PIGE method using 8 MeV proton beam from BARC-TIFR Pelletron facility, was also standardized for determination of Li, Ti and O simultaneously, in sol-gel synthesized Li_2TiO_3 samples. In this method, RBS method using thin gold foil was used for normalizing beam current variations during the experiment. The concentrations of Li, Ti and O were determined by measuring gamma-rays of 478, 983 and 6129

keV for Li, Ti and O from $^{7}Li(p, p'\gamma)^{7}Li$, $^{48}Ti(p, p'\gamma)^{48}Ti$ and $^{16}O(p, p'\gamma)^{16}O$ nuclear reactions, respectively, using high resolution gamma-ray spectrometry.

4.1 Introduction to lithium based ceramics: Lithium doped neodymium dititanate and lithium titanate in the present study

4.1.1 Lithium doped neodymium dititanate

Neodymium dititanate, $Nd_2Ti_2O_7$ (NTO), is a member of small family of rare earth titanates $Ln_2Ti_2O_7$ (Ln = La, Ce, Pr and Nd), which exhibits ferroelectric properties at high temperature. The ferroelectric properties of NTO can be modified by substituting Nd or Ti with lower oxidation state cations of alkali and alkaline earth metals. In order to study the effect of Li doping on ferroelectric properties, NTO samples with varying concentrations of Li were prepared by gel entrapment technique **[52,84,85]**.

Ferroelectric materials, for example, barium titanate and Rochelle salt, are composed of crystals in which the structural units are tiny electric dipoles, that is, in each unit the centres of positive and negative charge are slightly separated. Ferroelectric materials can be used to make capacitors with tunable capacitance and ferroelectric RAM [91]. Ferroelectric capacitors are used in medical ultrasound machines (the capacitors generate and then listen for the ultrasound ping used to image the internal organs of a body), high quality infrared cameras (the infrared image is projected onto a two dimensional array of ferroelectric capacitors capable of detecting temperature differences as small as millionths of a degree Celsius), fire sensors, sonar, vibration sensors, and fuel injectors on diesel engines.

4.1.2 Lithium titanate

Currently, studies on deuterium-tritium (D-T) reaction based fusion reactor under International Thermonuclear Experimental Reactor (ITER) programme are being carried out. It is based on the following nuclear fusion reaction:

$$D + T \rightarrow {}_{2}^{4}He\ (3.5\ MeV) + {}_{0}^{1}n\ (14.1\ MeV), \qquad [Q = 17.6\ MeV] - - - (4.1)$$

The prototype of ITER thermonuclear demonstrator reactor, are fueled by T and D. Due to very low abundance of tritium (T) in nature, it is required to produce T artificially. Lithium-containing ceramic (lithium titanate, lithium silicate, lithium aluminate etc.) pebbles can be used as solid breeder materials in a component known as a Helium Cooled Pebble Bed (HCPB) breeder blanket, for the production of tritium. The HCPB breeding blanket constitutes a key component of the ITER reactor design. In such reactor designs tritium is produced by neutrons leaving the plasma and interacting with ^{6}Li in the blanket as per following reaction:

$$ {}_{3}^{6}Li + {}_{0}^{1}n\ (14\ MeV) \rightarrow {}_{2}^{4}He\ (2.1\ MeV) + {}_{1}^{3}H\ (2.7\ MeV) - - - (4.2)$$

Tritium breeding materials in HCPB must exhibit high tritium release, low activation, good thermo-physical stability and low neutron activation characteristics [**87,88**]. The lithium based tritium breeders include Li_2O, Li_2ZrO_3, Li_2TiO_3, $LiAlO_2$ and Li_4SiO_4 **[89]**. Li_2O is a good tritium breeder but not considered because of high sensitivity towards moisture [**90**]. Out of these ceramics, lithium titanate (Li_2TiO_3) is considered as one of the suitable candidates for blanket material because of ease of tritium recovery at low temperature and good chemical stability **[91,92]**.

4.2 Synthesis of Li doped $Nd_2Ti_2O_7$ and Li_2TiO_3

4.2.1 Preparation of Li doped neodymium dititanate

Gel entrapment technique **[85, 92**] is an attractive solution based technique used for synthesizing homogeneous precursor powder of multi-component system, which on suitable heat treatment forms phase-pure powder at low temperature. This technique is simple, cost effective, does not involve filtration or washing and is capable of producing product with micro-homogeneity without repeated grinding and firing.

$Nd_{2-x}Li_xTi_2O_{7-\delta}$ samples in which x=0, 0.1, and 0.15 were synthesized by gel entrapment technique method [**85**]. For the preparation of the compounds, appropriate amounts of $Nd(NO_3)_3$, $TiOCl_2$, $LiNO_3$ and 0.2 moles of NH_4NO_3 were mixed in a 500 ml beaker. To this mixture, 1 M hexamethylene tetra ammine (HMTA) solution was added at room temperature leading to formation of a hard gel. The gel was dried at 180 °C and then ignited at 250 °C, leaving behind a fluffy mass. This precursor powder was further heated to 500 °C in flowing O_2 atmosphere to remove any leftover organic matter and finally to 800 °C for 6 h to get phase-pure compound.

4.2.2 Preparation of Li_2TiO_3

The internal gelation based sol–gel synthetic route was used for preparation of lithium titanate pebbles. The microspheres were prepared by dispersing feed solution prepared by mixing 3 M HMTA, urea solution with mixture of 3 M $TiOCl_2$ and 3 M $LiCl/LiNO_3$ solution in the required ratio (Li:Ti = 2:1 mole ratio). Feed solution was dispersed through a stainless steel capillary of 0.8 mm diameter in hot silicone oil which is circulated into a glass column. The feed droplets become hard as they travel down the column with counter current flow of silicone oil. The microspheres are separated from the oil and washed with CCl_4 to degrease the surface. Digestion of degreased microspheres were carried out in 1.55 M LiOH at 60 °C which was then washed with 1.55 M LiOH to remove left out chemicals and reaction products from the spheres.

This prevents the microspheres from cracking during drying and further heat treatment (100 °C). The spheres were dried and sintered at different temperatures (500–1250 °C) for 4 h **[93]**, to study its effect on Li contents in prepared samples.

4.3 Determination of Li concentration in Li based ceramics

Routinely used wet chemical methods like ICP-OES and ICP-MS techniques are precise and sensitive for Li estimation but demand sample to be brought in aqueous/solution phase for analysis. Dissolution of titanium based ceramics is difficult, as in present case, due to refractory nature of titania (TiO_2). Among the solid sample analysis techniques, laser ablation ICP–MS [**94**] and laser induced breakdown spectroscopy (LIBS) have the ability to determine Li and Ti directly in titania based ceramics of lithium. However, matrix interference is one of the major problems in LIBS technique for solid samples. Other non-destructive techniques such as instrumental neutron activation analysis (INAA) and prompt gamma neutron activation analysis (PGNAA) cannot be used for Li. X-ray based techniques like X-ray fluorescence (XRF) and particle induced X-ray emission (PIXE) are also not suitable for quantification of Li. This is due to the fact that the X-rays emitted by Li are of low energy and gets attenuated by the sample itself. NAA cannot be used for the estimation of Li, which is attributed to its unfavorable nuclear properties, whereas, Ti can be easily quantified by INAA and PGNAA as well as by XRF and PIXE. For quantification of Li in Li based ceramics (like Li doped NTO and lithium titanate), a non-destructive *in situ* PIGE method using F as current normalizer has been standardized **[63]**.

The standard and sample targets were mounted on stainless steel ladder and irradiated either by 4 or 8 MeV proton beam (current ~5-10 nA) from tandem accelerators. The gamma-rays of 197, 478, 983 and 6129 keV from $^{19}F(p,p'\gamma)^{19}F$, $^{7}Li(p,p'\gamma)^{7}Li$, $^{48}Ti(p,p'\gamma)^{48}Ti$ and

$^{16}O(p,p'\gamma)^{16}O$ nuclear reactions, respectively, were measured using 30% relative effeciency HPGe detector coupled to a PC based multi-channel analyzer (MCA). The detector was kept in a direction perpendicular to the beam direction for minimizing the Doppler broadening of gamma-rays. The variations in the beam current/fluence were normalized by the sensitivity of F measured from 197 keV (count rate/concentration of F) in order to get current normalized count rate of gamma-rays of interest from the target. The current normalized count rates were obtained using **Eq. 2.9** and **2.10**, given in **Chapter 2**. The methods were validated by analyzing the synthetic samples and stoichiometric chemical compound like Li_2CO_3.

Ti concentrations in lithium titanate samples were also determined by relative INAA method. Sample irradiations were carried out using pneumatic carrier facility (PCF) at Dhruva reactor, BARC, Mumbai. Sample, standard and synthetic samples, sealed in polyethylene and enclosed in polypropylene capsule were irradiated for 1 minute at a neutron flux of 5×10^{13} cm^{-2} s^{-1}. The gamma-rays of 320 keV from activated product of ^{50}Ti (^{51}Ti, $t_{1/2}$ = 5.76 min) were measured using high resolution gamma-ray spectrometer.

4.4. Results and discussion

4.4.1. Determination of Li in Li doped NTO

PIGE spectra of Li standard and Li doped NTO sample, irradiated using 4 MeV proton beam are shown in **Fig. 4.1 (a)** and **(b)**, respectively. The *in situ* current normalized sensitivity of Li (slope of calibration plot, **Fig. 4.2**) was obtained by plotting *in situ* current normalized count rate (counts per second, CPS) of 478 keV gamma-rays of Li against concentration of lithium in the in 'standard' pellets (600-8000 mg kg^{-1}). Current normalized count rates of 478 keV gamma-rays of different standards of Li were obtained by dividing the 478 keV CPS of Li with PIGE

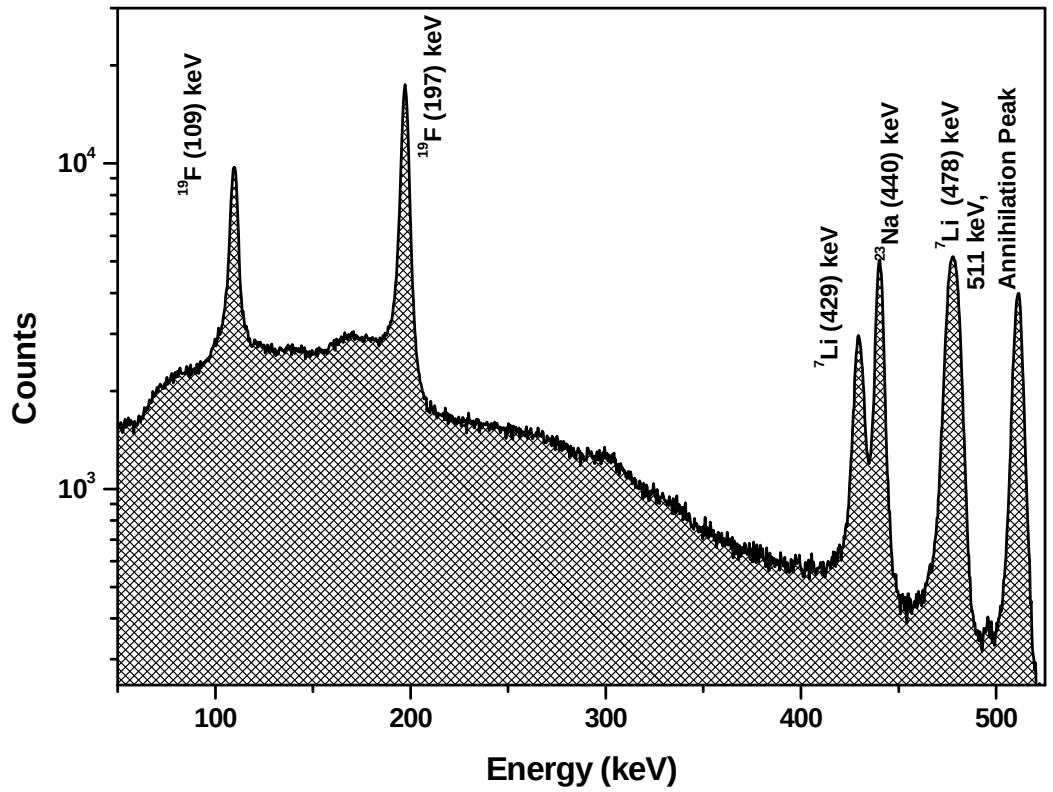

Fig. 4.1 (a): Gamma-ray spectrum of Li standard with *in situ* current normalizer F irradiated using 4 MeV proton beam.

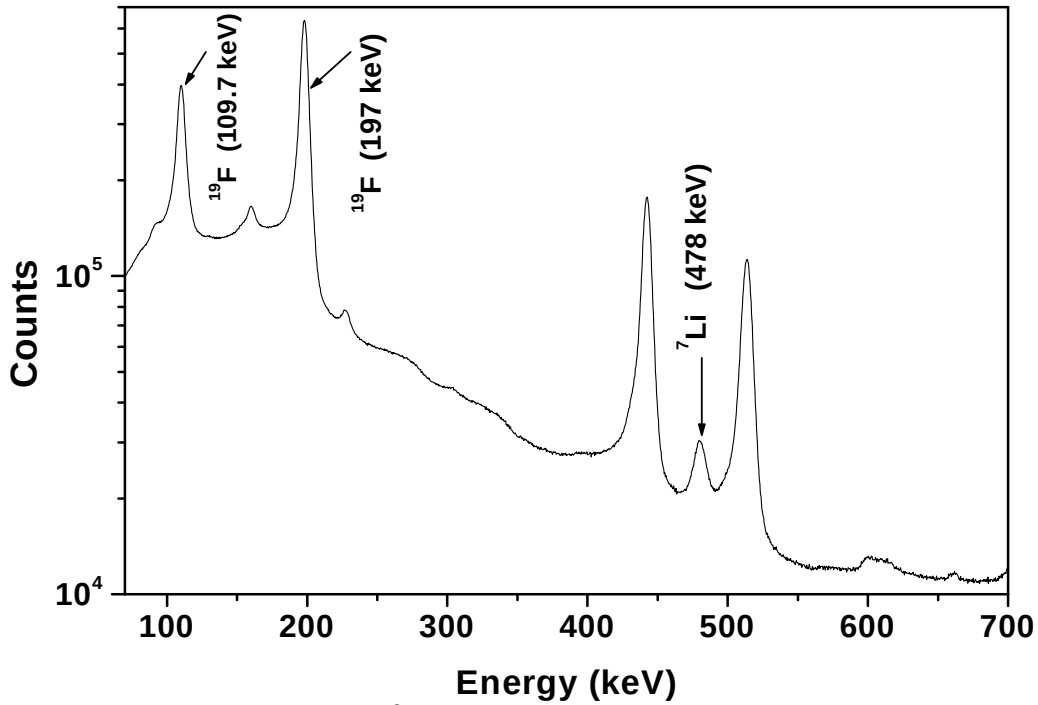

Fig. 4.1 (b): Gamma-ray spectrum of Li doped NTO sample irradiated by 4 MeV proton beam.

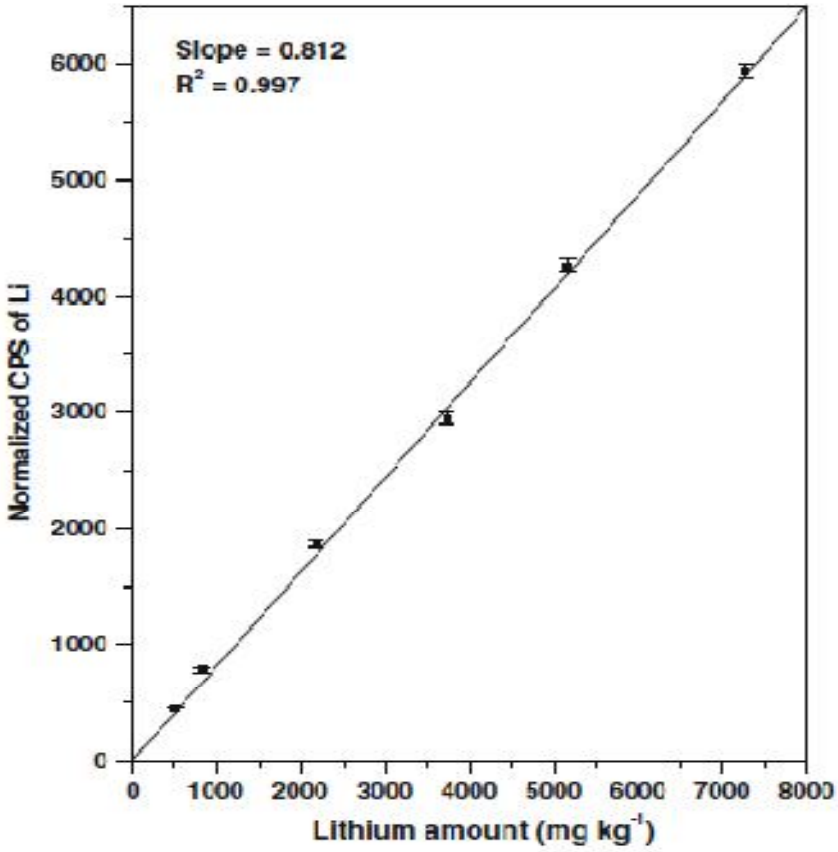

Fig. 4.2: Calibration plot for Li: current normalized count rate at 478 keV v/s Li amount.

method was applied for determining Li concentrations in four synthetic samples and in three precursor and heat treated (800 ^{o}C) samples of Li doped NTO. The concentrations of Li determined in synthetic samples were in good agreement with calculated values (**Fig. 4.3**). The concentrations of Li obtained in precursor and heat treated samples were in the range of 583–1696 mg kg^{-1} in the pellets that correspond to ~0.29–0.85 wt% of Li in actual samples. The results for lithium concentrations in these samples are given in **Table 4.1**. The concentration of Li in precursor samples were in the range of 615-1696 mg kg^{-1} (S-1 to S-3) in the pellets that corresponds to 0.31- 0.85 wt% of Li in original samples (**Table 4.1**). When these samples were

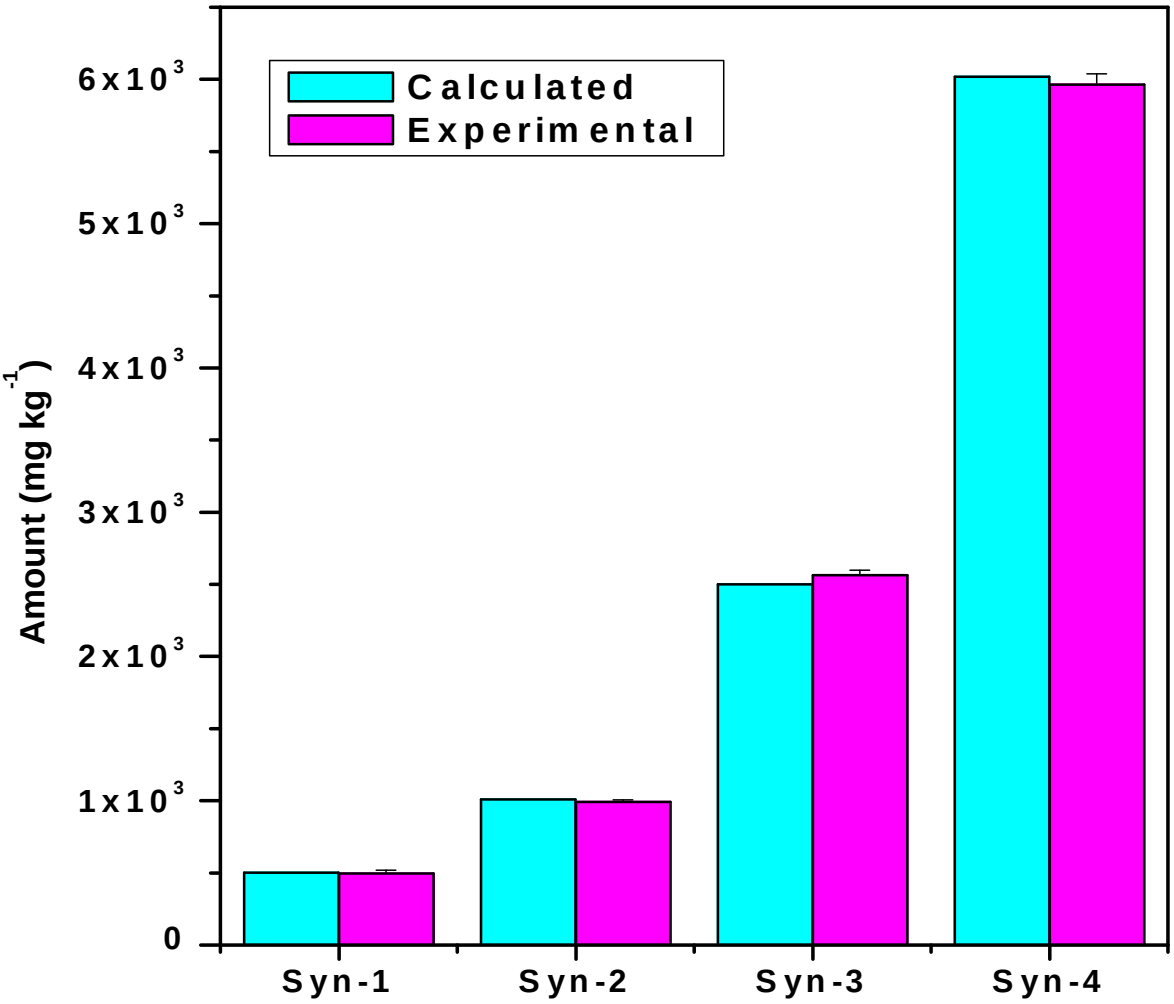

Fig. 4.3: Comparison of experimentally determined lithium concentrations with calculated values in synthetic samples.

heated (800 ^{o}C, 10 hour) and analyzed using PIGE, the Li concentrations were found in the range of 583-1097 mg kg^{-1} in pellet that corresponds to 0.29 - 0.55 wt% of Li in original samples. These results clearly reflect the loss of lithium in the heat treated samples of Li doped NTO. The loss of Li in respective precursor samples of Li doped NTO after heat treatment corresponds to 5-35%, respectively (**Table 4.1**). The results also showed that the loss of Li is dependent on initial Li concentration in the precursor samples but it has no linear correlation with the same.

The propagated uncertainties at ±1σ confidence limit, reported in **Table 4.1**, are in the range of 1.5–3.5 %. The uncertainties contributed in the final results are due to the (i) counting statistics and peak fitting errors of sample (1–2%), standard (~1 %) and current normalizing standard (0.2–0.5 %), (ii) concentration of Li in standards (~0.5 %) and (iii) masses of sample and standard (0.1–0.5 %).

Table 4.1: Li concentrations in pellets and actual samples of $Nd_2Ti_2O_7$ doped with Li obtained by *in situ* current normalized PIGE method.

Sam-Id	Precursor & heat treated Sample	Li conc. (in mg kg^{-1}) in pellet	Li conc. (in wt%) in actual sample	L_D (mg kg^{-1})
S-1	Precursor	615 ± 20	0.312 ± 0.010	7
	After Heating	583± 17	0.292 ± 0.009	7
S-2	Precursor	1288±27	0.640 ± 0.013	9
	After Heating	803±19	0.400 ± 0.009	8
S-3	Precursor	1696±25	0.851 ± 0.012	10
	After Heating	1097±22	0.550 ± 0.011	8

The detection limit (L_D) values for lithium were also calculated in each sample using **Eq. 1.14, Chapter 1** which were found to be in the range of 7-10 mg-kg^{-1} (**Table 4.1**) in the pellet (~750 mg) which corresponds to 22-33 mg kg^{-1} in the actual sample. The main reason behind the variations in the L_D values can be attributed to varying background counts under the gamma-ray peak (478 keV) of interest.

4.4.2. Compositional characterization of lithium titanate

The compositional characterization of Li_2TiO_3 prepared by sol-gel method was carried out by determining the concentrations of Li and Ti in eleven samples by *in situ* PIGE method and INAA method. The *in situ* PIGE method was used for determining Li concentrations and INAA method for determining Ti concentrations, respectively, for compositional characterization of sol-gel synthesized lithium titanate samples.

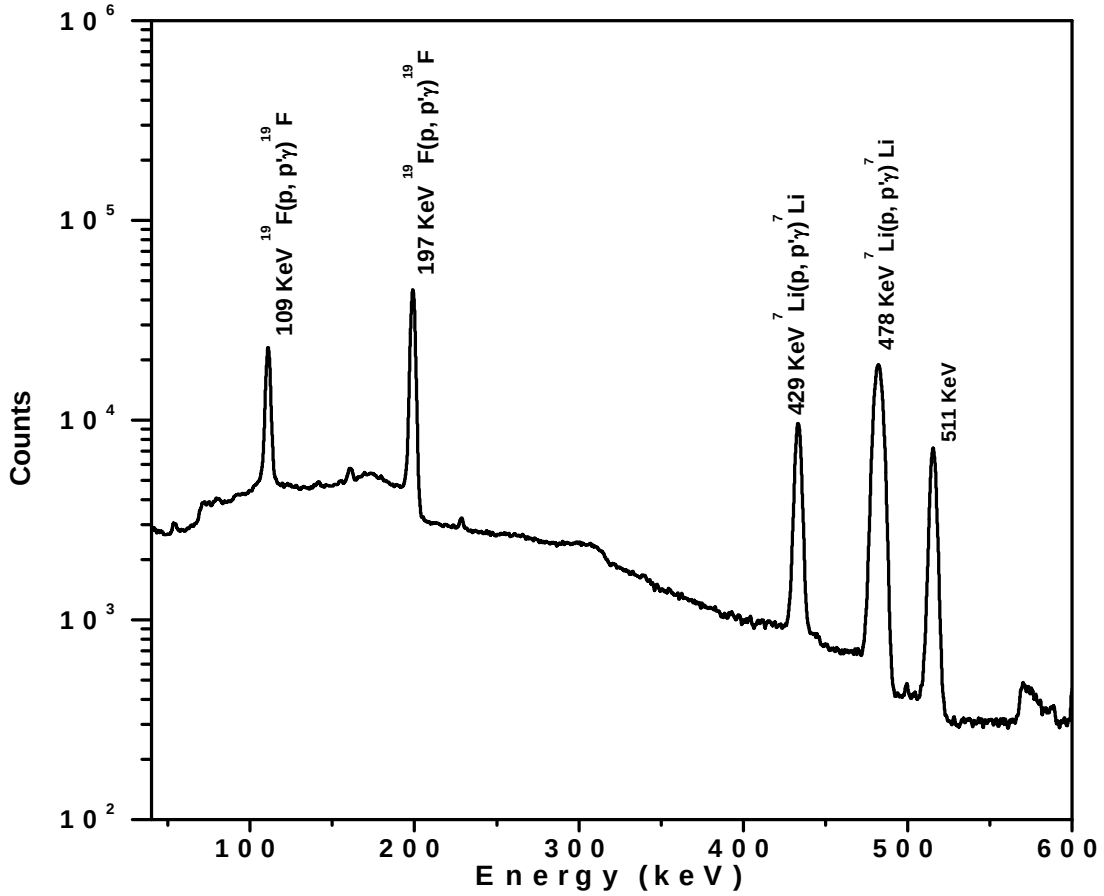

Fig. 4.4: A typical gamma-ray spectrum of lithium titanate sample in PIGE.

A typical PIGE spectrum of lithium titanate sample irradiated by 4 MeV proton beam containing F as *in situ* current normalizer is shown in **Fig. 4.4.** The PIGE method using F as *in situ* current normalizer was validated by determining the varying lithium concentrations (2.5-

14.0 wt% of Li) in synthetic samples of lithium titanate and one stoichiometric compound of Li (Li_2CO_3). The concentrations of Li in seven synthetic samples, one synthetic standard and eleven lithium titanate samples were determined using relative PIGE method (**Chapter 2, Eq. 2.10**). The concentrations of Li determined in synthetic targets are plotted as experimentally determined values along with calculated values of lithium in synthetic targets (**Fig. 4.5)**.There is a good

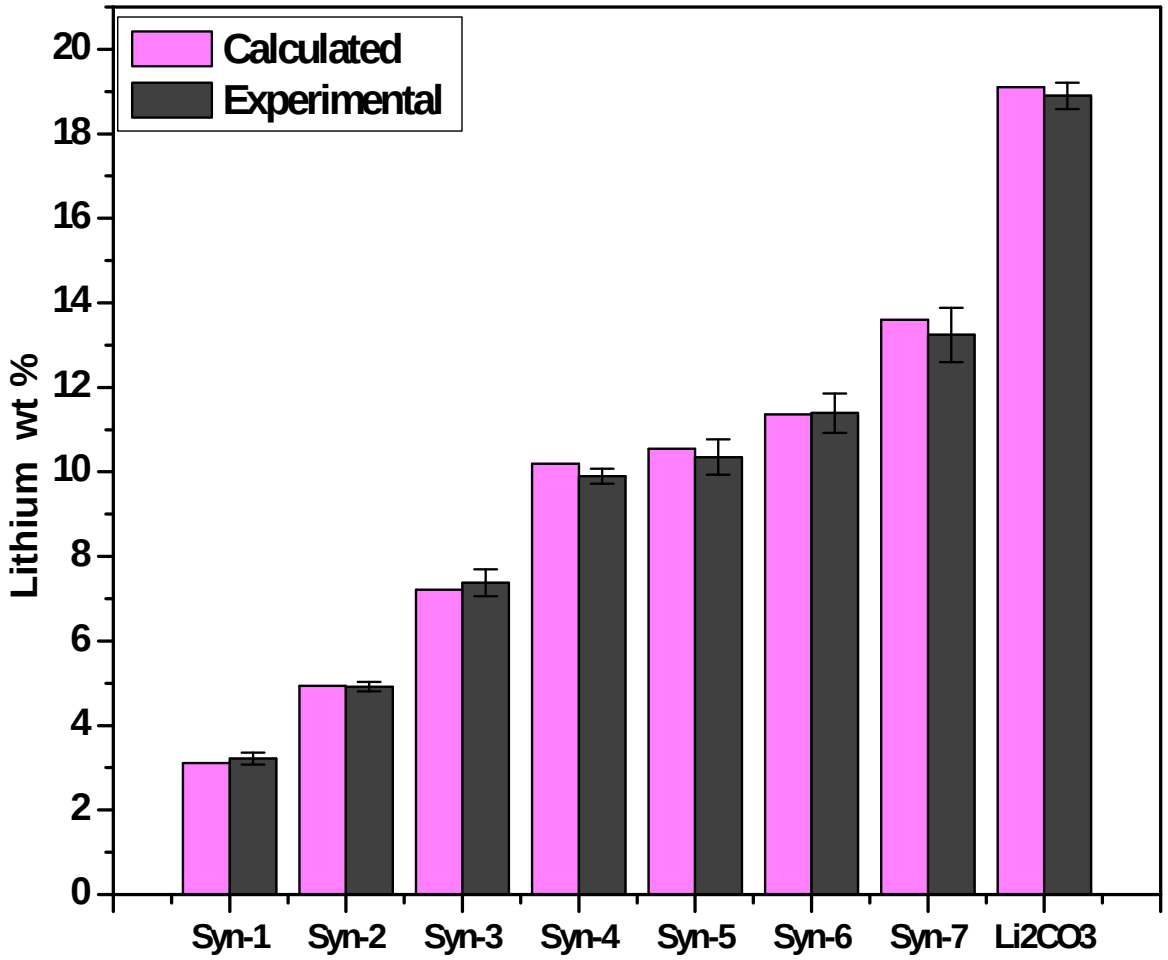

Fig. 4.5: Comparison of Li concentrations measured by PIGE with calculated Li contents.

agreement between experimental and calculated values of Li concentrations within ±3 %. The concentrations of Li in synthetic samples and synthetic standard (Li_2CO_3) obtained were in the range of 3.2–19 wt%. The concentrations of Li determined in eleven samples of lithium titanate

were in the range of 11.00-12.68 wt% which are summarized in **Table 4.2**. Fluorine normalized sensitivity of 478 keV gamma-ray of Li was used for concentration determination of Li in

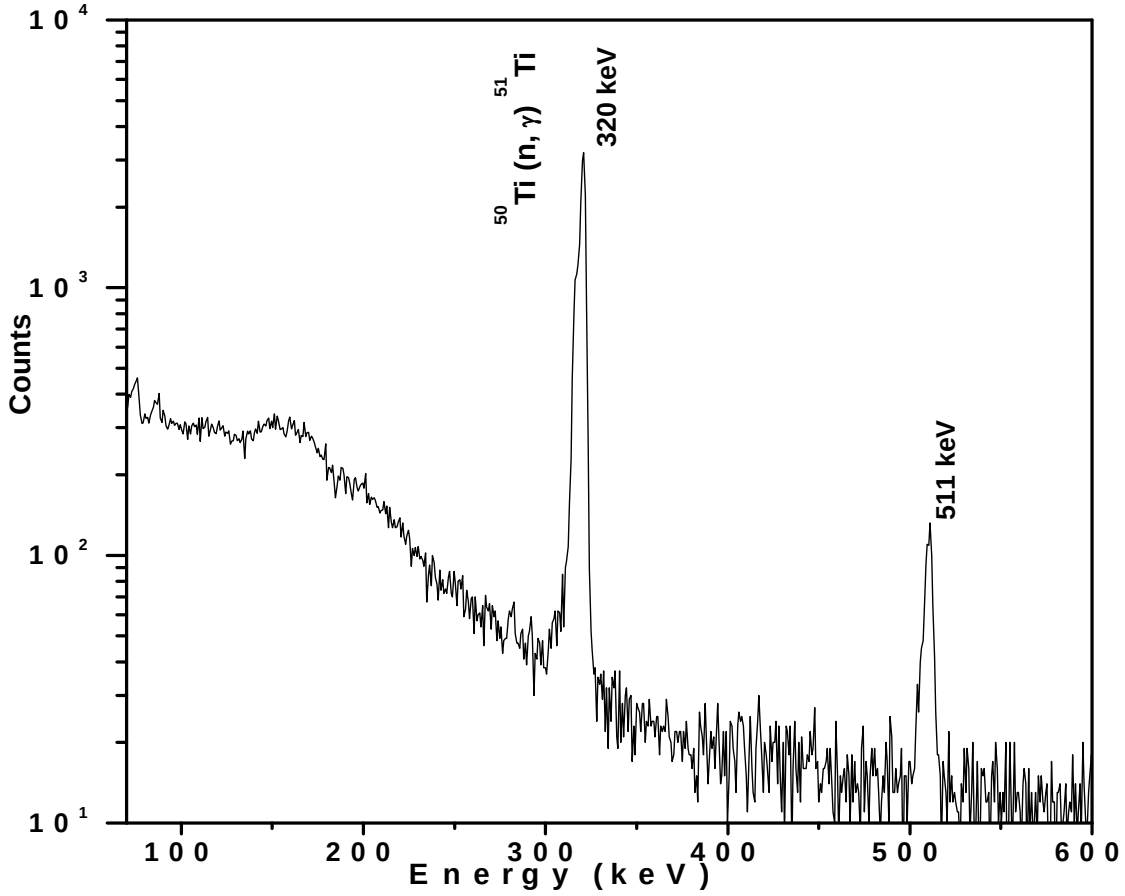

Fig. 4.6: Typical INAA γ-ray spectrum of neutron irradiated lithium titanate sample

synthetic samples, synthetic standard and samples of lithium titanate.

The relative INAA method, used for determination of Ti concentrations in eleven lithium titanate samples, was validated by quantifying Ti concentrations in three synthetic samples of lithium titanate. A typical INAA gamma-ray spectrum of lithium titanate sample is given in **Fig. 4.6**. The concentration of titanium obtained by relative INAA method, in three synthetic samples was in the range of 39.5–50 wt%. Experimentally obtained concentrations of Ti were within ±2.5 % of the expected or calculated value of Ti in synthetic samples (**Fig. 4.7**). The concentrations of

Ti obtained for eleven samples of lithium titanate were in the range of 42.7-44.7 wt% (**Table 4.2**) using **Eq. 2.25, Chapter 2**. The results of Li and Ti concentrations (in wt%) obtained for eleven samples by *in situ* PIGE and INAA methods, respectively, are summarized in **Table 4.2** along with Li to Ti mole ratios.

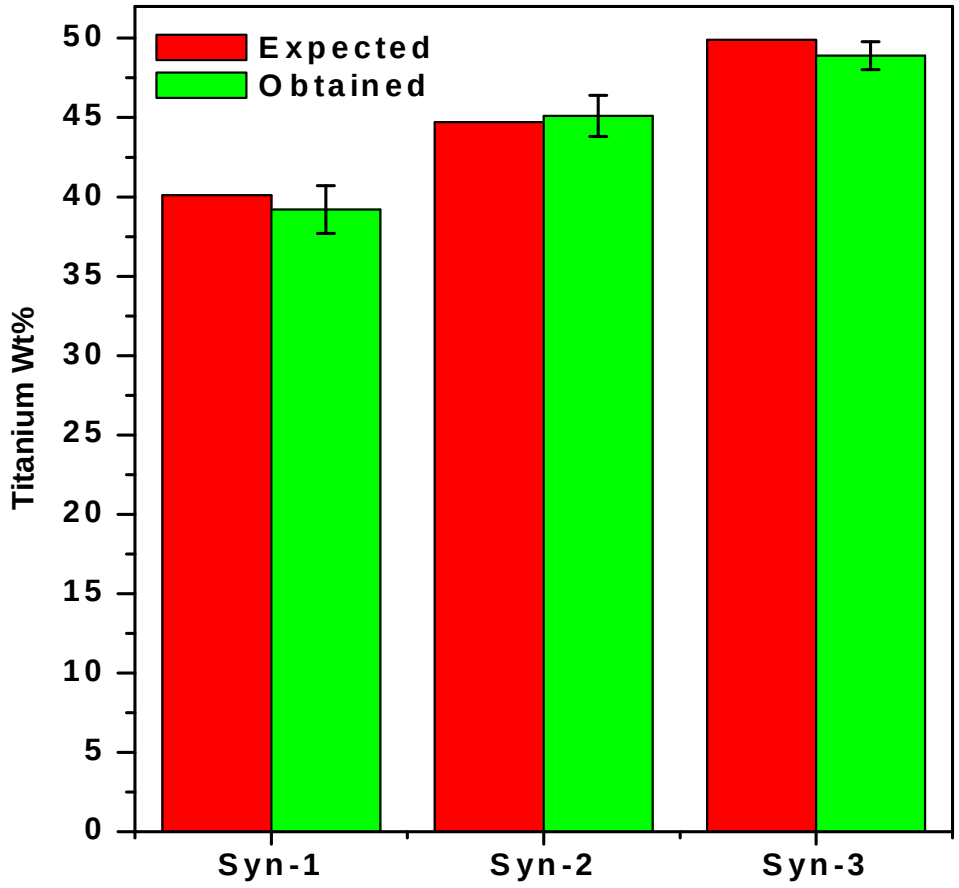

Fig.4.7: Comparison of experimentally determined concentration values of Ti with expected values in synthetic samples

The combined percentage uncertainties in the results of Li and Ti are about ±2 % for Li and ±2–3 % for Ti concentrations. The propagated uncertainties in Li concentrations are due to mass of Li_2TiO_3 (0.1–0.2 %), mass of Li standard (0.1–0.2 %), mass of F as *in situ* current

normalizer (0.5–1.0 %), peak fitting and counting statistics errors that corresponds to peak areas of γ-rays of ^{7}Li (478 keV) and ^{19}F (197 keV) in sample and standard (~0.5 %), respectively. Similarly in the case of Ti, the uncertainty due to mass of Ti in sample/standard is ~1.0 % and the uncertainties due to peak fitting and counting statistics errors that corresponds to peak areas under gamma-ray at 320 keV of standard and samples are 1.0 % and 1.0–2.0 %, respectively. Uncertainties on calculated concentrations of Li and Ti (used as standards) have been considered negligible, as stoichiometric compounds were used. The theoretical values of Li and Ti in

Table 4.2: Concentration and mole ratio (Li/Ti) values of Li and Ti in sol-gel synthesized Li_2TiO_3 samples.

S. No.	Starting material with $TiOCl_2$	Sintering temp (°C)	Li (wt %) (by PIGE)	Ti (wt %) (by INAA)	Li/Ti mole ratio
Sam-1	LiCl	500	12.00±0.23	42.7±1.3	1.94
Sam-2	LiCl	600	11.71±0.22	42.7±1.2	1.90
Sam-3	LiCl	700	12.68±0.24	43.6±0.9	2.01
Sam-4	LiCl	800	12.42±.23	44.6±1.0	1.92
Sam-5	$LiNO_3$	1000	12.38±0.23	44.0±0.8	1.94
Sam-6*	$LiNO_3$	1000	12.31±0.21	44.7±1.1	1.95
Sam-7	$LiNO_3$	1250	11.21±0.21	44.0±0.8	1.76
Sam-8	$LiNO_3$	1250	11.20±0.21	44.2±1.1	1.75
Sam-9	LiCl+$LiNO_3$ (1:1 mixture)	1000	11.50±0.22	44.0±1.4	1.80
Sam-10*	LiCl+$LiNO_3$ (1:1 mixture)	1000	12.13±0.23	43.5±1.2	1.92

(* without LiOH washing)

stoichiometric Li_2TiO_3, Li, O and Ti wt%, Li to Ti wt% ratio and mole ratio are 12.67 and 43.67 wt%, 0.29 and 2.0, respectively.

Li concentrations obtained for first four samples (Samples 1–4, sintering temperatures 500–800 °C) with LiCl as the starting material are in the range of 11.71–12.68 wt% which are close to Li concentrations in stoichiometric lithium titanate (12.67 wt%). The determined Ti concentrations by INAA are in the range of 42.7–44.6 wt%. The mole ratios of Li to Ti in these four samples were in the range of 1.9–2.0, indicating products are close to stoichiometric compound.

Lithium titanate samples which were prepared using $LiNO_3$ as starting material (Samples 5–8, sintering temperature 1000–1250 °C), the Li concentrations (wt%) are in the range of 11.2–12.4 wt % and the Ti values are in the range of 44–44.7 wt%. However, the mole ratios of Li/Ti are in the range of 1.75–1.95, which are lower than 2.0 in these four samples. The higher values of mole ratios for samples 5 and 6 are reasonable as these two samples were washed with LiOH after digestion and sintering temperature was 1000 °C. On the other hand, samples 7 and 8 showed lower mole ratio as no washing was done after digestion in addition to the high sintering temperature (1250 °C). Two mixture samples (samples 9 and 10) were synthesized using 1:1 mixture of LiCl and $LiNO_3$ as starting material. In sample 9 washing of finished product were not carried out with LiOH after digestion, whereas sample 10 was prepared with washing after digestion and in both cases the sintering temperature was kept 1000 °C. The Li contents were found to be 11.5 and 12.13 wt% for samples 9 and 10 respectively. The Li/Ti mole ratio for sample 10 was found to be higher (1.92) than sample 9 (1.8), as washing was carried out for sample 10. In the recycled batch (sample 11) Li concentration was found to be lower i.e. 11.0 wt% which is expected as recycled LiOH solution was used for lithium titanate washing after

digestion. This process will help in reducing Li concentration in the wash effluent, which is one of the important aspects of sol–gel based synthesis method.

4.5 Compositional analysis of lithium titanate using 8 MeV proton beam

In **Chapter 1** it has been explained (**Section 1.6, Eq. 1.7**) that the capability of PIGE technique can be enhanced beyond low Z elements by using high energy charged particle beam (like proton beam of energy ≥ 7 MeV) . Thus, it is possible to carry out complete compositional analysis of lithium titanate i.e., by determining Li, Ti and O, using higher energy proton beam. The thick target gamma-ray yields have direct dependence on energy of projectile (**Section 1.6, Eq. 1.7**). Therefore, gamma-ray yield and hence the sensitivity of isotope towards PIGE increases with increase in projectile energy **[20,43]**. Also, it becomes possible to high energy state in low Z elements like O using higher energy of proton beam. In view of this, a PIGE method using 8 MeV proton beam from BARC-TIFR Pelletron facility at TIFR, Mumbai, has been standardized for compositional characterization of sol-gel synthesized lithium titanate samples. A typical PIGE spectrum of lithium titanate sample irradiated using 8 MeV proton beam is shown in **Fig. 4.8**. The gamma-rays of energies 478, 983and 6129 keV were used for simultaneous quantification of Li, Ti and O. Normalization of beam current variations was carried out by RBS method using thin Au foil (1.5 mg/cm^2) (**Chapter 2, Section 2.5**). The current normalized sensitivities for Li, Ti and O were obtained using **Eq. 2.7, Chapter 2**. The concentrations of Li, Ti and O were determined in four lithium titanate samples using relative method (**Chapter 2, Eq. 2.8**). The method was validated by determining the concentrations of Li, Ti and O in two synthetic samples (**Table 4.3**). The results obtained were in good agreement with calculated concentration values of Li, Ti and O (within ±1-2%). The concentrations of Li,

Ti and O obtained in two synthetic samples are in the range of 11.1-13.5 wt%, 36.7-38.6 wt% and 62.5-70.5wt%, respectively. The concentrations for Li, Ti and O in four samples of lithium titanate are in the range of 11.8–12.7

wt%, 43.3–43.8 wt% and 43.7–44.3 wt%, respectively (**Table 4.4.**). The calculated values of Li, O and Ti in stoichiometric lithium titanate are 12.67 wt% for Li, 43.51 wt% for Ti and 43.85

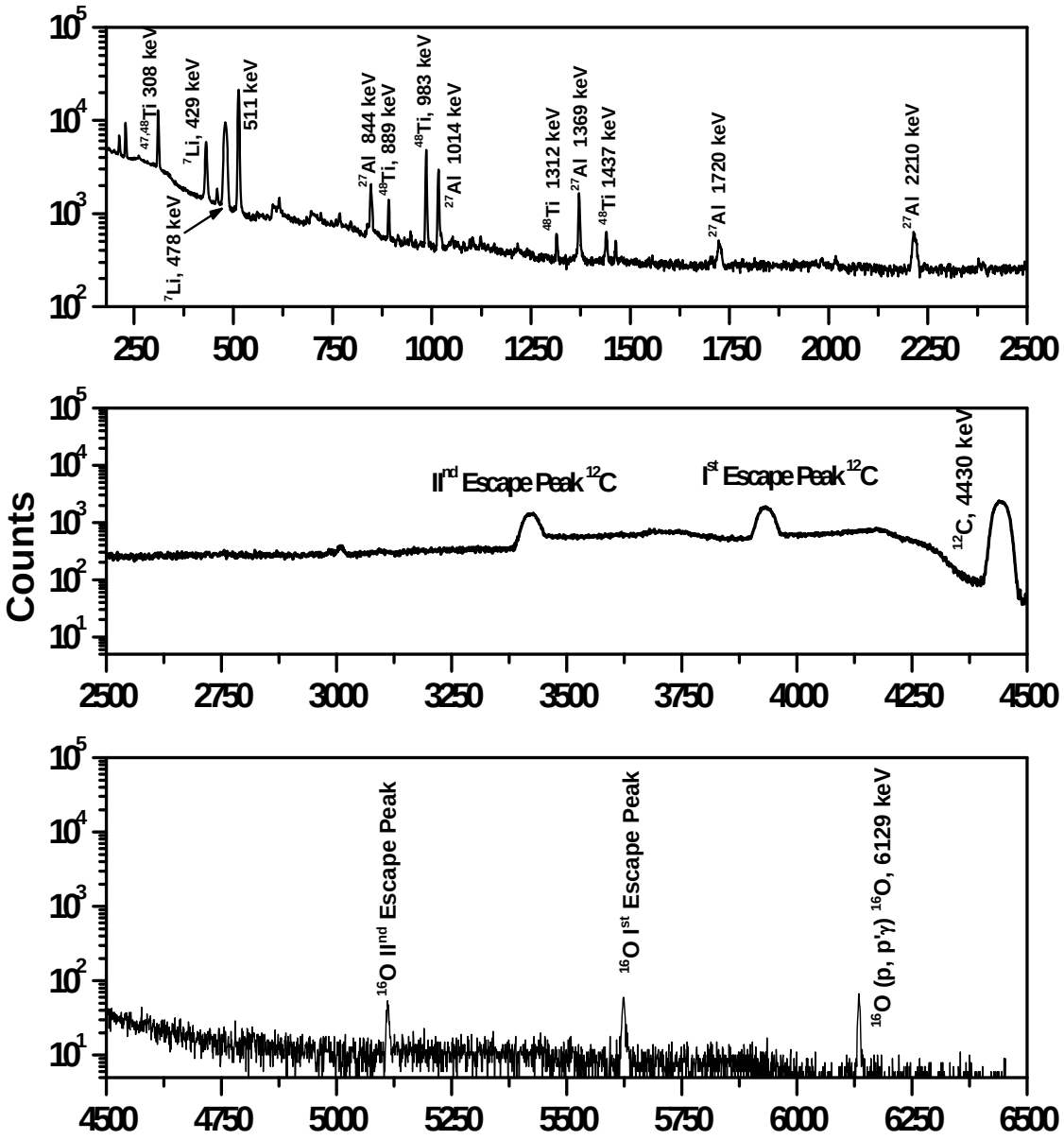

Fig. 4.8: PIGE spectrum of a lithium titanate (Li_2TiO_3) sample irradiated using 8 MeV proton beam.

wt% for O, respectively.

The combined propagated uncertainties in the results (**Tables 4.3** and **4.4**) obtained were due to counting statistics of sample, standard and current normalizing element (Au) (RBS count rate) as well as the respective masses of sample and standard. The uncertainty values for Li, Ti and O concentrations were in the range ±3%, ±3% and ±8%, respectively. Higher uncertainty for O is due to low γ-ray detection efficiency at 6129 keV γ-ray leading to higher counting statistics error.

Table. 4.3: Concentration values (wt %) of Li, Ti and O determined by PIGE method in two synthetic samples.

Element	Lithium		Titanium		Oxygen	
Sample Id	Calculated	Obtained	Calculated	Obtained	Calculated	Obtained
Syn-1	11.3	11.1±0.4	36.1	36.7±1.1	63.3	62.5±4.6
Syn-2	13.2	13.5±0.4	39.1	38.6±1.2	71.9	70.5±5.1

When LiCl was used as starting material for synthesizing Li_2TiO_3, the product obtained was crack-free and non-stoichiometric as loss of Li was there in the final product [**53,54**]. Li loss was negligible when $LiNO_3$ was used as starting material for synthesis of lithium titanate by sol-gel method, but the product obtained was not crack-free. Thus, attempts were made to prepare the said compound using 1:1 mixture of LiCl and $LiNO_3$ at sintering temperatures of 1000 and 1250°C to get crack-free stoichiometric compound. The composition of lithium titanate thus formed from LiCl and $LiNO_3$ mixture (1:1) sintered at 1000 °C temperature, compared to that sintered at 1250 °C, was found to be in good agreement with stoichiometric lithium titanate

(**Table 4.3**). The detection limits of PIGE method at 8 MeV proton beam for Li, Ti and O, in one of the representative samples of Li_2TiO_3, were calculated using sample background and respective elemental sensitivities by using **Eq. 1.14, Chapter 1.** The detection limits for Li, Ti and O were 4.0, 8.0 and 136 mg kg^{-1} (**Table 4.4**) in the sample. Although detection limit for oxygen using PIGE is slightly poorer compared to other techniques [**95-97**], its concentration could be determined simultaneously with Li and Ti without any interference. Thus, a non-destructive method for Ti and O concentration determination could be standardized which is an important application of PIGE using this medium (8 MeV) energy proton beam.

Table 4.4: Determined concentrations (wt %) of Li, Ti and O in lithium titanate samples by PIGE method along with corresponding detection limits (mg kg^{-1}) calculated in one sample

	Sam-1 1	Sam-2	Sam-3	Sam-4	Calculated Value	L_D (mg kg^{-1})
Starting material	LiCl	$LiNO_3$	(50%:50%) $LiCl+LiNO_3$	(50%:50%) $LiCl+LiNO_3$	-	-
Sintering Temp. (°C)	800	1000	1000	1250	-	-
Li (wt %)	12.0±0.2	12.7±0.3	12.5±0.3	11.8±0.3	12.67	4.0
Ti (wt %)	43.7±1.0	43.3±1.0	43.6±1.0	43.8±1.0	43.51	8.0
O (wt %)	44.3±3.3	43.7±3.3	43.8±3.3	43.9 ±3.3	43.82	136.0

Conclusions

In conclusion, PIGE method using 4 MeV proton beam and INAA method were standardized and applied to Li based ceramics namely Li doped NTO and lithium titanate. Li concentrations were determined in Li doped NTO in order to estimate the loss of Li content in the heat treated samples with respect to precursor samples. The concentration of Li in precursor samples were in the range of 0.31-0.85 wt% and in heat treated samples, 0.29-0.55 wt%, respectively. This shows that the loss of Li content in heat treated samples were in the range of 5-35 %.

In order to optimize sol-gel method, a synthesis procedure for preparation of lithium titanate, PIGE and INAA methods were standardized and used for compositional characterization of lithium titanate samples. The concentration of Li and Ti determined using relative PIGE and INAA methods, in eleven samples, were in the range of 11.00-12.68 wt% and 42.7-44.7 wt%, respectively. Additionally, PIGE method using 8 MeV proton beam was developed for the first time for simultaneous determination of Li, Ti and O as a part of compositional characterization of lithium titanate. These results using 8 MeV proton beam have been reported for the first time. The concentrations of Li, Ti and O obtained for four samples of lithium titanate were in the range of 11.8-12.7 wt%, 43.3-43.8 wt% and 43.7-44.3 wt%, respectively. These results helped in optimizing the sol-gel preparation method for lithium titanate and also for chemical quality control (CQC) of the prepared material.

Chapter 5

Simultaneous Determination of Isotopic Composition and Total Concentration of Boron by PIGE Methods

In this chapter, development of PIGE methodologies for simultaneous determination of isotopic composition (IC) and total concentration of boron have been described. PIGE methods using 4 MeV proton beam for simultaneous and non-destructive determination of IC of boron ($^{10}B/^{11}B$ atom ratio) and total boron concentrations have been standardized and applied to various natural and enriched samples with respect to ^{10}B. The PIGE method involves measurement of prompt gamma-rays at 429, 718 and 2125 keV from $^{10}B(p,\alpha\gamma)^{7}Be$, $^{10}B(p, p'\gamma)^{10}B$ and $^{11}B(p, p'\gamma)^{11}B$ reactions, respectively. IC of boron in natural and enriched samples was determined by comparing the peak area ratios of ^{10}B and ^{11}B of sample to natural boric acid standard. An in situ current normalized PIGE method, using F or Al, was standardized for total B concentration determination. The method was validated by analyzing stoichiometric boron compounds and applied to samples like boron carbide, elemental boron, carborane and borosilicate glass. Total boron concentrations were in the range of 5-78 wt% and isotopic compositions of boron were in the range of 0.247-2.0 corresponding to ^{10}B atom% in the range of 19.8–67.0. Total B concentration values obtained by PIGE were compared with that obtained by conventional wet chemical methods.

5.1 Importance of boron in nuclear technology

Boron and boron based materials find extensive applications in the field of science and technology including nuclear technology. Boron has two isotopes, ^{10}B and ^{11}B, respectively. Boron is used as neutron poison (due to large thermal neutron capture cross-section of ^{10}B), and neutron reflector material (due to low neutron absorption cross-section of ^{11}B) in the nuclear reactor. The basic requirements associated with the safe operation of nuclear reactor and development of nuclear reactor technology is control and containment of neutrons which helps in sustaining the reactor operation. The control rod material is composed of elements, compounds or alloys which are capable of absorbing neutrons without undergoing fission.

The choice of material is influenced by the energy of neutrons in the reactor, their resistance to neutron-induced swelling, and the required mechanical and lifetime properties. Chemical elements whose isotopes have high neutron capture cross-section include B, Cd, Gd, Eu, Sm, Hf and In. Alloys or compounds of these elements like high-boron steel, Ag-In-Cd alloy, boron carbide, boric acid, borated wood, borated paraffin wax, zirconium diboride, titanium diboride, hafnium diboride, gadolinium nitrate, gadolinium titanate, and dysprosium titanate may also be used for neutron absorption. Out of these, boron, its compounds (boric acid, boron carbide, rare-earth and refractory metal borides) and alloys (high boron steel, BORAL) are extensively studied for the development of nuclear technology.

The effectiveness of boron as neutron absorber is due to the high thermal neutron absorption cross-section of ^{10}B isotope, 3837 barn. The neutron absorption cross-section of natural boron (containing ~20% ^{10}B) is sufficiently high (764 barn) which makes it an excellent candidate for use in thermal reactors. Boron based material are used as neutron sensors, human and instrument shielding against neutrons, nuclear/neutron poison, control/shutoff rods and for storing nuclear materials in nuclear industry, because of high neutron absorption cross-section of boron. ^{10}B after neutron absorption undergoes a nuclear reaction [$^{10}B(n,\alpha\gamma)^{7}Li$] whose products ($^{7}Li$ and ^{4}He) are stable and non-radioactive, which is another advantage over other potential neutron absorber materials. As the reaction products do not emit nuclear radiation, decay heating problems during reactor shutdowns and transfer of depleted control rods are minimal. Boron as boric acid is used in the primary coolant system of pressurized water reactors (PWRs) and as sodium pentaborate for standby liquid control systems in boiling water reactors (BWRs).

In Indian Nuclear Industry, boric acid along with boron carbide is used for constructing reactor buildings in concrete. Boron carbide is used as control rod in Boiling Water Reactor (BWR) at Tarapur. Also, the dense pellets of ^{10}B enriched boron carbide are being used as

control rod material in Prototype Fast Breeder Reactor (PFBR) at Kalpakkam. The other borated materials like BORAL (boron carbide in aluminum matrix), bocarsil (boron carbide in silicon rubber), polyboron (boric acid in polyethylene) borated wax and borated wood are used as neutron shields in reactors and for storing nuclear materials. Boron composites like TiB_2 and B_4C+ZrO_2 also finds useful applications in control and shielding of advanced nuclear reactors.

5.2 Various applications boron based materials

Boron and nitrogen based materials like $LiBH_4+2LiNH_2$, $NaBH_4+2H_2O$, NH_3BH_3, $NH_3BH_3+2H_2O$, $LiNH_2+LiH$, NH_3 and N_2H_4 are used as good hydrogen carrier for proton exchange membrane (PEM) **[98]**. Borosilicate glasses are used for vitrification of nuclear waste in geological repositories **[99]**. Boron fibers (boron filaments) have tensile high-strength and light in weight and finds useful applications in advanced aerospace structures **[100]**. In non-nuclear applications boron carbide is used in the making tank armor, bulletproof vests, and numerous other important structural applications due to its great structural strength. Other compounds of boron like boron nitride (BN) is iso-electronic to carbon can be used as a lubricant (due to high temperature stability) and as an abrasive (due to its high chemical stability) **[101]**. The metal borides are used as surface coating tools. These coatings increase the resistance of surface and micro-hardness. These borides are used as alternative to diamond coated tools **[102]**. Boron compounds like boric acid have insecticidal **[103]**, antiseptic, antifungal, and antiviral properties and for these reasons is applied as a water clarifier in swimming pool water treatment **[104]**. Mild solutions of boric acid have been used as eye antiseptics. Diboride of boron like magnesium diboride, an important superconducting material with the transition temperature of 39 K, can be used in designing superconducting magnets **[105,106].** The amorphous form of boron is used as a

melting point depressant in nickel-chromium brazes alloys **[107]**. Boron (^{10}B) is used boron neutron cancer therapy (BNCT) for treating brain tumors using $^{10}B(n,\alpha)^{7}Li$ nuclear reaction. **[108-110]**.

5.3 Methods for determining total boron and its isotopic composition

Conventional analytical techniques used for total boron concentration determination in solid and aqueous samples include spectrophotometry, titrimetry, ion chromatography, inductively coupled optical emission spectroscopy (ICP-OES), inductively coupled mass spectrometry (ICP-MS), and isotope dilution thermal ionization MS (ID-TIMS) **[113-123]**. This low atomic number element (B) is difficult to be analysed by X- ray based radio-analytical techniques such as X-ray fluorescence (XRF) and particle induced X-ray emission (PIXE). It is difficult to determine B concentration directly by conventional neutron activation analysis (NAA) due to unfavourable nuclear properties of ^{10}B and ^{11}B. Nuclear analytical techniques, namely the alpha track technique, prompt gamma-ray NAA (PGNAA), and particle induced gamma-ray emission (PIGE), are capable of determining total boron concentration [**124-132]** The concentration of boron can be determined non-destructively by the PGNAA and PIGE methods, whereas PIGE is also capable of determining the isotopic composition (IC) of boron ($^{10}B/^{11}B$ atom ratio). For determination of the IC of boron, TIMS, ICP-MS, and secondary ion MS (SIMS) are routinely used **[111-119]**. Static SIMS can determine the IC of boron in solid samples without destroying them, though it is strongly demands matrix matching composition of the sample and the standard. Among these, TIMS is one of the best methods for precise determination of the $^{10}B/^{11}B$ atom ratio **[113-119]**. However, TIMS and ICP-MS methods are destructive in nature, wherein samples need to be brought to solution form by dissolving or decomposing the solid samples **[119]**. In some cases a chemical separation procedure is used for pre-concentrating the boron and eliminating

the sample matrix effect **[119, 122]**. As some of the mass spectrometry methods including TIMS are destructive, they need special care during dissolution as well as for evaporation loss of boron, if any, while analyzing complex matrix solid samples. Hence, development of an alternate, simple, and non-destructive analytical method for simultaneous determination of IC and total B concentration in solid samples is desirable. In this respect PIGE is a suitable nuclear analytical technique for non-destructive determination of total boron including IC of boron. PIGE, a complementary technique to NAA, XRF, and PIXE, is an isotope specific nuclear analytical technique capable of determining low Z elements (like Li to S or even higher Z) using a low to medium energy (2−9 MeV) proton beam **[19,20,25,29,37,43,129-133]**.

5.4 Determination of total boron and its isotopic composition by PIGE

The pellets of solid samples namely boron carbide (natural and enriched), borazine, boric acid (enriched), elemental boron, borosilicate glass and carborane along with stoichiometric compounds like borax pellets were prepared in cellulose/graphite matrix, were irradiated using 4 MeV proton beam from FOTIA. It utilizes measurement of prompt gamma-rays at 429 keV from $^{10}B(p, p'\gamma)^{7}Be$ and at 718 keV from $^{10}B(p, p'\gamma)^{10}B$ and at 2125 keV from $^{11}B(p, p'\gamma)^{11}B$ for quantification of ^{10}B, ^{11}B, and total B concentrations as well as $^{10}B/^{11}B$ atom ratios. For total concentration of B, the *in situ* current normalized PIGE method was used whereas for IC can be determined by directly comparing the peak area ratios of sample with standard.

5.5 Results and discussion

5.5.1 Validation of PIGE method for boron concentration determination

Total boron concentrations (in wt %) have been determined from individual

concentrations of ^{10}B and ^{11}B using relative PIGE method. For calculating total boron concentrations, calibration plots of *in situ* current normalized count rates (using F as *in situ* current normalizer) of all three gamma-rays of boron (429 and 718 keV of ^{10}B and 2125 keV of ^{11}B) against varying boron concentrations (4400−44000 mg kg^{-1}) in standards were obtained. The results showed good linearity values (R^2 = 0.995−0.998) in the above boron concentration range. This indicates good homogeneity of the prepared mixture of standards as well as *in situ* current normalizer F or Al. The concentrations of boron obtained for stoichiometric compounds including a B_4C sample are given in **Table 5.1**. The table also shows the individual concentrations of ^{10}B and

Table 5.1: Validation of *in situ* PIGE method: Comparison of calculated and determined values of concentrations of ^{10}B, ^{11}B and total B (in wt%) obtained by PIGE method*.

Sample Id	Using 429 keV		Using 718 keV		Using 2125 keV		Average	Calculated
	^{10}B	Total Boron	^{10}B	Total Boron	^{11}B	Total Boron	Total Boron	Boron
$LiBO_2$	4.35 (0.6)	21.98	4.26 (1.4)	21.52	17.43 (1.0)	21.73	21.74 (1.1)	21.71
$Na_2B_4O_7.10H_2O$	2.23 (0.6)	11.27	2.28 (1.5)	11.52	9.12 (1.0)	11.37	11.38 (1.1)	11.33
$B_3N_3H_6$	7.93 (0.6)	40.03	7.91 (1.4)	39.96	32.12 (0.9)	40.05	40.05 (1.0)	40.30
B_4C	15.52 (0.9)	78.38	15.53 (1.1)	78.40	63.11 (0.8)	78.69	78.50 (1.0)	78.26

*Total percentage uncertainties are given in parenthesis

^{11}B as well as corresponding total B concentrations calculated from ^{10}B and ^{11}B. The average B concentrations obtained (in the range of 11.4−78.5 wt %) are in good agreement (≤ ±2%) with the calculated values, indicating good accuracy of the *in situ* current normalized PIGE method. Total uncertainty values at ±1σ confidence limit on measured concentrations of ^{10}B, ^{11}B, and total boron are within ±1.5%. Thus, it can be inferred that any gamma-ray (429, 718,

and 2125 keV) can be used for obtaining total B concentrations for samples in the natural composition. When sample contains a low concentration of boron, 429 and 2125 keV gamma-rays are preferred over 718 keV because of their higher thick target gamma-ray yields at a 4 MeV proton beam **[37,43,122]**.

5.5.2 Determination of total boron by in situ current normalized PIGE method

(a) Using fluorine as in situ current normalizer

The *in situ* PIGE method thus standardized was applied to four different samples, namely natural B_4C (four replicates), enriched B_4C (enriched with ^{10}B, three replicates), carborane, and two borosilicate glass samples. The results of ^{10}B, ^{11}B, and total boron concentrations are given in **Table 5.2**. Here, concentrations of ^{10}B were obtained using 718 keV γ-rays. It is to be noted that if the sample

Table 5.2: Concentrations ^{10}B, ^{11}B and total B (wt%) determined by *in situ* PIGE method using F as *in situ* current normalizer boron based in natural (N) and enriched (E) samples.

Sample	**^{10}B Conc. (718 keV)**	**^{11}B Conc. (2125 keV)**	**Total B Conc.**
B_4C (N) (n=4)	15.55 (1.1)	62.74 (0.7)	78.29 (1.3)
B_4C (E) (n=3)	51.75 (1.0)	25.83 (0.7)	77.58 (1.2)
Carborane	1.06 (1.6)	4.26 (1.0)	5.32 (1.9)
BSG-1	1.05 (2.5)	4.40 (2.3)	5.39 (3.4)
BSG-2	1.14 (2.3)	4.45 (2.2)	5.68 (3.2)

is enriched, the total boron concentration determination should be done through its isotopic (^{10}B and ^{11}B) concentrations. Thus, for an unknown sample, total boron concentration should be calculated through addition of the isotopic concentrations. This has been reflected in the

results of both natural and enriched boron carbide samples. **Table 5.2** also gives the results of boron concentrations in two borosilicate glass samples, which could be analyzed non-destructively in the presence of other major matrix elements, such as Si, Al, and Na. The uncertainties for B_4C (N and E) were arrived at from standard deviation at $\pm 1\sigma$ confidence limit from replicate samples. The total propagated uncertainty values are in the range of 0.7−1.9%, except for two borosilicate glass samples. The individual results from four replicates and mean concentration values with % relative standard deviation (%RSD) of natural B_4C are given in **Table 5.3**. It is seen that the %RSD values for ^{10}B, ^{11}B, and total

Table 5.3: Concentrations (wt %) of ^{10}B, ^{11}B and total boron in four sub-samples of natural B_4C for evaluating the reproducibility of the analysis

Sample	**^{10}B (wt %) Using 718 keV**	**^{11}B (wt %) Using 2125 keV**	**Total B (wt %)**
1	15.8 (0.7)	62.44 (0.5)	78.24 (0.9)
2	15.47 (0.7)	62.35 (0.6)	77.82 (0.9)
3	15.49 (1.1)	63.17 (0.8)	78.66 (1.3)
4	15.43 (1.5)	63.02 (1.0)	78.45 (1.4)
Mean	15.55	62.74	78.29
± SD	0.17	0.41	0.36
% RSD	1.1	0.7	0.5

boron are 1.1, 0.7, and 0.5%, for their concentrations of 15.6, 62.7, and 78.3 wt%, respectively.

(b) Using thin Al foil as in situ current normalizer

In addition, another *in situ* current normalized PIGE method was standardized using thin Al. Energy loss is about 100 keV at a 4 MeV proton beam for 1.5 mg cm^{-2} aluminum foil. As relative PIGE method was used, this loss in energy does not alter the results, since the energy experienced by sample and standard is the same. The results obtained by this method for three samples (natural and enriched B_4C and enriched H_3BO_3) are given in **Table 5.4**. The results are in good agreement with that obtained by the *in situ* method using F (**Table 5.2**). The propagated uncertainty values are in the range of 0.7−1.4%.

Table 5.4: Concentrations (wt%) of ^{10}B, ^{11}B and total B in B_4C (N and E) and H_3BO_3 (E) boron by PIGE using Al as *in-situ* current normalizer

Sample	**^{10}B Conc. Using 718 keV**	**^{11}B Conc. Using 2125 keV**	**Total B Conc. (*in situ* Al method)**
B_4C (N)	15.5 (1.0)	62.7 (1.1)	78.2 (1.2)
B_4C (E)	52.1 (1.0)	25.4 (0.7)	77.5 (1.2)
H_3BO_3 (E)	11.7 (1.0)	5.7 (1.0)	17.4 (1.4)

5.5.3 Determination of isotopic composition of boron using PIGE method

Typical gamma-ray spectra of boron for enriched and natural boron carbide samples are shown in **Fig. 5.1** and **5.2**, respectively. The PIGE method is simple for IC determination of boron as it requires comparison of peak area ratios of $^{10}B/^{11}B$ (429 keV/2125 keV and 718 keV/2125 keV) of sample and standard only, and is independent of masses of sample and standard and proton beam current. For determination of boron IC, standard and sample target pellets of boron (natural boric acid and samples) were irradiated separately, and their corresponding peak area ratios (429 keV/2125 keV and 718 keV/2125 keV) were obtained

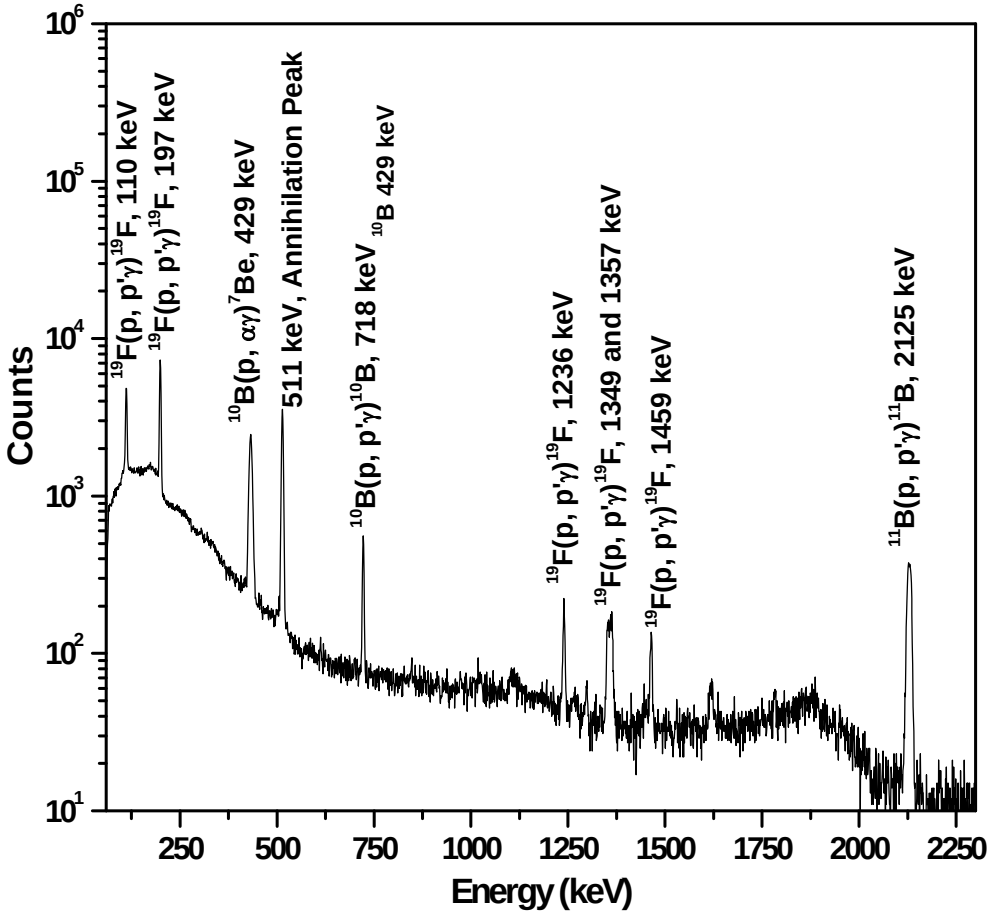

Fig. 5.1: PIGE spectrum of a natural composition B_4C sample with F as *in situ* current normalizer.

under similar experimental conditions. The $^{10}B/^{11}B$ atom ratio can directly be obtained from peak areas under the γ-rays of boron isotopes as given below:

$$(^{10}B/^{11}B)_{Atom\ Ratio} = \frac{\left(\frac{PA(^{10}B)}{PA(^{11}B)}\right)_{Sam}}{\left(\frac{PA(^{10}B)}{PA(^{11}B)}\right)_{Ref}} \times \left(\frac{\theta(^{10}B)}{\theta(^{11}B)}\right)_{Ref} \quad ---(5.1)$$

where $[\theta(^{10}B)/\theta(^{11}B)]_{ref}$ for natural boron composition is 0.247. Then the atom % of ^{10}B can be calculated using the following expression:

$$^{10}B(Atom\%) = \frac{(^{10}B/^{11}B)_{Atom\ Ratio}}{(^{10}B/^{11}B)_{Atom\ Ratio}} \times 100 \quad ---(5.2)$$

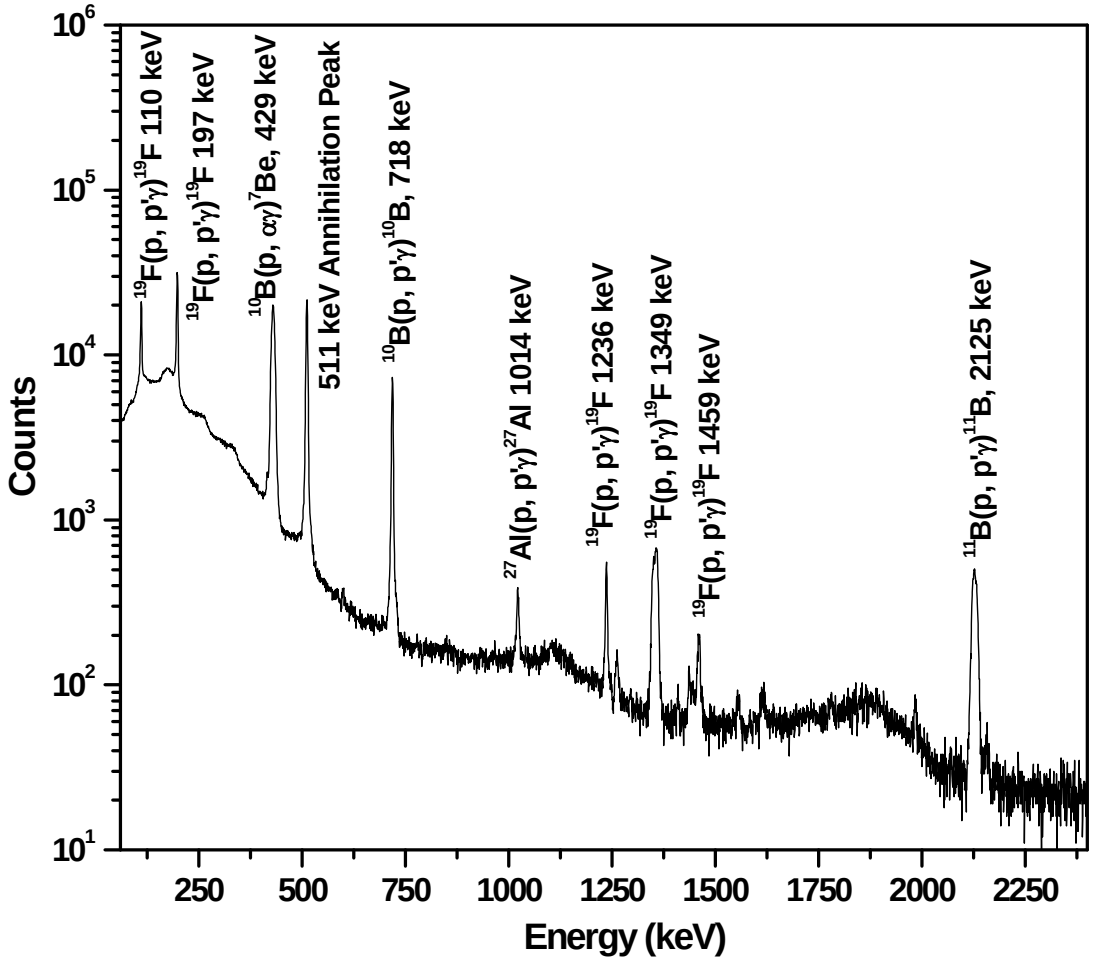

Fig. 5.2: PIGE spectrum of an enriched B_4C sample F as *in situ* current normalizer.

The results for $^{10}B/^{11}B$ atom ratio and enrichment percentage with respect to ^{10}B atom percent are presented in **Table 5.5**. The atom ratio values for all natural composition samples are in the range of 0.247−0.253, and the corresponding ^{10}B atom % values are in the range of 19.8−20.2%. For two enriched samples (of boric acid and boron carbide) the $^{10}B/^{11}B$ atom ratios are about 2.0 which correspond to ^{10}B enrichment values are about 67%. The results of three synthetic boron carbide samples **(Table 5.5)** are found to be in good agreement (within ±3%) with calculated values. The propagated uncertainty values on determined atom ratios as well

as on ^{10}B atom percent are in the range of 0.8−1.9%, which were arrived at from counting statistical errors of sample, standard, and current normalizing standard. However, in addition

Table 5.5: Isotopic composition of boron ($^{10}B/^{11}B$ atom ratio and ^{10}B atom %) measured in different natural and enriched samples of boron based compounds by PIGE method.

Sample	Using 429 keV of ^{10}B and 2125 keV of ^{11}B		Using 718 keV of ^{10}B and 2125 keV of ^{11}B	
	$^{10}B/^{11}B$ atom ratio (Uncertainty %)	^{10}B atom%	$^{10}B/^{11}B$ atom ratio (Uncertainty %)	^{10}B atom%
Borazine	0.251 (1.0)	20.0	0.247 (1.6)	19.8
$Na_2B_4O_7.10H_2O$	0.247 (1.1)	19.8	0.249 (1.8)	19.9
$LiBO_2$	0.252 (1.1)	20.1	0.249 (1.7)	19.9
Carborane	0.248 (1.1)	19.9	0.249 (1.9)	19.9
Elemental B	0.251 (1.1)	20.1	0.253 (1.7)	20.2
H_3BO_3 (E)	2.011(1.2)	66.8	1.987 (1.0)	66.5
B_4C (N)	0.249 (0.9)	19.9	0.249 (1.2)	19.9
B_4C (E)	2.032 (0.9)	67.0	2.009 (1.0)	66.8
Syn-1	0.528 (0.9)	34.6	0.518 (1.2)	34.1
Syn-2	0.916 (1.4)	47.8	0.913 (1.6)	47.7
Syn-3	1.349 (0.8)	57.4	1.425 (0.9)	58.7

**Syn=Synthetic Samples*

to the knowledge of isotopic composition of B, it is necessary to quantify total boron concentration, as IC does not give the idea about total amount of boron present in the sample.

5.6 Uncertainty measurements and detection limits

The total uncertainties at ±1σ confidence limit were evaluated by propagating individual uncertainties based on the expressions used for calculation of total boron concentrations **[55]** and determination of IC **(Eq. 5.1 & 5.2)**. Propagated uncertainty values were arrived at from the (i) counting statistics of samples, standard, *in situ* current normalizer, (ii) uncertainties on their corresponding masses, and (iii) uncertainty on the concentration of B standard and F *in situ* current normalizer. The individual uncertainty values are: counting statistics of standards (~0.1−0.8%), samples (~0.1− 1%), current normalizing standard (0.1−0.4%), and masses of samples and standards (~0.05−0.4%) and concentration of standard (negligible to 0.3%). The energy uncertainty of the proton beam is about 0.2% on a 4 MeV proton beam **[134]**. Since we have used the relative method, this uncertainty value was not considered in our calculations. The propagated uncertainty values on determined $^{10}B/^{11}B$ atom ratios were obtained from counting statistics of sample, standard, and current normalizing element, and they are in the range of ±0.8−1.9% (**Table 5.6**), whereas total uncertainty values at ±1σ confidence limit on measured concentrations of ^{10}B, ^{11}B, and total boron are within 2.0% (**Tables 5.1−5.4**).

5.6.1 Detection limits of boron by PIGE

The 3σ detection limits (L_D in mg kg^{-1}) of boron (in terms of ^{10}B and ^{11}B) by the PIGE method at a 4 MeV proton beam were evaluated using sample background and respective sensitivities for all three gamma-rays (429, 718, and 2125 keV) **[61,63]**. Calculated detection limits for selected samples are given in **Table 5.6**. The detection limit values are in the range of 0.3−1.9 mg kg^{-1} using 2125 keV of ^{11}B, and 0.3−2.6 mg kg^{-1} and 1.3−6.0 mg kg^{-1} using 429 and 718 keV of ^{10}B, respectively. The variations of detection limits are due to varying backgrounds obtained from samples having varying matrix composition. The detection limits

can be improved further by using a higher energy proton beam and a higher efficiency detection system.

Table 5.6: Experimental detection limits (mg kg^{-1}) for boron (^{10}B and ^{11}B) in selected samples by the PIGE method using a 4 MeV proton beam

Sample	L_D using 429 keV	L_D using 718 keV	L_D using 2125 keV
Carborane	0.8	2.8	0.3
Borax	2.5	5.0	1.9
Borazine	1.9	5.1	0.7
Boron Carbide (N)	0.3	1.3	0.7
Boron Carbide (E)	0.5	2.3	1.2
Boric Acid (E)	2.6	6.0	1.1

(N = Natural composition, E = Enriched with ^{10}B)

5.7 Comparison of total boron contents in borosilicate glass samples and boron carbide samples using PIGE and wet chemical methods

As a part of quality assurance, total B determinations of a few samples of borosilicate glass and boron carbide were also analyzed by titrimetry and ICP-OES other than PIGE, results of which are tabulated in **Table 5.7**. The relative standard deviation (%RSD) values obtained for PIGE method was found to be 2–3 % for triplicate analysis. The %RSD on boron concentrations in borosilicate glass and boron carbide samples by titrimetry and ICP-OES are within ±1.5 and ±0.6%, respectively, from triplicate analyses. The results of boron contents in different boron samples were obtained using three analytical methods, which are given in **Table 5.7.** The table shows that boron content obtained in three different samples were in good agreement with each other. The total propagated % uncertainty in the boron contents of two borosilicate glass samples obtained by Titrimetry, ICP-OES and PIGE is less than 2%,

6% and 2.5%. For boron carbide samples the results of PIGE and Titrimetry were compared and the uncertainty in the measured boron contents is less than 2% and 1% respectively. The boron carbide samples were not analyzed using ICP-OES for determination of boron concentrations

Table 5.7: Comparison of B contents (in wt%) determined by titrimetry, ICP-OES and PIGE

Sample Id	Boron (titrimetry)	Boron(ICP-OES)	Boron (PIGE)
BSG-1	5.4 ± 0.1	5.2 ± 0.3	5.48 ± 0.12
BSG-2	5.6 ± 0.1	5.5 ± 0.3	5.41 ± 0.12
B_4C-1	78.3 ± 0.5	NM*	78.2 ±1.5
B_4C-2	78.5±0.6	NM*	78.6 ± 1.4

*(NM=Not measured)

Conclusions

PIGE methods using 4 MeV proton beam have been optimized for simultaneous determination of IC and total boron concentrations in solid samples of boron based natural and enriched materials. Total boron concentration determination was carried out by *in situ* current normalization using F and Al as *in situ* current normalizer. The obtained experimental results showed a good agreement with the calculated values in a wide range of concentrations as well as isotopic compositions of boron. Isotopic compositions of boron in the range of 0.247-2.0 corresponding to ^{10}B in the range of 19.8–67.0 atom% and total B concentrations in the range of 5-78 wt% were determined. The uncertainty in the results of total boron concentrations were less than ±2%. The results of total boron concentrations in two boron carbide and two BSG samples obtained by PIGE were compared with the results obtained from wet chemical methods. The main advantage of standardized PIGE method is that it is a relatively fast quantitative analysis approach for determination of total B and its isotopic composition.

Chapter 6

Conclusions and Future Scope

Conclusions

Particle induced gamma-ray emission (PIGE) methods using 4 and 8 MeV proton beams have been optimized for quantification of low Z elements like Li, B, O, F, Na, Al, Si and Ti. These methods have been utilised for non-destructive analysis of samples of borosilicate glass, lithium based ceramics and boron based samples including boron carbide. Tandem accelerators, namely 6 MV FOlded Tandem Ion Accelerator (FOTIA) at BARC, 3 MV Tandetron at IOP and 14 MV BARC-TIFR Pelletron at TIFR, Mumbai, were utilized for energetic proton beams in the present work. In addition to conventional current measurement methods (using RBS method or from conducting target), an *in situ* current normalized method was developed in the present work. In this method, an element (like F or Li) was externally mixed to the target pellet and the variations of count rate per unit concentration (sensitivity) of the current normalizing element was taken as relative variation of beam current. The plot of current normalized count rate of elemental standards v/s concentrations showed linearity from trace to major concentration levels validating the *in situ* current normalization approach. Current normalized count rate of sample and standard were used for concentration calculations in thick targets (cellulose and graphite used as matrix) using relative PIGE method. The methods were validated by analyzing stoichiometric compounds of elements of interest, reference materials (from IAEA and NIST) and/or synthetic samples, and, the results obtained for the measured low Z elements were found to be in good agreement (within ±3%) with calculated values. The results of various samples and the conclusions made are summarized as below.

Both conventional and *in situ* current normalized (using Li) PIGE methods, using 4 MeV proton beam from FOTIA, BARC and IOP, Bhubaneswar, were applied to different borosilicate glass samples for quantification of: (i) F in the range of (0.1-4.0 wt%) and simultaneous quantification of (ii) F along with Si, B and Na at major concentration level and

(iii) B, Li, F, Na, Al and Si. For third set of samples where Li, F and Al are present along with other elements, current measurement from the target of graphite matrix was performed instead of using a current normalizing element. Thus, a simple non-destructive nuclear analytical method has been optimized for low Z elements in borosilicate glass samples and the results obtained helped in evaluating loss of F (which is about 10% or more) and giving actual composition of simulated barium borosilicate glass after vitrification.

Like F, PIGE has got high sensitivity for Li. The *in situ* current normalized method using 4 MeV proton beam was extended for quantification of Li at trace to major concentrations in two types of Li based ceramics namely, lithium doped neodymium dititanate (NTO, ferroelectric material) and sol-gel synthesized lithium titanate (Li_2TiO_3) samples. The element F (in the form of CaF_2) was used as *in situ* current normalizer. The concentrations of Li, in precursor and heat treated (800 ^oC) NTO samples, were in the range of 0.29-0.85 wt% of Li. The actual concentrations of Li in heat treated samples were less by 5-35% with respect to initial concentrations in precursor samples. It was also seen that the loss is more with increasing Li concentration in precursor.

The PIGE method was further extended for quantification of Li in lithium titanate ceramic samples. Lithium titanate samples, prepared by three different methods (variation of starting material, sintering material and washing with LiOH) were analyzed by PIGE using 4 MeV proton beam, and, the concentration of Li were in the range of 11.0-12.7 wt%. Concentrations of Ti and O could not be determined by PIGE using 4 MeV proton beam due to low beam current and/or lower thick-target gamma-ray yield. INAA using PCF at Dhruva reactor was utilized to determine Ti concentrations. In order to obtain crack free and dense material, our results indicated that the optimum synthesis procedure could be 1:1 LiCl and $LiNO_3$, processed at 1000 ^oC with LiOH washing. For complete characterization of Li_2TiO_3 under CQC, a PIGE method using 8 MeV proton beam from Pelletron was developed for

simultaneous determination Li, Ti and O. This developmental work using medium energy proton beam, which gives higher thick-target gamma-ray yield, is useful for many low as well as medium Z elements including C, N and O determination in samples relevant to nuclear technology.

Isotope specific nature of PIGE was advantageously utilized for simultaneous quantification of total boron as well as its isotopic composition (IC) i.e. $^{10}B/^{11}B$ atom ratio in natural and enriched boron based samples. The PIGE method using 4 MeV proton beam was applied to various stoichiometric compounds, natural and enriched boric acid as well as boron carbide. In situ current normalization was carried out using F (by mixing in the target pellet) or thin foil of Al (using as a wrapper) for total boron concentration determination. The total boron concentrations obtained in various boron based compounds were in the range of 5-78 wt% and ^{10}B atom % was in the range of 19.8-67%. For analyzing the IC values, the method was rather simple, in which current normalization is not a requirement. Results of IC and total boron concentrations in natural stoichiometric compounds were used or evaluating the accuracy of the method. For method validation, total boron concentration were also determined by conventional ICP-OES and titrimetry. It was shown that for solid and complex matrix samples including carbide and alloy matrices, PIGE is a simple and fast method for determination of IC as compared to TIMS and ICP-MS with added advantage of giving total B concentration simultaneously from the same experiment.

As a part of QA/QC, in addition to validation of methods, total propagated uncertainty in the measurements and detection limits all elements of interest were evaluated. The total propagated uncertainties were arrived at from the (i) counting statistics of samples, standard, *in situ* current normalizer, (ii) uncertainties on their corresponding masses, and (iii) uncertainty on the concentration of current normalizer. The energy uncertainty of the proton beam is about 0.2% for 4 MeV proton beam which was arrived from ±2 kV uncertainties at 2

MV of terminal voltage of accelerator. The propagated uncertainties for elements of interest like F, Li, B, Si, Na, Al and Ti were in the range of ±1-3 % except for O in which propagated uncertainty was about ±8%.

The 3σ detection limits determined using 4 MeV proton beam were in the range of 5-20, 22-33 and 0.3−5.0 mg $kg^{-1}$for F, Li and B, respectively, depending on the experimental conditions and energy of gamma-rays (197 keV for F, 478 keV for Li and 429 and 2125 keV for B). The detection limits estimated for Li, Ti and O were 4, 8 and 136 mg kg^{-1}, respectively, in lithium titanate sample using 8 MeV proton beam. In summary, PIGE methods developed were simple, sensitive and non-destructive in nature and applied to materials relevant to nuclear technology for low Z elements. The results helped in CQC of finished products as well as process/preparation method optimization.

6.2 Future scope

In addition to the elements estimated by PIGE covered in this thesis, exploratory work on elements like Be, C, N, O, P, S, Cl and K was also carried out using 4 as well as 8 MeV proton beams. It is worthwhile to pursue further work on PIGE using medium and high energy proton beams for quantification of many medium to high Z elements. Higher energy proton beams from 14 MV BARC-TIFR Pelletron facility and Cyclotron at VECC will enhance the capability of PIGE for many elements starting from Li and improve the detection limits compared to PIGE using low energy proton beam (2-5 MeV). Additionally, thick target gamma-ray yields of elements above 7 MeV proton beams will be worth pursuing. PIGE can be applied to various samples of environmental, biological, biomedical and pharmaceutical importance as well as to advanced materials including nuclear reactor materials, namely, zircaloys, stainless steels and U-Th based oxides. For example, PIGE can be applied for determination of F in environmental, food and biological samples, Li in Li–ion

batteries and Pb-Li alloy as well as B, C, N, O, F, P, S, Cl in nuclear materials. *In situ* current normalized PIGE method using thin Al will be of immense help to analyze samples like paraffin wax, Pb-Li alloy, other metallic alloys, borated rubber and wood that are difficult to destroy or convert to fine homogenous powder for making target pellets.

References

1. Y. Leng, **2009**, *Materials Characterization: Introduction to Microscopic and Spectroscopic Methods, Wiley*, ISBN: 9780470822999.
2. S. Zhang, **2008**, *Materials Characterization Techniques, CRC Press*, ISBN 1420042947.
3. Vogels, **2003**, *Textbook of Quantitative Chemical Analysis, 6th edition*, ISBN: 8178085380.
4. M.B.H. Breese, D.J. Jamieson, P.J.C. King, **1996**, *Materials Analysis Using a Nuclear Microprobe, John Wiley & Sons, New York*, ISBN: 0471106089.
5. R.F. Sippel, E.D. Glover, **1960**, *Nucl. Instrum.Methods*, 9, p.37–48.
6. T.B. Pierce, P.F. Peck, W.M. Henry, **1965**, *Analyst*, 90, p.339–345.
7. T.B. Pierce, P.F. Peck, D.R.A. Cuff, **1965**, *Anal. Chim. Acta*, 39, p.433–436.
8. G. Deconninck, **1972**, *J. Radioanal. Chem.*, 12, p.157–169.
9. I.S. Giles, M. Peisach, **1979**, *J. Radioanal. Chem.*, 50, p.307–360.
10. R.B. Boulton, G.T. Ewan, **1977**, *Anal. Chem.*, 49, p.1297–1304.
11. B. Borderie, J.N. Barrandon, **1978**, *Nucl. Instrum. Methods*, 156, p.483–492.
12. G. Deconninck, **1978**, *Introduction to Radioanalytical Physics, Akademia Kiado, Budapest,*
13. S.N. Ghoshal, **1950**, *Phys. Rev.*, 80, p.929-936.
14. B. Borderie, J.N. Barrandon, **1978**, *Nucl. Instrum. Methods*, 156, p.483–492.
15. *Nuclear Data and Nuclear Data Sheets*, Academic Press, New York & London.
16. J.F. Ziegler, B.F. Biersack, U. Littmark, **1985**, *The Stopping and Ranges of Ions in Solids B*, Pergamon Press, New York.
17. P. Trocellier, Ch. Engelmann, **1986**, *J. Radioanal. Nucl. Chem.*, 100, p.117-127.
18. F. Xiong, F. Rauch, C. Shi, Z. Zhou, R.P. Livi, T.A. Tombrello, **1987**, *Nucl. Instrum. Methods B*, 27, p.432-441.
19. Anttila, R. Hanninen, J. Raisanen, **1981**, *J. Radioanal. Chem.*, 62, p.293–306.

20. A.Z. Kiss, E. Koltay, B. Nyako, E. Somorjai, A. Anttila, J. Raisanen, **1985**, *J. Radioanal. Chem.*, 89, p.123–141.

21. G. Deconninck, **1972**, *J. Radioanal. Chem.*, 12, p.157–169.

22. P.J. Clark, G.F. Neal, R.O. Allen, **1975**, *Anal. Chem.*, 47, p.650–658.

23. B. Borderie, J.L. Pinault, J.N. Barrandon, 1977, *Analusis*, 5, p.280-283.

24. B. Borderie, J.N. Barrandon, **1978**, *Nucl. Instrum. Methods*, 156, p.483–492.

25. Borderie, **1980**, *Nucl. Instrum. Methods*, 175, p.465–482.

26. P.H.A. Mutsaers, **1996**, *Nucl. Instrum. Methods B*, 113, p.323–329.

27. M.J. Kenny, J.R. Bird, E. Clayton, **1980**, *Nucl. Instrum. Methods*, 168, p.115–120.

28. R. Lappalainen, A. Anttila, J. Raisanen, **1983**, *Nucl. Instrum.Methods*, 212, p.441–444.

29. J. Raisanen, R. Hanninen, **1983**, *Nucl. Instrum. Methods*, 205, p.259–268.

30. E. Moller, N. Starfelt, 1967, *Nucl. Instrum. Methods*, 50, p.225-228.

31. T.B. Pierce, P.F. Peck, D.R.A. Cuff, **1967**, *The Analyst*, 92, p.143-150.

32. R.B. Boulton, G.T. Ewan, **1977**, *Anal. Chem.*, 49, p.1297–1304.

33. E.S. Macias and J.H. Barker, **1978**, *J. Radioanal. Chem.* 45, p.387-394.

34. L.J. van IJzendoorn, M. Haverlag, A. Verbeek, J. Politiek, M.J.A. de Voigt, **1996**, *Nucl. Instrum. Methods B*, 113, p.411–414.

35. G.E. Coote, **1992**, *Nucl. Instrum. Methods B*, 66. P.191-204.

36. M. Volfinger, J.L. Robert, **1994**, *J. Radioanal. Nucl. Chem.* 185, p.273–291.

37. Savidou, X. Aslanoglou, T. Paradellis, M. Pilakouta, **1999**, *Nucl. Instrum. Methods B*, 152, p.12-18.

38. Nsouli, A. Bejjani, S.D. Negra, A. Gardon, J.P. Thomas, **2010**, *Anal. Chem.* 82, p.7309–7318.

39. M. Mosbah, N. Metrich, P. Massiot, **1991**, *Nucl. Instrum. Meth. B*, 58, p.227–231.

40. K.Yosnda, V.H. Hai, M. Nomachi, Y. Sugaya, H. Yamamato, **2007**, *Nucl. Instrum. Meth. B*, 260, p.207–212.
41. S.S. Macias Edward, C. Radcliffe, R. David, W. Lewis Charles, R. Sawicki Carole, **1978**, *Anal. Chem.* 50, p.1120–1124
42. O. Valkovic, M. Jaksic, S. Fazinic, V. Valkovic, G. Moschini, E. Menapace, **1995**, *Nucl. Instrum. Meth. B*, 99, p.372–375.
43. J. Raisanen, T. Witting, J. Keinonen, **1987**, *Nucl. Instrum. Meth. B,* 28, p.199-204.
44. K.E. Saarela, L. Harju, J.O. Lill, J. Rajander, A. Lindroos, S.J. Heselius, **2000**, *Talanta*, 51, p.717–725.
45. J. Raisanen, R. Lapatto, **1990**, *Nucl. Instrum. Meth. B,* 30, p.90-93.
46. R. Tripathi, S. Sodaye, B.S. Tomar, **2004**, *Nucl. Instrum. Meth. A*, 533, p.282–286.
47. Z. Smit, P. Pelicon, H. Hole, M. Kos, **2002**, *Nucl. Instrum. Meth. B*, 189, p.344-349
48. R.L. Moore, C. Goodall, J.L. Hepworth, R.A. Watts, **1957**, *Ind. Eng. Chem.*, 49, p.885–887.
49. K. Raj, K.K. Prasad, N.K. Bansal, **2006**, *Nucl. Eng. Des.*, 236, p.914–930.
50. B.G. Parkinson, D. Holland, M.E. Smith, A.P. Howes, C.R. Scales, **2007**, *J. Non-Cryst. Solids*, 353, p.4076–4083.
51. W.E. Lee, M.I. Ojovan, M.C. Stennett, N.C. Hyatt, **2006**, *Adv. Appl. Ceram.*, 105, p.3-12.
52. R.V. Pai, S.K. Mukerjee, V. Venugopal, **2011**, *Solid State Ionics*, 187, p.85–92.
53. Sumit Chhillar, R. Acharya, T.V. Vittal Rao, Y.R. Bamankar, S.K. Mukerjee, P.K. Pujari, S.K. Aggarwal, **2013**, *J. Radioanal. Nucl. Chem.*, 297, p.1597-1603.
54. Sumit Chhillar, R. Acharya, R. Tripathi, S. Sodaye, K. Sudarshan, P.C. Rout, S.K. Mukerjee, P.K. Pujari, *J. Radioanal. Nucl. Chem.*, **2015**, DOI 10.1007/s10967-015-4037-1.

55. Sumit Chhillar, Raghunath Acharya, Suparna Sodaye, Pradeep K. Pujari, **2014**, *Anal. Chem.*, 86(22), 11167−11173.

56. P. Singh, S.K. Gupta, M.J. Kansara, A. Agarwal, S. Santra, Rajesh Kumar, A. Basu, P. Sapna, S.P. Sarode, N.B.V. Subrahmayam, J.P. Bhatt, P.J. Raut, S.S. Pop, P.V. Bhagwat, S. Kailas, B.K. Jain, **2002**, *J. of Physics*, 59, p.739–744.

57. http://www.iopb.res.in/~ibl_btr/

58. K.G. Prasad, **1989**, *Nucl. Instrum. Meth. B*, 40/41, 916-920.

59. H.C. Jain, U.T. Raheja, P.J. Bhalerao, V.M. Datar, M.Y. Vaze, **1991**, *Ind. J. Phy.*, 34B, p.383.

60. S.A. Kori, M.M. Date, S.K. Kataria, R.P. Thakkar, R.R. Hosangdi, S.K. Sarkar, S.K. Mitra, 1991, *International Conference on Data Acquisition and Control of Accelerators*, VECC, Calcutta, 155.

61. S. Chhillar, R. Acharya, S. Sodaye, K. Sudarshan, S. Santra, R.K. Mishra, C.P. Kaushik, R.K. Choudhury, P.K. Pujari, **2012**, *J. Radioanal. Nucl. Chem.*, 294, p.115–119.

62. S. Chhillar, R. Acharya, R.K. Mishra, C.P. Kaushik, P.K. Pujari, (***Communicated***).

63. S. Chhillar, R. Acharya, R.V. Pai, S.K. Mukerjee, S. Sodaye, P.K. Pujari, S.K. Aggarwal, **2012**, *J. Radioanal. Nucl. Chem.*, 293, p.212-216.

64. B.S. Tomar, **2002**, *Nuclear Analytical Techniques, IANCAS Bulletin*, BARC, Mumbai, India, p.162–170.

65. R.D. Evans, **1982**, *The Atomic Nucleus*, Krieger, New York, ISBN: 0898744148.

66. G.F. Knoll, **1989**, *Radiation detection and measurement*, 2nd Edition, John Wiley & Sons, New York.

67. W.D. Davis, **1958**, *J. Appl. Phys.*, 29, p.231–232.

68. E.M. Pell, **1960**, *J. Appl. Phys.*, 31, p.291–302.

69. W.D. Ehmann, D.E. Vance, **1991**, *Radiochemistry and nuclear methods of analysis*, John Wiley & Sons, New York.

70. D.D. Sood, A.V.R. Reddy, N. Ramanmoorthy, **2007**, *Fundamentals of radiochemistry*, 4th Edition, IANCAS, BARC, Mumbai.

71. A.V.R. Reddy, T.N. Nathaniel, A.G.C. Nair, R. Acharya, D.K. Lahiri, U.S. Kulkarni, C, Sengupta, S. Duraisamy, D.K. Shukla, K. Chakrabarty, R. Ghosh, S.K. Mondal H.S. Gujar, **2007**, *The pneumatic carrier facility in Dhruva reactor utilization*, BARC Report, Mumbai, India.

72. L. Moore, C. Goodall, J.L. Hepworth, R.A. Watts, **1957**, *Ind. Eng. Chem.*, 49, p.885–887.

73. K. Raj, K.K. Prasad, N.K. Bansal, **2006**, *Nucl. Eng. Des.* 236, p.914–930.

74. R.K. Mishra, V. Sudarsan, C.P. Kaushik, K. Raj, S.K. Kulshreshta, A.K. Tyagi, **2006**, *J. Nucl. Mater.*, 359, p.132–138.

75. R.K. Mishra, V. Sudarsan, A.K. Tyagi, C.P. Kaushik, K. Raj, S.K. Kulshreshta, **2006**, *J. Non. Cryst. Solids.*, 352, p.2952–2957.

76. R.K. Mishra, V. Sudarsan, C.P. Kaushik, K. Raj, R.K. Vatsa, M. Body, A.K. Tyagi, **2009**, *J. Non. Cryst. Solids*, 355, p.414–419.

77. H. Scholze, **1991**, *Glass Nature, Structure and Properties*, Springer-Verlag (NewYork), ISBN: 9781461390718.

78. K.J. Rao, **2002**, *Structural Chemistry of Glasses*, Elsevier (Amsterdam), ISBN: 9780080439587.

79. H. Bach, D. Krause, **1991**, Analysis *of the Composition and Structure of Glass*, Schott Series on Glass and Glass Ceramics, Springer-Verlag (Berlin, Heidelberg), ISBN: 3540586105.

80. S. Shuttleworth, J.E. Monteith, **1997**, *Mater. Res. Soc. Symp. Proc.*, 465, p.123.

81. Borbely-Kiss, M. Jozsa, A.Z. Kiss, E. Koltay, B, Nyako, E, Somorjai, G. Szabo, S. Seif El-Nasr, **1985**, *J. Radioanal. Nucl. Chem.*, 92, p.391–398.
82. C. Boni, E. Caruso, E. Cereda, G.M.B. Marcazzan, P. Redaelli, **1989**, *Nucl. Instrum. Meth. B*, 40/41, p.620–623.
83. K.B. Dasari, Sumit Chhillar, R. Acharya. N.L. Das, P.K. Pujari, **2014**, *Nucl. Instrum. Meth. B*, 339, p.37-41.
84. N. Ishizawa, F. Marumo, S. Iwai, M. Kimura, T. Kawamura, **1982**, *Acta Cryst.* B38, p.368– 372.
85. R.V. Kamat, K.T. Pillai, V.N. Vaidya, D.D. Sood, **1996**, *Mater. Chem. Phys.*, 46, p. 67–71.
86. J.F. Scott, **2000**, *Ferroelectric Memories, Berlin, Springer,* ISBN: 3540663878
87. N. Roux, J. Avon, A. Floreancig, J. Mougin, B. Rasneur, S. Ravel, **1996**, *J. Nucl. Mater.*, 233–236 p.1431–1435.
88. P. Gierszewski, J. Miller, J. Sullivan, R. Verrall, J. Earnshaw, D. Ruth, R. Macauley-Newcombe, G. Williams, **2005**, *Fusion Eng. Des.*, 75–79, p.877–880.
89. L. Giancarli, V. Chuyanov, M. Abdou, M. Akiba, B.G. Hong, R. Lasser, C. Pan, Y. Strebkov, TBWG Team, **2007**, *J. Nucl. Mater.*, 367, p.1271–1280.
90. R. Govindan, D. Alamelu, R.V. Shah, T.V. Vittal Rao, Y.R. Bamankar, A.R. Parab, B.K. Sasi, S.K. Mukerjee, S.K. Aggarwal, **2010**, *Anal. Meth.*, 2, p.1752–1755.
91. P. Gierszewski, **1998**, *Fusion Eng. Des.*, 39–40, p.739–743.
92. S. Nanamatsu, M. Kimura, S. Matsushita, M. Takahashi, **1973**, *Jpn. Electron. Eng*., 33, p.
93. T.V. Vittal Rao, Y.R. Bamankar, S.K. Mukerjee, S.K. Aggarwal, **2012**, *J. Nucl. Mater.*, 426, p.102–108.

94. J.D. Pedarnig, J. Heitz, T. Stehrer, B. Praher, R. Viskup, M. Siraj, A. Moser, A. Vlad, M.A. Bodea, D. Bauerle, N. Hari Babu, D.A., Cardwell, **2008**, *Spectrochim. Acta B*, 63, p.1117–1121.

95. D.P. Chowdhury, J. Arunachalam, Rakesh Verma, Sujit Pal, S. Gangadharan, **1992**, *J. Radioanal. Nucl. Chem.*, 158, p.463-470.

96. W.D. Ehmann, B.F. Ni, **1992**, *J. Radioanal. Nucl. Chem.*, 160, p.169-179.

97. Inoue Ryo, Suito Hideaki, **1991**, *Mater. Trans.*, 12, p.1164-1169.

98. Tetsuo Umegaki, Jun-Min Yan, Xin-Bo Zhang, Hiroshi Shioyama, Nobuhiro Kuriyama, Qiang Xu, **2009**, *Inter. J. Hydro. Ener.*, 34, p.2303–2311.

99. H.G. Pfaender, **1996**. *Schott Guide to Glass*, Springer, IInd Edition, ISBN:041262060-X

100. Cooke, F. Theodore, **1991**, *Journal of the American Ceramic Society*, 74, p.2959–2978.

101. R.H. Wentorf, **1957**, *J. Chem. Phys.*, 26, p.956-962.

102. Y.G. Gogotsi, R.A. Andrievski, **1999**, *Materials Science of Carbides, Nitrides and Borides*. Springer, ISBN: 9789401145626

103. J.H. Klotz, J.I. Moss, R. Zhao, Jr. L.R. Davis, R.S. Patterson, **1994**, *J. Econ. Entomol*. **87**, p.1534–1536

104. Boric Acid, *chemicalland21.com.*

105. C. Paul Canfield, W. George Crabtree, **2003**, *Physics Today*, **56**, p.34–41.

106. Valeria Braccini, D. Nardelli, R. Penco, G. Grasso, **2007**, *Physica C: Superconductivity* 456, p.209–217.

107. Xiaowei Wu, R.S. Chandel, Hang Li, **2001**, *J. Mater. Sci.*, 36, p.1539–1546.

108. Rolf F. Barth, **2003**, *J. Neuro-Onco.*, 62, p.1–5.

109. Jeffrey A. Coderre, G.M. Morris, **1999**, *Rad. Res.*, 151, p.1–18.

110. Rolf F. Barth, **1990**, *Cancer Research*, 50, p.1061–1070.

111. J.E. Riley, R.M. Lindstrom, **1987**, *J. Radioanal. Nucl. Chem.*, 109, p.109−115.

112. S.D. Kumar, B. Maiti, P.K. Mathur, **1999**, *Anal. Chem.*, 71, p.2551−2553.

113. J.K. Aggarwal, M.R. Palm, **1995**, *Analyst*, 120, p.1301−1307.

114. A.J. Spivack, J.M. Edmond, **1986**, *Anal. Chem.*, 58, p.31−35.

115. M. Joseph, N. Sivakumar, P. Manoravi, R. Balasubramanian, **2003**, *Mass Spectrom.*, 18, p.231−234.

116. M. Rosner, W. Pritzkow, J. Vogl, S. Voerkelius, **2011**, *Anal. Chem.*, 83, p.2562−2568.

117. R.M. Rao, A.R. Parab, K. Sasibhushan, S.K. Aggarwal, **2009**, *Int. J. Mass Spectrom.*, 285, p.120−125.

118. N.C. Porteous, N.J. Walsh, K.E. Jarvis, **1995**, *Analyst*, 120, p.1397−1400.

119. R. Sah, P.J. Brown, **1997**, *Microchem.*, 56, p.285−304.

120. Farhat, F. Ahmad, H. Arafat, **2003**, *Desalination*, 310, p.9−17.

121. W.H. Christie, R.E. Eby, R.J. Warmack, L. Landau, **1983**, *Anal. Chem.*, 53, p.13−17.

122. J.K. Aggarwal, D. Sheppard, K. Mezger, E. Pernicka, **2003**, *Chem. Geol.*, 199, p.331−342.

123. V. Devulder, P. Degryse, F. Vanhaecke, **2013**, *Anal. Chem.*, 85, p.12077−12084.

124. Y.J. Park, H.Y. Pyo, K. Song, B.C. Song, K.Y. Jee, W.H. Kim, **2006**, *Korean Chem. Soc.*, 27, p.609−1612.

125. E.S. Gladney, E.T. Jurney, D.B. Curtis, **1976**, *Anal. Chem.*, 48, p.2139−2142.

126. R. Acharya, **2009**, *J. Radioanal. Nucl. Chem.*, 281, 291−294.

127. K. Sudarshan, R. Tripathi, A.G.C. Nair, R. Acharya, A.V.R. Reddy, A. Goswami, **2005**, *Anal. Chim. Acta*, 549, p.205−211.

128. G.L. Molnar, **2004**, *Handbook of Prompt Gamma Activation Analysis with Neutron Beams*, Kluwer Academic Publishers, London, ISBN: 9780387233598

129. F.S. Romolo, M.E. Christopher, M. Donghi, L. Ripani, C. Jeynes, R.P. Webbc, N.L. Ward, K.J. Kirkby, M. Bailey, **2013**, *J. Forensic Sci. Int.*, 231, 219−228.

130. S. Savolinen, J. Raisanen, V. Etelaniemi, U.A. Ramadan, M. Kallio, **1995**, Appl. *Radiat. Isot.*, 46, p.855−858.

131. B. Nsouli, T. Darwish, K. Zahraman, A. Bejjani, M. Roumie, J.P. Thomas, **2006**, *Nucl. Instrum. Meth. B*, 249, p.566−570.

132. R. Mateus, A.P. Jesus, B. Braizinha, J. Cruz, J.V. Pinto, J.P. Riberio, **2002**, *Nucl. Instrum. Meth.B*, 283, p.117−121.

133. A.E. Pillay, M. Peisach, **1992**, *Nucl. Instrum. Meth. B*, 66, p.226−229.

134. S. Santra, K. Mahata, P. Singh, C.V. Fernandes, M. Hemalatha, S. Kailas, **2003,** *Nucl. Instrum. Meth. A*, 496, p.44−50.

List of Publications

Journal

1. Application of particle induced gamma-ray emission for non-destructive determination of fluorine in barium borosilicate glass samples, **Sumit Chhillar**, R. Acharya, S. Sodaye, K. Sudarshan, S. Santra, R.K. Mishra, C.P. Kaushik, R.K. Choudhury, P.K. Pujari, *J. Radioanal. Nucl. Chem.*, **2012**, 294, 115–119.
2. A simple and sensitive particle induced gamma-ray emission method for non-destructive quantification of lithium in lithium doped $Nd_2Ti_2O_7$ ceramic sample, **Sumit Chhillar**, R. Acharya, R.V. Pai, S. Sodaye, S.K. Mukerjee, P.K. Pujari, *J. Radioanal. Nucl. Chem.*, **2012**, 293, 212-216.
3. Non-destructive compositional analysis of sol–gel synthesized lithium titanate (Li_2TiO_3) by particle induced gamma-ray emission and instrumental neutron activation analysis, **Sumit Chhillar**, R. Acharya, T.V. Vittal Rao, Y.R. Bamankar, S.K. Mukerjee, P.K. Pujari, S.K Aggarwal, *J. Radioanal. Nucl. Chem.*, **2013**, 298, 1597-1603.
4. Compositional characterization of lithium titanate ceramic samples by determining Li, Ti and O concentrations simultaneously using PIGE at 8 MeV proton beam, **Sumit Chhillar**, R. Acharya, R. Tripathi, S. Sodaye, K. Sudarshan, P. C. Rout, S. K. Mukerjee, P. K. Pujari, *J. Radioanal. Nucl. Chem.*, **2015**, DOI 10.1007/s10967-015-4037-1
5. Simultaneous determination of Si, Al and Na concentrations by particle induced gamma-ray emission and applications to reference materials and ceramic archaeological artifacts K.B. Dasaria, **Sumit Chhillar**, R. Acharya, D.K. Ray, A. Behera, N. Lakshmana Das, P.K. Pujari, *Nucl. Instrum. Meth. B*, **2014,** 339, 37-41.

6. Development of particle induced gamma-ray emission methods for nondestructive determination of isotopic composition of boron and its total concentration in natural and enriched samples, **Sumit Chhillar**, Raghunath Acharya, Suparna Sodaye, Pradeep K. Pujari, *Anal. Chem.*, **2014**, 86(22), 11167-11173.
7. Compositional Characterization of borosilicate glass samples for low Z elements using *in situ* current normalized particle induced gamma-ray emission methods, **Sumit Chhillar**, R. Acharya, R.K. Mishra, C.P. Kaushik, P.K. Pujari *(Submitted)*

Conference

1. Non-destructive Determination of Fluorine in Borosilicate Glass Samples by a PIGE Method; **S. Chhillar**, R. Acharya, S. Sodaye, K. Sudarshan, S. Santra, R.K. Mishra, C.P. Kaushik, R.K. Choudhury, P.K. Pujari, Fourth International Symposium on Nuclear Analytical Chemistry (NAC-IV), BARC, Mumbai, **November 15-19, 2010**, p.196.
2. Setting up of PIGE facility at FOTIA, BARC and its application to Borosilicate Glass Samples for determination of fluorine by an internal standard method; **S. Chhillar**, R. Acharya, S. Sodaye, K. Sudarshan, S. Santra, R.K. Mishra, C.P. Kaushik, S.K. Gupta, A. Agarwal, P. Singh, R.K. Choudhury, P.K. Pujari, Proceedings of DAE Symposium on Nuclear Physics (SNP-55), BITS, Pilani, Rajasthan, **December 20-24, 2010**, p.780-781.
3. An internal standard particle induced gamma ray emission methodology for non-destructive determination of Lithium in ceramic samples, **S. Chhillar**, R. Acharya, S. Sodaye, R. Pai, S. K. Mukerjee, P. K. Pujari, Proceedings of Tenth DAE-BRNS biennial symposium on

Nuclear and Radiochemistry (NUCAR-2011), GITAM University, Visakhapatnam, **February, 22-26, 2011**, p.523-524.

4. Proton Induced Gamma-ray Emission Reaction for Quantification of Lithium in Lithium Titanate Samples, **S. Chhillar**, R. Acharya, K.B. Dasari, R. Tripathi, P.K. Pujari, T.V. Vittal Rao, Y. R. Bamankar, S. K. Mukerjee, S.K Aggarwal, Proceedings of DAE Symposium on Nuclear Physic (SNP-56), Andhra University, Visakhapatnam, **December 26-30, 2011**, p.630-631.
5. Non-destructive quantification of boron and ^{10}B to ^{11}B ratios in neutron absorber materials by PIGE using proton beam from FOTIA, BARC, **S. Chhillar**, R. Acharya and P.K. Pujari, Proceedings of DAE Symposium on Nuclear Physic (SNP-57), Delhi University, Delhi, **December 3-7, 2012**, p. 920-921.
6. Applications of PIGE and PIXE for analysis of ceramic and archaeological artifacts, K.B. Dasari, R. Acharya, **Sumit Chhillar**, D.K. Ray, A. Behera, N.L. Das, P.K. Pujari, Proceedings of Eleventh DAE-BRNS biennial symposium on Nuclear and Radiochemistry (NUCAR-2013), R.D. University, Jabalpur, **February 19-23, 2013**, p.473-474.
7. Application of particle induced gamma-ray emission methodology for simultaneous quantification of low Z elements in borosilicate glass, **Sumit Chhillar**, R. Acharya, R. K. Mishra, C. P. Kaushik and P. K. Pujari, Proceedings of Eleventh DAE-BRNS biennial symposium on Nuclear and Radiochemistry (NUCAR-2013), R.D. University, Jabalpur, **February 19-23, 2013**, p.479-480.
8. Application of *in situ* current normalized PIGE method for determination of total boron and its isotopic composition, **Sumit Chhillar**, R. Acharya, S. Sodaye, P.K. Pujari, Fifth

Symposium on Nuclear Analytical Chemistry (NAC-V), BARC, Mumbai, **January 20-24, 2014**, p.224-225.

9. Simultaneous quantification of Li, Ti and O in lithium titanate by particle induced gamma-ray emission using 8 MeV proton beam, **S. Chhillar**, R. Acharya, R. Tripathi, S. Sodaye, K. Sudarshan, P.C. Rout, S.K. Mukerjee, P.K. Pujari, Proceedings of Fifth Symposium on Nuclear Analytical Chemistry (NAC-V), BARC, Mumbai, **January 20-24, 2014**, p.210-211.
10. R&D work on particle induced gamma-ray emission using proton beam at FOTIA, BARC: Present status and future Prospects, R. Acharya, **S. Chhillar**, P.K. Pujari, A. Agarwal, S.K. Gupta and P. Singh, Fifth Symposium on Nuclear Analytical Chemistry (NAC-V), BARC, Mumbai, **January 20-24, 2014**, p.212-213.
11. Determination of isotopic composition of boron in various neutron absorbers by a Particle Induced Gamma-ray Emission method, R. Acharya, **Sumit Chhillar**, J.K. Sonber, D.S. Arati, T.S.R. Ch Murthy, P. K. Pujari, Proceedings of Twelfth DAE-BRNS biennial symposium on Nuclear and Radiochemistry (NUCAR-2015), BARC, Mumbai, **January 20-24, 2015**, p.417-418.